2007

The Role of Silicates in Interstitial Lung Disease

Francisco Jose Leyva
The University of Montana

THE ROLE OF SILICATES IN INTERSTITIAL LUNG DISEASE

By

Francisco Jose Leyva

B.S., Universidad Peruana Cayetano Heredia, Lima, Peru, 1995
M.D., Universidad Peruana Cayetano Heredia, Lima, Peru, 1995

Dissertation

presented in partial fulfillment of the requirements
for the degree of

Doctor of Philosophy.
in Toxicology

The University of Montana
Missoula, MT

Spring 2007

Approved by:

Dr. David A. Strobel, Dean
Graduate School

Andrij Holian, Chair
Department of Biomedical & Pharmaceutical Sciences

Mark A. Pershouse, Co-Chair
Department of Biomedical & Pharmaceutical Sciences

Jean C. Pfau
Department of Biomedical & Pharmaceutical Sciences

Kevan Roberts
Department of Biomedical & Pharmaceutical Sciences

Scott A. Wetzel
Division of Biological Sciences

Leyva, Francisco, Ph.D., May 2007 Toxicology

The Role of Silicates in Interstitial Lung Disease

Chairperson or Co-Chairperson: Mark A. Pershouse

Interstitial Lung disease (ILD), produces disruption of alveolar walls with loss of functionality and accumulation of scar tissue. Asbestosis and silicosis are the ILD produced by the inhalation of asbestos fibers or silica particles respectively. An increase in prostacyclin release after exposing endothelial cells to asbestos has been reported. This study attempts to elucidate the role of lung epithelial cells in the generation of asbestos induced ILD. A cell model to study crocidolite-induced toxicity was developed using LA-4 cells, previously characterized as alveolar type II cells. LA-4 cells when exposed to crocidolite had a decrease in viability and an increase in the release of LDH and 6-keto $PGF_{1\alpha}$, a prostacyclin metabolite. Prostacyclin release was Cox 2 and vitronectin receptor (VNR) mediated. Coating crocidolite asbestos with vitronectin enhances its internalization via VNR, which also recognize the Arg-Gly-Asp (RGD) motif present in a variety of ligands (e.g., vitronectin, fibronectin). These findings propose that crocidolite is coated by an RGD protein and binds VNR inducing Cox 2 expression promoting prostacyclin release. Cytotoxicity did not follow the same model. In silica studies, it has been previously reported that Scavenger receptor A I/II (SR-A I/II) plays a role in silica-induced apoptosis. The cytoplasmic domain of the SR-AI/II has four aminoacids: Ser25, Ser32, Ser53, Thr34 that can be phosphorylated, and the extracellular region contains a lysine-rich cluster that is required for Acetylated Low density lipoprotein (AcLDL) binding. SR-AI contains a cysteine-rich domain, which is absent in SR-AII. This study evaluated the role of the four aminoacids that could be phosphorylated, and differences between SR-AI and SR-AII in silica binding. Constructs expressing SR-AII, and mutated SR-AIIs containing deletions to Ser25, Ser32, Ser53, Thr34 and KE (lysine cluster) were generated and CHO cells were transfected. Receptor functionality was verified by AcLDL uptake. Silica binding or silica-induced apoptosis was not statistically significant different from transfected controls. In addition, no statistically significant difference was found between SR-AI and SR-AII in AcLDL uptake, silica binding, and silica-induced apoptosis. This study shows that asbestos or silica alone cannot induce its effect, and asbestos required to be coated by RGD proteins.

TABLE OF CONTENTS

LIST OF TABLES

LIST OF FIGURES

LIST OF ABBREVIATIONS

AcLDL	Acetylated low density lipoprotein
AM	Alveolar macrophages
BALF	Bronchoalveolar lavage fluid
CHO	Chinese hamster ovary cells
COX	Cyclooxygenase
DNA	Deoxyribonucleic acid
ECL	Enhanced chemiluminiscense
ECM	Extracellular matrix
EV	Empty vector
FCS	Fetal calf serum, fetal bovine serum
GAPDH	Glyceraldehyde-3-phosphate dehydrogenase
HSP	Heat shock protein
ILD	Interstitial lung disease
IP	Immunoprecipitation
LAP	TGFβ latency-associated peptide
LDH	Lactate dehydrogenase
LDL	Low density lipoprotein
LPS	Lipopolysaccharide
LSC	Laser Scanning Cytometer
mRNA	Messenger ribonucleic acid
OD	Optical density
PCR	Polymerase chain reaction
PGI2	Prostaglandin I2, Prostacyclin
PI	Propidium iodide
PM	Peritoneal macrophages
PolyI	Polyinosinic acid
RGD	Arginine-Glycine-Aspartic acid
SR-A	Scavenger receptor A
SRCR	Scavenger receptor cysteine rich domain
TGFβ	Transforming growth factor beta
TUNEL	Terminal deoxynucleotide transferase dUTP nick end labeling
VNR	Vitronectin receptor
WB	Western blot

Chapter 1

Interstitial Lung Disease

Interstitial lung diseases (ILD) are a large and heterogeneous group of lower respiratory tract disorders that share certain pathogenic mechanisms and histopathologic features. ILD is also known as “Interstitial pulmonary fibrosis” or “Diffuse parenchymal lung disease.” The prevalence of ILD in the general population is estimated to be 20 to 40 per 100,000 and accounts for 100,000 hospital admissions each year (Toews, 2000). Several factors such as an increase in the use of pneumotoxic drugs prescribed to treat malignancies, cardiovascular diseases, or organ transplantation, and the increase in the identification of occupationally-induced ILD have contributed to an increase in its incidence.

The human respiratory system includes the following regions: the nasal cavity, pharynx, larynx, trachea, bronchi and their smaller branches, and the lungs. (Figure 1.1). The histology of the respiratory system is complex in the proximal regions and simple in the distal regions as shown in Figure 1.2 (Marieb & Hoehn, 2007; Powel, 1998). The human respiratory tract contains over 40 different cell types, such as epithelial cells lining in the airways, alveoli and blood vessels as well as connective tissue cells. The affected structure in ILD is the alveolar interstitium, which involves the space between the alveolar epithelium and the capillary endothelium including the connective tissues surrounding blood vessels, lymphatic vessels, and airways. Despite the presence of some

pathologic differences, the common denominator among ILDs is the widespread disruption of alveolar walls with loss of functional alveolar capillary units and accumulation of collagenous scar tissue also described as fibrosis.

The clinical presentation of ILD includes the triad: progressive dyspnea or shortness of breath, evident radiographic interstitial infiltrates, and pulmonary function tests showing a decrease in volume and gas diffusion. The clinical classification of ILD is described in Table 1.1. It shows that ILDs could be divided into five groups. This study focuses in the Environment/Occupation–associated ILD. Occupational diseases affecting the pulmonary interstitium and producing ILD include primarily the pneumoconiosis or dust diseases of the lung, and hypersensitivity pneumonitis. The principal pneumoconioses are shown in Table 1.2. The term pneumoconiosis can be defined as "the accumulation of dust in the lungs and the tissue reactions to its presence" (R. S. Fraser et al., 2005). The most prevalent pneumoconioses are the ones caused by silicates such as asbestos and silica. Pneumoconiosis as a consequence of silicate exposure produced significant morbidity and mortality during the early part of the twentieth century. Today silicate exposure in the workplace has been reduced through enforcement of strict regulations in US, but due to the latency period between exposure and disease, new cases of silicate pneumoconiosis are still detected in the general population (Kelley, 1998).

Silicate is chemically defined as a compound with one or more central silicon atoms surrounded by electronegative ligands, most often oxygen atoms. Because the most abundant elements in the continental crust are oxygen (45.2% weight) and silicon (27.2% weight), high silicate abundance (30%) in the Earth's crust is not surprising (Covey,

2006; Whitehead, 2001). Structurally, silicates are classified into six subclasses: Nesosilicates, Sorosilicates, Inosilicates, Cyclosilicates, Phyllosilicates, and Tectosilicates (Table 1.3). Silica belongs to the tectosilicate and the asbestos amphibole crocidolite to the inosilicate sub class (Figure 1.3).

Every day the respiratory system is exposed to large amounts of air through respiration. The calculated amount of air mobilized by an adult is 15 to 20 m^3 per day. Due to this large amount of air volume, a considerable amount of inhaled particles could accumulate in the lungs despite their low concentrations in the environment. The principal mechanisms of inhaled particle deposition in the respiratory tract are impaction, sedimentation, interception, and diffusion (Figure 1.4) (McClellan, 1999; Raabe, 1999).

A. Impaction is the dominant mechanism of deposition of particles larger than 3 μm in aerodynamic diameter. It occurs when the particles follow their initial path because of inertia rather than following changes in direction or speed of the airflow, resulting in collision with the wall of the airway usually near a bifurcation.

B. Sedimentation of particles occurs when the airflow is slow and particle deposition is influenced by gravity. As particles increase in aerodynamic diameter the sedimentation increases.

C. Interception is a non-inertial incidental contact with the airway wall. It is more important for fibers (e.g. asbestos) because their length (not their diameter) increases the probability that the ends of the fiber will deposit by interception on the walls of the airway.

D. Diffusion is responsible for the deposition of particles smaller than 0.5 μm in diameter. As particle size decreases, diffusion increases. Deposition by diffusion is highest in the alveoli where the airflow is very slow

Particle deposition can occur in any portion of the respiratory system, but for the development of pneumoconioses, the deposit has to occur in the distal regions, such as the terminal bronchioles and alveoli. The great majority of particles that penetrate to the alveoli are 1 μm or less in diameter. Larger particles are deposited on the upper respiratory tract, trachea, and larger bronchi (Figure 1.5). Asbestos fibers are the exception because they can penetrate the lung parenchyma despite their length of 30 μm or more (R. S. Fraser, Colman et al., 2005). After the noxious agent (e.g. silica or asbestos) reaches the lung, several factors in exposed individuals may play a role in their susceptibility to develop ILD. Nemery et al., proposed four factors: First: differences in delivery and/or persistence of the noxious agent could be related to innate anatomical or physiological characteristics, and to acquired changes. Second: genetic or acquired variations in enzymatic and non-enzymatic defense systems mainly related to protection against oxidative stress. Third: the immunological sensitization that is dependent on genetic and environmental factors. And fourth, the propensity to develop particular types of reaction such as granulomas, and the ability to regulate and resolve inflammation and fibrogenesis (Nemery et al., 2001).

The cause of most ILDs is unknown. Different agents such as bacteria, virus, fungi, toxic agents, and environmental agents have been implicated. It has been proposed that these agents can activate inflammatory or immune cells in the lung, or alternatively

these agents could produce direct injury to the resident pulmonary cells leading to an inflammatory response initiated by the injured lung tissue. Because most of the time more than one agent is present, it is possible to conclude that ILD is produced by a combination of factors that induce direct and indirect inflammation, and affect the self-limited inflammatory response. In the past it was proposed that an insult initiated an inflammatory response leading to a cycle of chronic inflammatory injury leading to fibrosis. As a consequence, anti-inflammatory therapy was the primary therapy in the hope that an interruption of the inflammatory cascade before irreversible tissue injury occurred would benefit patients with ILD. However, in many cases, the use of anti-inflammatory agents such as glucocorticoids and cytotoxics failed to improve the outcome (Mason et al., 1999). Therefore, a new hypothesis has been proposed focusing on the alveolar surface of the lung. It has been suggested that a stimulus (e.g. asbestos, beryllium) produces repeated episodes of lung injury and the damaged alveolar epithelium induces accumulation and activation of immuno-inflammatory cells, with subsequent migration and proliferation of fibroblasts and extracellular matrix deposition leading to the development of foci of fibroblasts/myofibroblasts in the alveolar interstitium. This wound healing process leads to fibrosis and loss of lung function (Clement et al., 2004; Gross & Hunninghake, 2001) (Figures 1.6 and 1.7).

The pathogenesis of ILD can be divided into three steps:

I. Epithelial damage: Epithelial cell injury is a hallmark of ILD. In situations of extensive cell damage and/or inappropriate re-epithelialisation of the lung surface, the normal

interaction between alveolar epithelial cells, inflammatory cells and interstitial fibroblasts is altered resulting in an unbalanced production of inflammatory mediators.

II. Intra-alveolar inflammation: Inflammatory exudate accumulates and inflammatory cells such as macrophages, neutrophils and lymphocytes increase in number in the alveolar walls and in the alveolar air spaces. The inflammatory cell recruitment process, which depends on production of cytokines and chemokines, includes the following four steps: sequestration of inflammatory cells in pulmonary vessels, transmigration of the vascular wall, migration through the extracellular matrix, and selective tissue retention.

III. Intra-alveolar fibrosis/alveolar collapse: The local population of fibroblasts and myofibroblasts increases, leading to a progressive aberrant tissue remodeling process with deposition of extracellular matrix components, including fibrillar collagen, elastic fibers, fibronectin and proteoglycans. Under the influence of growth factors and angiogenic molecules, epithelial cells proliferate and convert the fibrin-rich exudate in fibrotic tissue producing scars and changes in the normal lung architecture.

In order to understand the mechanisms involved in the cellular activation during the interaction between particle and cells from the lung, the agents chosen in this study were crocidolite and silica. Crocidolite was chosen due to its high ability to induce pulmonary fibrosis, and silica because is the most studied silicate in our laboratory. Understanding this response will contribute the development of new strategies for clinical intervention in silicate pneumoconiosis.

Crocidolite Asbestos

Asbestos is a naturally occurring fibrous hydrated silicate mineral widely used in the past for commercial applications. In the last century, more than 30 million tons of asbestos have been mined, processed and applied in the United States (Mossman et al., 1990; Mossman & Gee, 1989). Asbestos exposure can be classified into two groups: occupational and non-occupational. Occupational exposure occurs during mining and milling of the fibers, or during industrial application of asbestos in textiles, insulation, shipbuilding, brake lining mechanics, etc. Non-occupational exposure is related to fugitive asbestos fibers released into the environment and material inadvertently brought home and released from contaminated clothing or other asbestos contaminated materials (Kamp & Weitzman, 1997).

Despite the fact that most occupational asbestos exposure ceased in the late 1970's due to governmental legislation, asbestos-related disease is still a public health concern because: a) approximately 27 million workers in U.S. have been exposed, b) the latency period involved between initial exposure and asbestos-related disease which is 20 years or longer, c) the continued presence of construction material containing great amounts of asbestos, d) it is still used in over 3,000 products in US and e) the increase in death rate due to asbestos-related disease (Kamp & Weitzman, 1997). Asbestos-related diseases integrate several different kinds of diseases related to previous exposure to asbestos fibers. The spectrum of thoracic diseases includes benign pleural effusion, pleural plaques, diffuse pleural thickening, rounded atelectasis, asbestosis, mesothelioma, and lung cancer. Asbestosis is the ILD produced by the inhalation of asbestos fibers.

Asbestos forms fine, fibrous crystals and exhibits different properties such as high tensile strength and durability, flexibility and malleability, thermal and chemical resistance, and low electrical conductivity. Due to these properties, asbestos had been used widely in many industrial and commercial applications. There are two primary classes of asbestos: serpentine and amphibole (Figure 1.8). Serpentine fibers are curly-stranded structures. Chrysotile ($Mg_6Si_4O_{10}(OH)_8$), a white or greenish colored asbestos generally considered to be a less toxic fiber is the only commercial serpentine asbestos and accounts more than 90% of asbestos used in the United States. Amphiboles fibers are straight, rigid and needlelike. Three examples of amphiboles fibers are: crocidolite ($Na_2Fe^{2+}{}_3Fe^{3+}{}_2Si_8O_{22}(OH)_2$) a blue sodium iron silicate fiber that may be woven or spun into cloth or tape, tremolite a white to yellowish calcium magnesium silicate that has been a major ingredient in industrial and commercial talc, and amosite ($Fe_7Si_8O_{22}(OH)_2$) a brownish-yellow to white asbestos mineral used for heat insulation (Faust, 1995). Despite their differences in physical properties, all types of asbestos fibers are fibrogenic, but crocidolite is considered the most carcinogenic (Khan et al., 2004).

In the last 30 years numerous studies have been performed using different kinds of asbestos and cell types. It has been established that alveolar macrophages (Bissonnette et al., 1990; Tatrai et al., 2005), alveolar type II cells (Tatrai, Brozik et al., 2005), mesothelial cells (Boylan et al., 1995; Wu et al., 2000), fibroblasts (MacCorkle et al., 2006), and endothelial cells (Garcia et al., 1989; Garcia et al., 1988) can generate different responses when exposed to asbestos fibers. These different responses include DNA damage, gene transcription, and expression of proteins modulating cell proliferation, cell death, and inflammation (Kamp et al., 1992; Mossman & Churg, 1998;

Mossman, Kamp et al., 1996; Rom et al., 1991). In addition, several factors have been found related to the pathogenesis of asbestos induced lung injury: a) chemical and structural properties of the fiber, b) fiber burden in the lung, c) uptake by pulmonary epithelial cells, d) iron catalysed free radicals, e) DNA damage, f) induction of cytokines and growth factors, and g) cigarette smoke (Kamp & Weitzman, 1999). All these findings give an idea about the complexity of the lung response after asbestos exposure (Figure 1.9). In a PubMed search performed on March 2007, the phrase "asbestos related disease" was used. Approximately 15% of publications were about asbestosis, while most of the published work were about mesothelioma a malignancy associated with asbestos exposure.

In order for asbestos to initiate asbestosis or other asbestos related disease it needs to come in contact with and be recognized by the target cell. In 1995 Boylan et al, reported in rabbit mesothelial cells that coating crocidolite asbestos with vitronectin enhanced its internalization via the alpha V integrin vitronectin receptor $\alpha v\beta 5$ (Boylan, Sanan et al., 1995). Integrins are a large family of cell surface receptors described as heterodimeric, transmembrane glycoproteins composed of an α and a β subunit noncovalently associated. Each $\alpha\beta$ combination has its own binding specificity and signaling. Most integrins can recognize more than one extracellular matrix (ECM) protein and conversely, ECM proteins such as fibronectin, laminins, collagens, and vitronectin can bind to more than one different integrin as well. Integrins can signal through the cell membrane in either direction: inside-out signaling (induce changes in the environment) and outside-in signaling (induce changes inside the cell); and transmit signals that regulate the activities of cytoplasmic kinases, growth factor receptors, and ion channels

and control the organization of actin cytoskeleton. Many integrin signals converge on cell cycle regulation, directing cells to survive or die, proliferate, or exit the cell cycle and differentiate (Giancotti, 2000; Giancotti & Ruoslahti, 1999; Kampman & McDonald, 1996). Vitronectin receptors (VNRs) comprise a group of integrins sharing a common αv subunit. Based on their β subunit five different VNRs have been described: αvβ1, αvβ3, αvβ5, αvβ6, and αvβ8. VNR and some integrins recognize the Arg-Gly-Asp (RGD) motif present in a variety of ligands such as vitronectin, fibronectin, osteopontin, bone sialoprotein, thrombospondin, fibrinogen, von Willebrand factor, tenascin, and agrin (Converse, 2006; Roberts et al., 1991; Ruoslahti, 2003; Sheppard, 2005). Vitronectin is a multifunctional protein present in blood serum and in the extracellular matrix. Structurally, vitronectin contains an RGD motif that binds integrins, and other binding domains for plasminogen activator inhibitor-1, urokinase receptor, thrombin-antithrombin III complex, collagen, plasminogen, and heparin. It also contains proteolytic cleavage and phosphorylation sites (McKusick, 1989; Schvartz et al., 1999). Vitronectin promotes diverse biological functions such as cell adhesion, spreading and migration, fibrinolysis, cell proliferation, etc (Figure 1.10). Its deposition has been detected in areas of fibrosis and necrosis in different diseases (Seiffert, 1997). Following the observations by Boylan et al. additional studies have reported the involvement of the VNR and RGD motif in crocidolite internalization and toxicity (Boylan, Sanan et al., 1995; W. Liu et al., 2000; Pande et al., 2006; Wu, Liu et al., 2000).

In studies performed in endothelial cells, an increase in the release of PGI_2 (Prostacyclin) has been reported after asbestos exposure (Garcia, Dodson et al., 1989; Garcia, Gray et al., 1988). Prostacyclin is a product of arachidonic acid metabolism

(Figure 1.11) and is well established as a potent vasodilator and inhibitor of platelet aggregation in contrast to the Thromboxane effect (Helliwell et al., 2004; McKusick, 2001). Due to this effect, it has been suggested that changes in the homeostasis between prostacyclin and thromboxane could lead to endothelial damage, a component for the development of ILD. Due to the lack of studies attempting to elucidate the role of lung epithelial cells in the generation of asbestos induced ILD, we propose the following general hypothesis: “Lung epithelial cells have the ability to respond when exposed to asbestos.” The results of these studies examining the roles of VNR and prostacyclin in epithelial response to crocidolite asbestos are detailed in Chapter 2.

Silica

Silicosis and asbestosis, which share similar clinical findings, have been classified as occupational diseases. Both are caused by the inhalation of silicates (silicon dioxide, SiO_2), which leads to a severe lung inflammation, accompanied by destruction of lung tissue, development of ILD, and death. Silicosis is induced by the inhalation of free crystalline silica (tectosilicate). The crystalline forms include cristobalite, tridymite and quartz. All of them can produce ILD (Kelley, 1998). Silica exposure occurs more frequently in granite quarrying and processing, crushed stone industries, foundries, ceramics industry, and in construction and sandblasting operations (Table 1.4). Unlike many other inhalation diseases, silicosis and asbestosis are diseases that progress even after exposure has ceased (R. S. Fraser, Colman et al., 2005). In the U.S. between 1979 and 1992, 4882 death certificates listed silicosis as the cause of death. In European countries the silicosis mortality ranged from 0.91 to 7.36 per 100,000 men (Wagner, 1997). This broad ranged was due to differences in degree of exposure, occupations, and mortality reports among different countries. Silica particles, after reaching the alveoli, are phagocytized by the resident alveolar macrophages (AM). Macrophages containing silica undergo apoptosis releasing the particles that will be taken up by other AM. This permanent cycle of phagocytosis-apoptosis contributes to the induction of ILD (Wang et al., 2003; Wang et al., 2005).

Macrophage cell membrane receptors can recognize a broad range of endogenous and exogenous ligands. The macrophage scavenger receptor A (SR-A) is a pattern recognition receptor able to interact with polyanionic ligands with different levels of

affinity (Gordon, 2002). SR-A was initially described as a binding site on macrophages mediating the uptake and degradation of acetylated low density lipoprotein (AcLDL) (Goldstein et al., 1979). It has been reported that SR-A has an important role in the process of silica-induced apoptosis but the mechanism is still unknown (Chao et al., 2001; R. F. Hamilton et al., 2000; R. F. Hamilton et al., 1996; Iyer et al., 1996). SR-A has the ability to bind different kind of ligands such as modified LDL, silica, asbestos, LPS, etc; and also has an important role in cell adhesion (I. Fraser et al., 1993; Peiser & Gordon, 2001; Platt & Gordon, 2001) (Table 1.5). SR-AI, SR-AII, and SR-AIII are three alternative splice variants of the scavenger receptor A gene. SR-AIII is not functional and stays in the endoplasmic reticulum (Gough et al., 1998). Structurally SR-A is a trimeric transmembrane protein with an N-terminus cytoplasmic region and a glycosylated fibrous coiled extracellular region. SR-A contains five domains: 1) cytoplasmic, 2) transmembrane, 3) spacer, 4) α-helical coiled-coiled, and 5) collagenous. SR-AI contains an additional 6^{th} domain called cysteine-rich (Kodama et al., 1990) (Figure 1.12). The role of the cytoplasmic domain in receptor surface expression and modified LDL internalization has been already described by Morimoto et al. and Kosswig et al. (Kosswig et al., 2003; Morimoto et al., 1999). The cytoplasmic region in the human, rabbit, bovine, dog and mouse contains between 50 to 55 amino acids, with a consensus of more than 40% amino acids. The mouse sequence of SRA-II contains twelve amino acids that could be phosphorylated (Ser and Thr). Four of these amino acids are common in the SR-A sequence of five species (Figure 1.13). These amino acids correspond to Ser25, Ser32, Ser53, and Thr34 in the SR-A mouse sequence. Based on this information, it is possible that these four amino acids play an important role in the SR-A signaling.

Currently, it is unknown how SR-A initiates its intracellular signaling. In one study heat shock proteins 90 (HSP90), HSP70 and GAPDH were found to interact with a synthetic peptide containing the sequence of the cytoplasmic domain of SR-A (T. Nakamura et al., 2002), but it was not possible to conclude that these proteins bind SR-A after activation. In another study, where AcLDL was used to activate SR-A, it was found that the cytoplasmic tyrosine kinase Lyn interacts with SR-A (Miki et al., 1996). Unfortunately, it is not possible to conclude that SR-A responds to silica in the same way as to AcLDL. Most of the research studies in SR-A and macrophages were done using modified LDL and measuring binding and uptake of these lipoproteins, with no reported studies on the cellular mechanism of silica-induced apoptosis in macrophages.

A highly conserved lysine cluster is found in the extracellular collagenous domain of SR-A corresponding to human, murine, rabbit, bovine, and dog when they are aligned (Figure 1.14). It has been proposed that this structure forms a positively charged groove that interacts with negatively charged ligands such as modified LDL (Yamamoto et al., 1997) and crocidolite asbestos (Resnick et al., 1993). Doi et al and Andersson et al independently mutated these lysines in bovine SR-AI and rabbit SR-AII respectively reporting a remarkable reduction in AcLDL binding and degradation (Andersson & Freeman, 1998; Doi et al., 1993). An interesting finding reported in both papers was that when binding experiments were performed at 4°C, the SR-A lacking the lysines was still able to bind AcLDL.

Levels of expression of each SR-A splicing variant have been studied. Geng et al reported similar levels of SR-AI and SR-AII mRNA in human circulating monocytes, however when monocytes were differentiated into macrophages or macrophage-derived

foam cells, a selective increase in SR-AI mRNA levels was found (Geng et al., 1994). Dufva et al reported, using monocyte derived macrophages, greater down-regulation of SR-AII mRNA after LPS exposure, and in the presence of cycloheximide, selective degradation of SR-AI mRNA (Dufva et al., 1995). A third study performed by Kim et al with peritoneal macrophages (PMs) found no SR-A protein in freshly isolated PMs and minimal AcLDL uptake. However, when PMs were cultured in vitro for 3 days, expression of SR-A protein and AcLDL uptake were considerably increased. Due to the lack of differences in SR-A mRNA levels between the fresh and 3-days cultured PMs, it was concluded that SR-A expression is post-transcriptionally regulated (Kim et al., 1997).

As mentioned above, the key difference between SR-AI and SR-AII is that SR-AI contains a cysteine rich domain also known as scavenger receptor cysteine rich domain (SRCR). Because previous studies comparing SR-AI and SR-AII binding properties including the mutated lysines were performed using modified LDL as ligands, the general affirmation that SR-AI and SR-AII bind the same ligands is limited only to modified LDL. Ashkenas et al in 1993 reported no difference in polyanion binding specificity between SR-AI and SR-AII, but in an experiment using ReLPS as a competitive inhibitor, SR-AII transfected cells showed almost a complete inhibition of AcLDL degradation in comparison with SR-AI transfected cells (Ashkenas et al., 1993). In addition, Resnick et al reported that bovine SR-AI binds crocidolite asbestos more efficiently than bovine SR-AII (Resnick, Freedman et al., 1993). One explanation for these two findings is that the SCRC domain of SR-AI is functional and able to interact with ReLPS and Crocidolite asbestos. Moreover, another SR-A receptor called MARCO,

also has a SRCR domain, which is functional and very important for its ligand-binding function (Chen et al., 2006).

Since there are no studies evaluating the role of the SR-A cytoplasmic domain in silica-induced apoptosis or comparing binding properties between SR-AI and SR-AII using silica as particulate ligands, the following general hypothesis was generated: “Silica binding to SR-A results in an induction of apoptosis mediated by a signal transduction mechanism beginning at specific cytoplasmic domains, and the presence of the SCRC domain in SR-AI increases the binding efficiency of silica.” This study is presented in Chapter 3.

Table 1.1
Clinical Classification of Interstitial Lung Disease (ILD)(Toews, 2000)

Primary Lung Diseases
- Idiopatic pulmonary fibrosis
- Sarcoidosis
- Bronchiolitis obliterans with organizing pneumonia
- Lymphocytic interstitial pneumonia
- Histiocytosis X
- Lymphangioleiomyomatosis

ILD Associated with Systemic Rheumatic Disorder
- Rheumatoid arthritis
- Systemic lupus erythematous
- Polymyositis-dermatomyositis
- Sjogren's syndrome
- Mixed connective tissue disease
- Ankylosing spondylitis

ILD Associated with Drug or Treatments
- Antibiotics
- Anti-inflammatory agents
- Cardiovascular drugs
- Antineoplastic agents
- Illicit drugs
- Dietary supplements
- Oxygen
- Radiation
- Paraquat

Environment/Occupation-Associated ILD
- Organic dust/hypersensitivity pneumonitis (>40 known agents)
  - Farmer's lung
  - Air conditioner-humidifier lung
  - Bird breeder's lung
  - Bagassosis
- Inorganic dusts
  - Silicates
    - Silicosis
    - Asbestosis
  - Coal workers' pneumoconiosis
  - Berylliosis
- Gases/fumes/vapors
  - Oxides of nitrogen
  - Sulfur dioxide
  - Toluene diisocyanate
  - Oxides of metals
  - Hydrocarbons
  - Thermosetting resins

Alveolar Filling Disorders
- Diffuse alveolar hemorrhage
- Goodpasture's syndrome
- Idiopathic pulmonary hemosiderosis
- Pulmonary alveolar proteinosis
- Chronic eosinophilic pneumonia

ILD Associated with Pulmonary Vasculitis
- Wegener's granulomatosis
- Churg-Strauss syndrome
- Hypersensitivity vasculitis
- Necrotizing sarcoid granulomatosis

Inherited Disorders
- Familial idiopathic pulmonary fibrosis
- Neurofibromatosis
- Tuberous sclerosis
- Gaucher's disease
- Niemann-Pick disease
- Hermansky-Pudlak syndrome

Table 1.2

Principal Pneumoconioses Caused by Mineral Dust (Samet, 2000)

AGENT	DISEASE
Asbestos	Asbestosis
Coal dust	Coal workers' pneumoconiosis
Cobalt	Hard metal disease
Silica	Silicosis
Talc	Talcosis

Table 1.3

Silicate Subclasses (Covey, 2006; Whitehead, 2001)

Silicate subclass	Arrangement	Formula	Common Minerals
- Nesosilicates	Single tetrahedron	$(SiO_4)^{4-}$	Olivine Garnet Kyanite Sillimanite Andalusite Staurolite
- Sorosilicates	Double tetrahedral	$(Si_2O_7)^{6-}$	Epidote
- Inosilicates			
	Single chain	$(Si_nO_{3n})^{2n-}$	Pyroxene
	Double chain	$(Si_{4n}O_{11n})^{6n-}$	Amphibole
- Cyclosilicates	Rings	$(Si_nO_{3n})^{2n-}$	Tourmaline Beryl
- Phyllosilicates	Sheets	$(Si_{2n}O_{5n})^{2n-}$	Illite Chlorite Serpentine Kaolinite Talc Vermiculite
- Tectosilicates	3D frameworks	$(Al_xSi_yO_{2(x+y)})^{x-}$	Quartz Feldspars Zeolites

Table 1.4

Occupations and Industries Associated with Silicosis (Wagner, 1997)

Occupations	Industries
Mining-machine operators	Coal-mining
Laborers	Construction
Managers and administrators	Metal-mining
Supervisors, precision production occupations	Blast furnaces, steelworks, rolling and
Janitors and cleaners	finishing mills
Operators of molding and casting machines	Non-metallic mining and quarrying
Supervisors and proprietors, sales occupations	Iron and steel foundries
Operating engineers	Structural clay products
Machinists	
Hand-molding, casting, and forming occupations	

Table 1.5

Macrophage Scavenger Receptor A Ligands (Peiser & Gordon, 2001; Platt & Gordon, 2001)

Ligand	*Non-ligand*
Oxidized low density lipoprotein	Native low density lipoprotein
Acetylated low density lipoprotein	Native high density lipoprotein
Oxidized high density lipoprotein	Bovine serum albumin
Maleylated bovine serum albumin	Heparin
Malondialdehyde bovine serum albumin	Chondroitin sulfate
Fucoidan	Polycytidylic acid
Dextran sulfate	Polyadenylic acid
Polyguanylic acid	Phosphatidylserine
Polyinosinic acid	Phosphatidylcholine
Crocidolite asbestos	
Silica	
Lipopolysaccharide	
Lipoteichoic acid	
Gram negative bacteria	
Gram positive bacteria	
Apoptotic cells	
AGE-modified proteins	
β-amyloid	

Figure 1.1

The Airway Tree (Weibel, 1963)

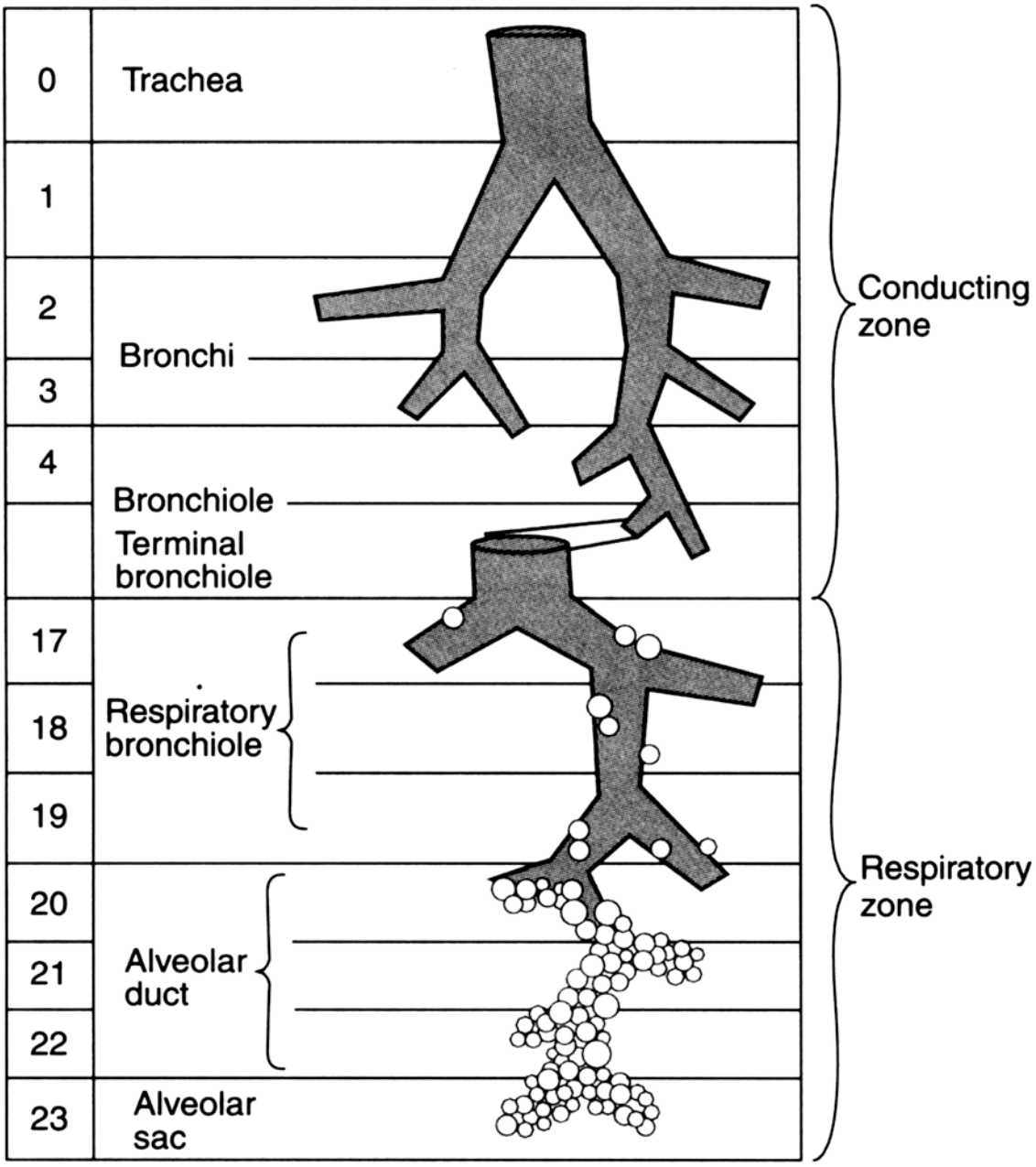

Figure 1.2

Cellular Structure of Airways (Burri & Weibel, 1973)

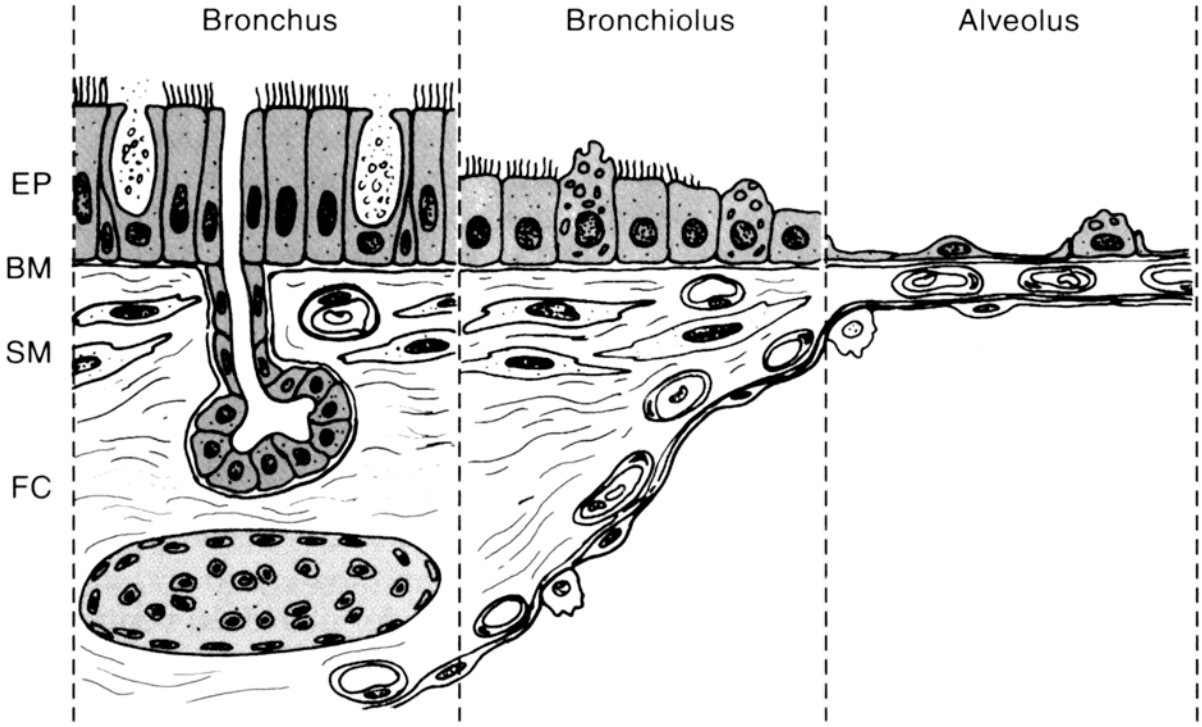

EP, epithelium; BM, basement membrane; SM, smooth muscle; FC, fibrous coat and connective tissue.

Figure 1.3

A. Crocidolite asbestos fibers and B. Cristobalite silica (Mossman & Churg, 1998)

A

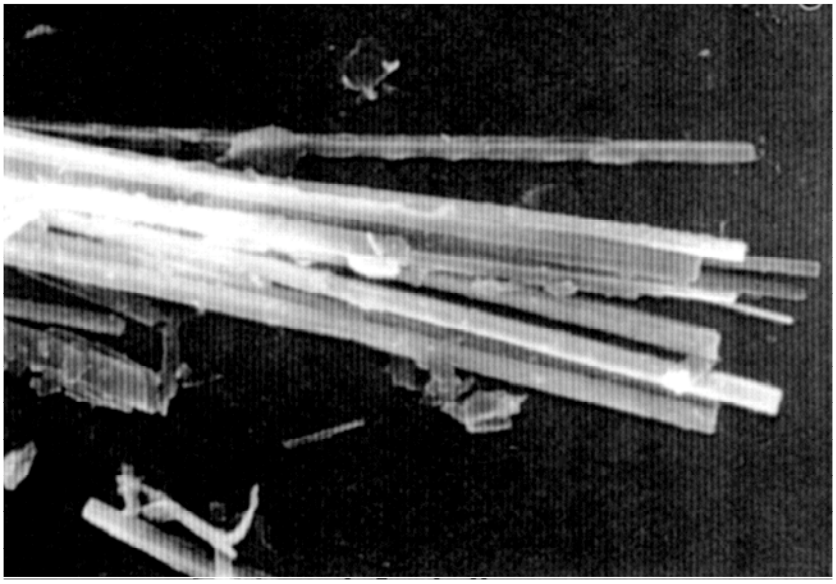

B

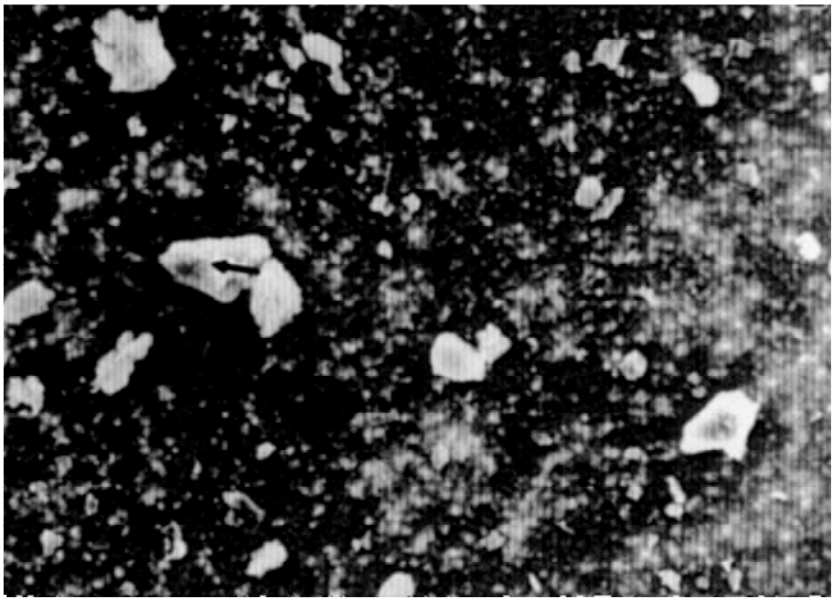

Figure 1.4

Primary Mechanisms of Deposition of Inhaled Particles in the Respiratory Tract (McClellan, 1999)

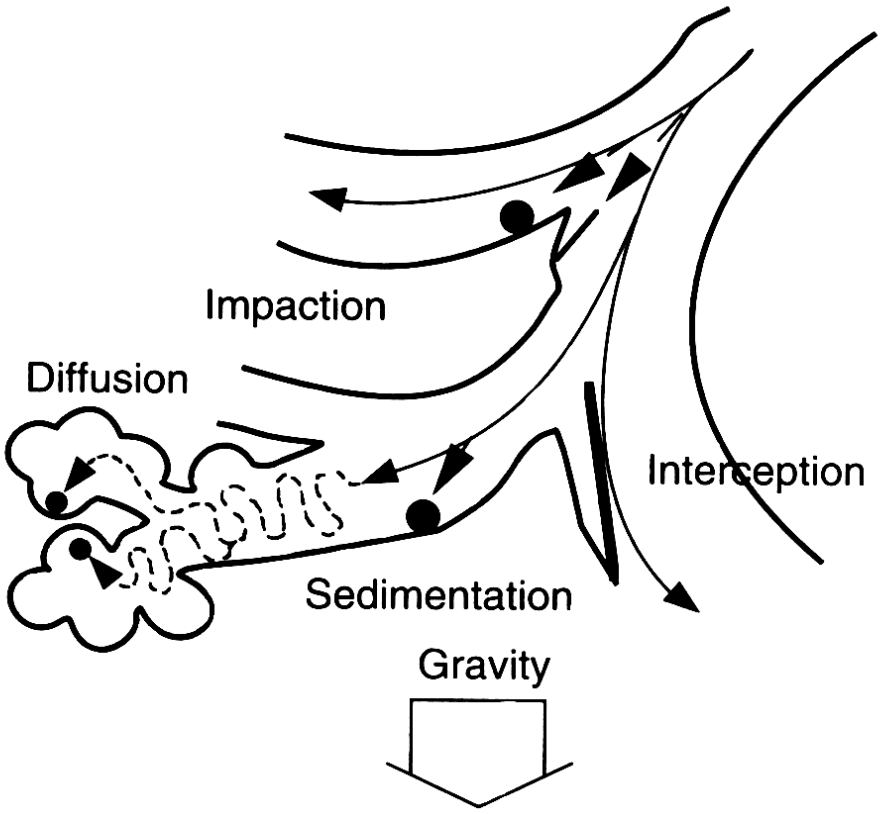

Figure 1.5

Fractional Deposition of Inhaled Particles Related to Aerodynamic Particle Diameter (McClellan & Miller, 1997)

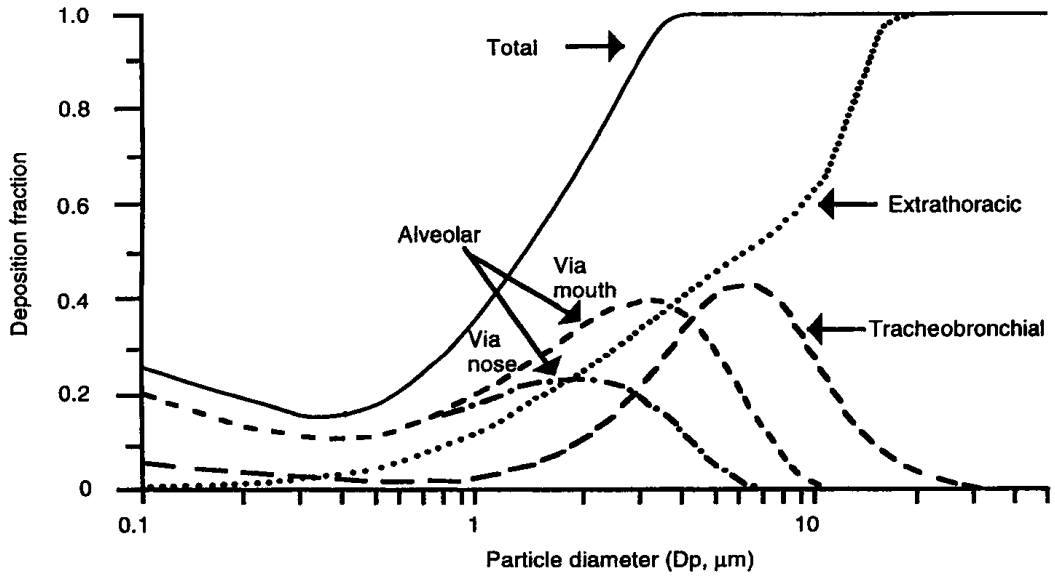

Figure 1.6

Original and New Hypothesis for the Pathogenesis of ILD (Gross & Hunninghake, 2001)

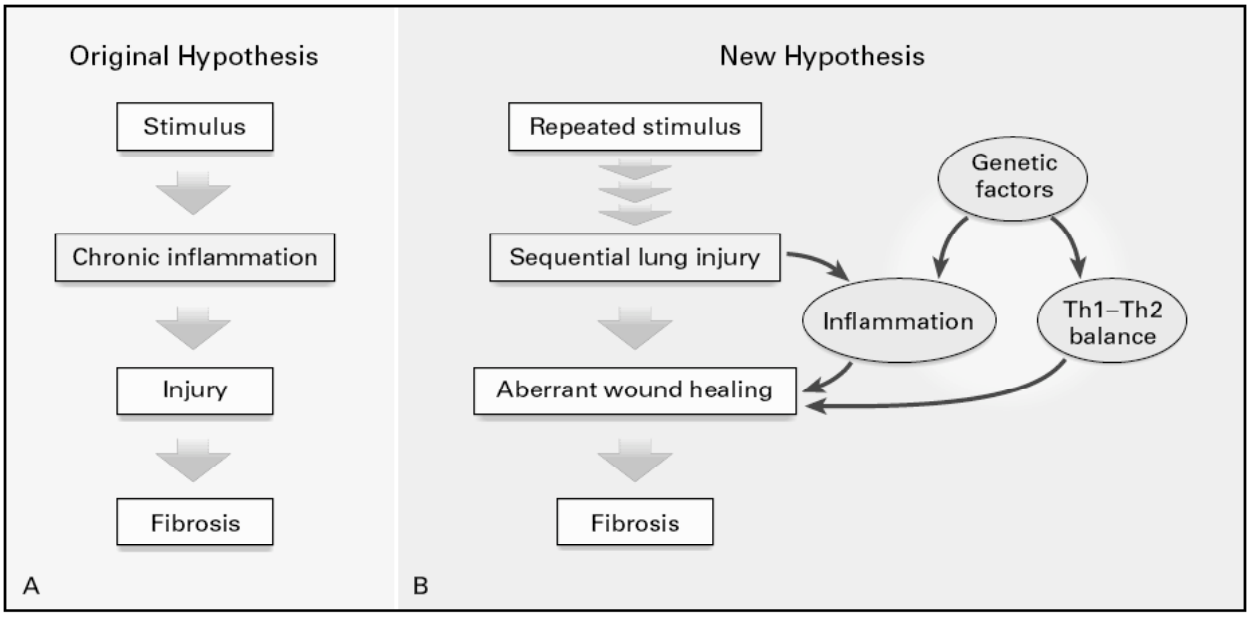

Figure 1.7

The Process Involved in the Development of ILD (Peterson & Schwartz, 1999)

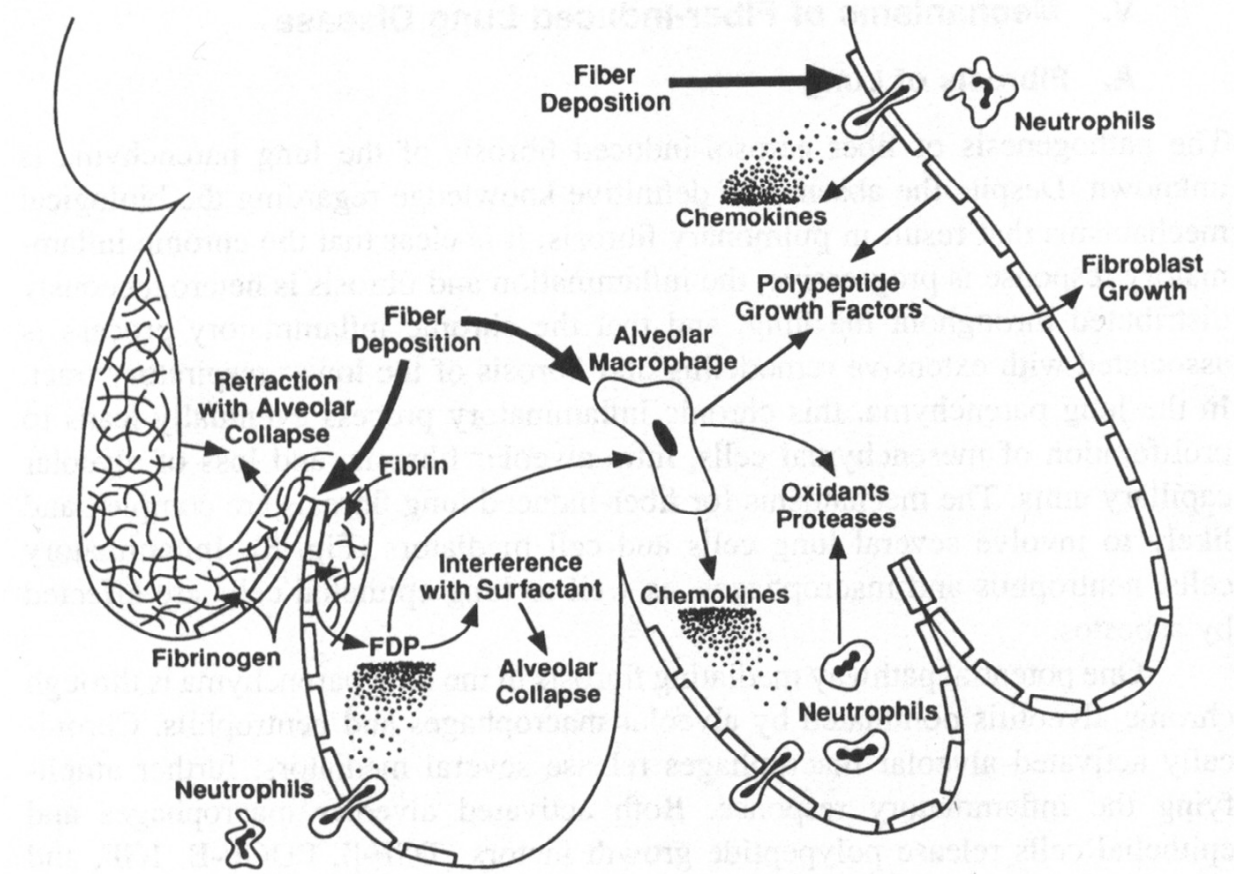

Figure 1.8

Schematic picture of the crystal structure of the asbestos class (A) serpentine, and (B) Amphibole (Ottaviani et al., 2001)

A

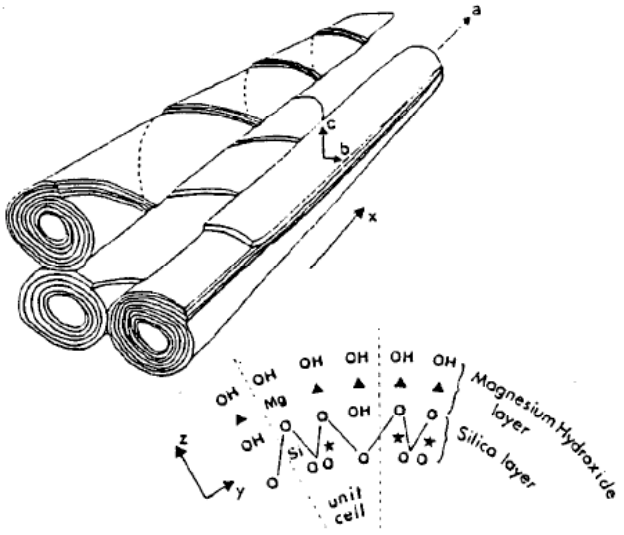

B

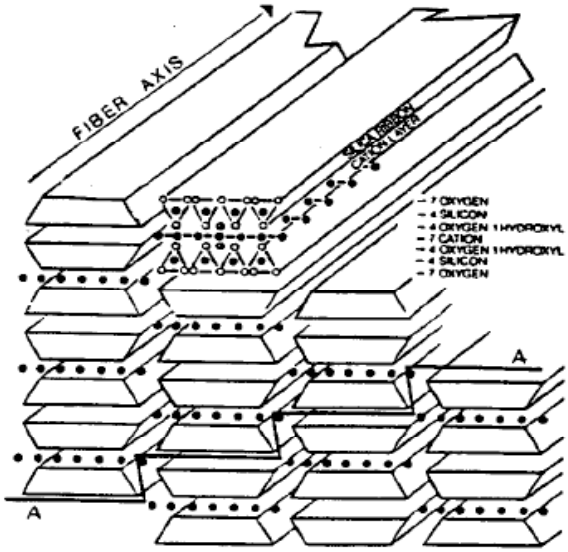

Figure 1.9

Mechanisms of Asbestos Induced Pulmonary Toxicity (Kamp & Weitzman, 1999)

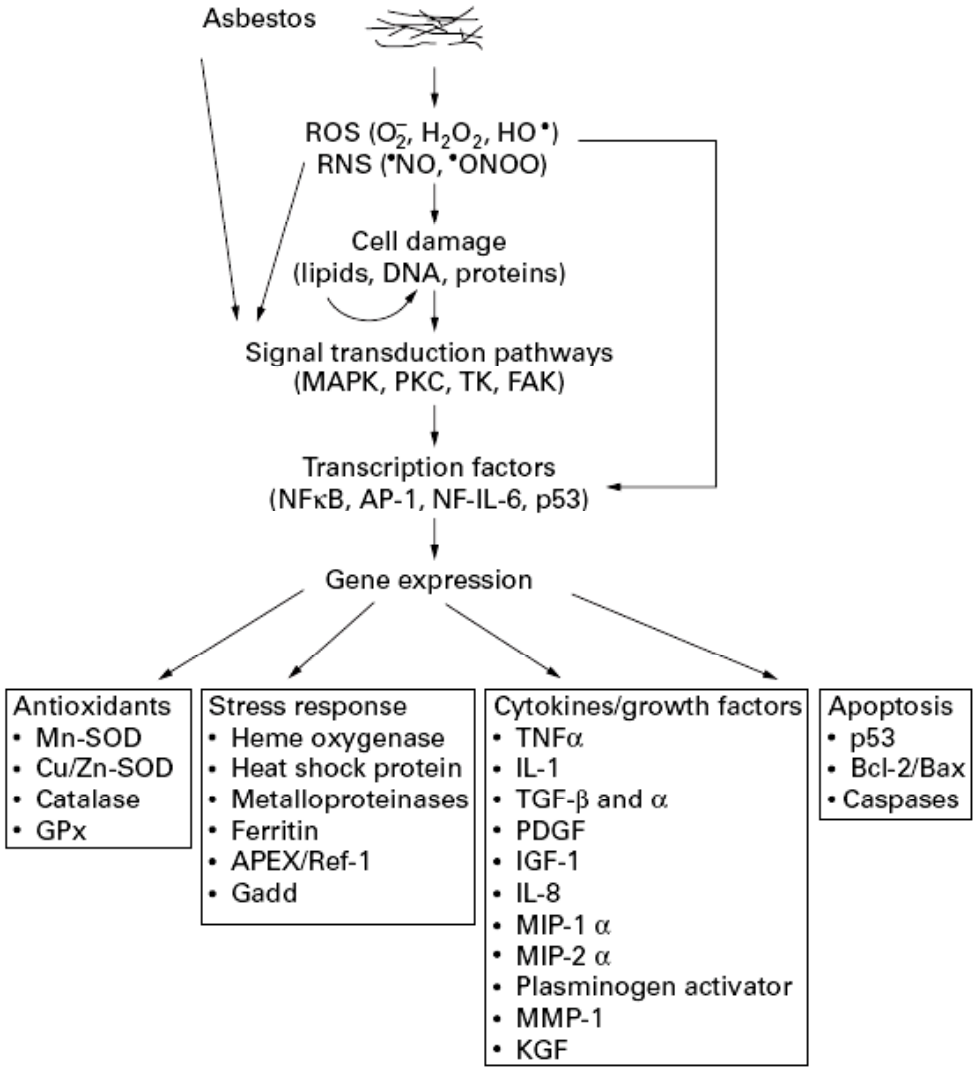

Figure 1.10

Major Biological Functions in which Vitronectin has been Implicated (Schvartz, Seger et al., 1999)

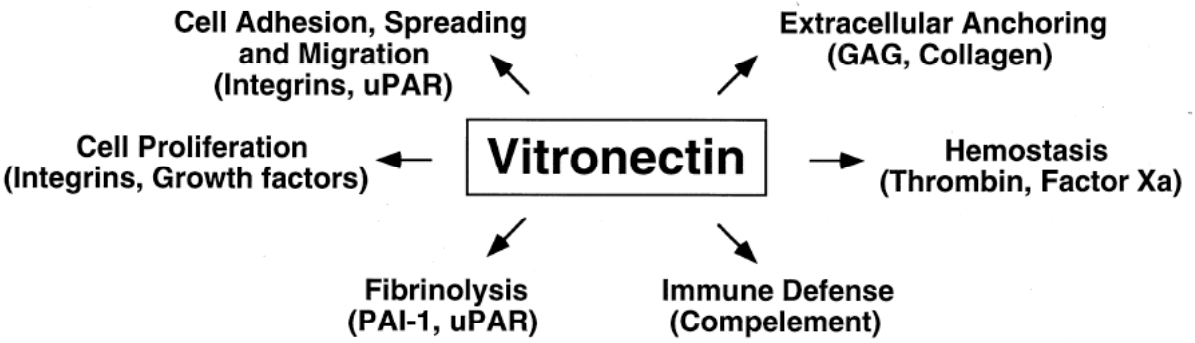

GAG: glycosaminoglycan binding domain
UPAR: urokinase receptor
PAI-1: plasminogen activator inhibitor-1

Figure 1.11

Prostacyclin Biosynthetic Pathway

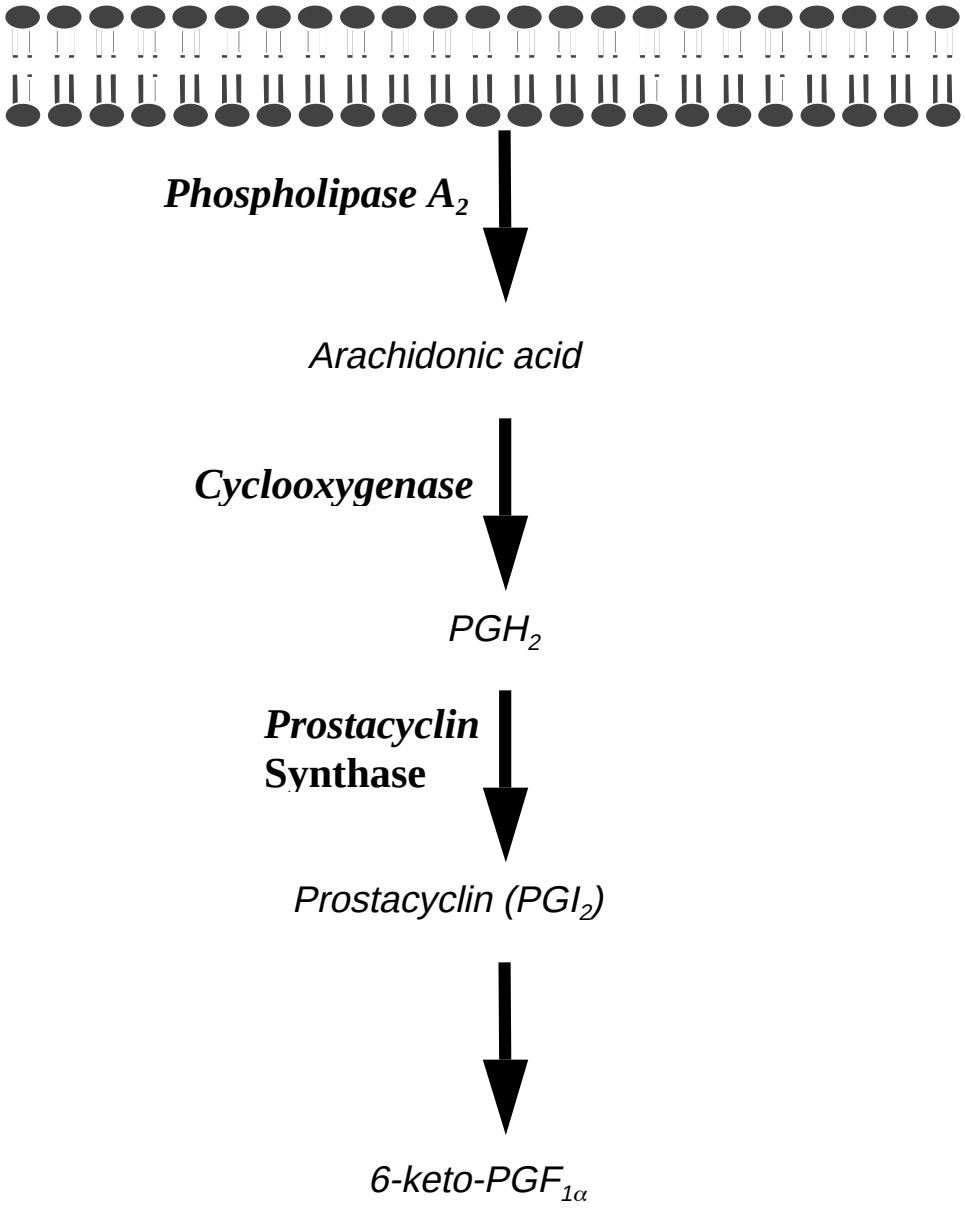

Figure 1.12

Domains of Human Macrophage Scavenger Receptor A type I and II (Platt & Gordon, 2001)

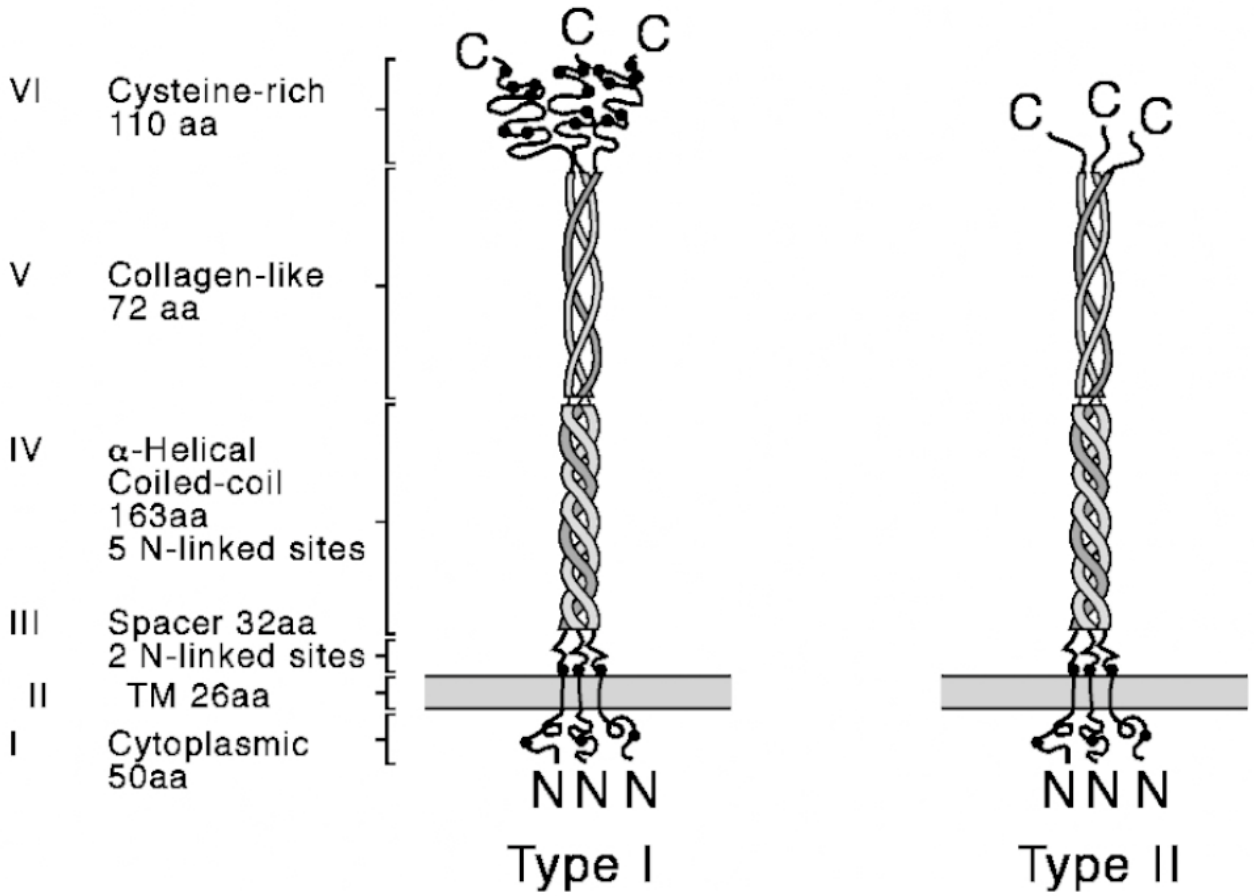

Figure 1.13

Protein Alignment of the SRA Cytoplasmic Domain Among Different Species.

Figure 1.14

Protein Alignment of the SRA Lysine Cluster Among Different Species.

Chapter 2

The Biological Response of Lung Epithelial Cells to Asbestos

Asbestosis is the ILD elicited by the inhalation of asbestos fibers. ILD are a large and heterogeneous group of lower respiratory tract disorders. ILD is also known as “Interstitial pulmonary fibrosis” or “Diffuse parenchymal lung disease. The cause of most ILDs is unknown. It has been suggested that certain agents (e.g. asbestos, beryllium) cause repeated episodes of lung injury. The damaged alveolar epithelium subsequently induces accumulation and activation of inflammatory cells, which is coincident with the migration and proliferation of fibroblasts and extracellular matrix deposition in the alveolar interstitium leading to fibrosis and loss of lung function (Clement, Henrion-Caude et al., 2004; Gross & Hunninghake, 2001).

A number of studies have shown that asbestos is cytotoxic for epithelial/endothelial cells. Different mechanisms have been described to be involved in the development of asbestos-induced pulmonary disease such as DNA damage, signaling mechanisms, gene transcription and protein expression, mutagenicity, cell death/apoptosis and inflammation (Kamp, Graceffa et al., 1992; Mossman, Bignon et al., 1990; Mossman & Churg, 1998; Mossman, Kamp et al., 1996; Rom, Travis et al., 1991). It has been postulated that asbestos-induced pathogenesis derives from an interplay between persistent free radical production and expression of cytokines, growth factors, and inflammatory cell products (Kamp & Weitzman, 1999). In addition, since the

epithelial layer of the lung has a barrier function and serves as a likely sentinel following asbestos inhalation, its chronic cell injury will compromise its protective function and promote the development of ILD.

Coating crocidolite asbestos with vitronectin enhances its internalization via the alpha V integrin VNR αvβ5 in mesothelial cells (Boylan, Sanan et al., 1995). VNRs, and many other members of the integrin family such as α4β1, α5β1, α8β1, and αIIbvβ3 recognize the Arg-Gly-Asp (RGD) motif (Takagi, 2004) present in a variety of ligands such as vitronectin, fibronectin, osteopontin, bone sialoprotein, thrombospondin, fibrinogen, von Willebrand factor, tenascin, and agrin (Converse, 2006; Roberts, Yokoyama et al., 1991; Ruoslahti, 2003; Sheppard, 2005). Additional studies have reported the involvement of VNR and RGD motif in crocidolite internalization and toxicity (W. Liu, Ernst et al., 2000; Pande, Mosleh et al., 2006; Wu, Liu et al., 2000). Besides, in endothelial cells, an increase in the release of Prostacyclin has been reported after asbestos exposure (Garcia, Dodson et al., 1989; Garcia, Gray et al., 1988). It has been suggested that changes in the prostacyclin homeostasis could lead to endothelial damage, a component for the development of ILD. Due to the lack of understanding of the lung epithelial cell response to asbestos exposure and in the development of asbestos induced ILD, and to determine VNR and/or prostacyclin involvement, this study was performed in order to answer the following hypothesis.

Hypothesis

Lung epithelial cells interact with asbestos via vitronectin receptor resulting in cellular toxicity and the initiation of an inflammatory response.

Aims

I. Develop a cell model to study asbestos-induced lung toxicity.

II. Evaluate the ability of asbestos to induce the inflammatory mediator PGI_2 (Prostacyclin).

III. Evaluate the role of Vitronectin receptor in asbestos-induced response.

Aim I. Develop a cell model to study asbestos-induced lung toxicity

This aim focused on the downstream consequences of lung epithelial cells exposed to asbestos. Numerous studies have been performed evaluating different cells in asbestos-induced response. Mesothelial cells are the most studied due to the relationship between asbestos exposure and mesothelioma, a malignant pleural disease. Studies not performed with mesothelial cells, had used primary (alveolar macrophages or neutrophils) or immortalized cell lines (A549, WI-26, BEAS 2B, MET 5A, or HTE), both obtained from different sources such as human, rat, and hamster (Kamp et al., 1994; Kamp et al., 1998; Kinnula et al., 1995; Mossman, Surinrut et al., 1996; Tsuda et al., 1999). In a PubMed search performed on April 2007, the terms “asbestos AND epithelium AND murine” were used. Results showed 30 studies, most of them in-vivo experiments or in mesothelial cells. It was not possible to find a study evaluating murine lung epithelial cell line and asbestos exposure. In order to find an appropriate murine epithelial cell line to perform crocidolite studies, this aim will compare immortalized lung epithelial cells lines in order to determine which one is a better model for the study of asbestos-induced responses. Initially two cell lines were selected due to laboratory availability.

Methods

Cell Lines

Two epithelial cell lines were used:

1) LA-4 cells: lung adenoma clone 4, derived from A/He mouse. Tumor was induced by urethane exposure, and characterized as alveolar type II cell-like (Stoner et al., 1975). Cell cultures were maintained in Ham's F12K medium (Mediatech, Inc., Herdon, VA) supplemented with 2 mM L-glutamine adjusted to contain 100 units/ml of penicillin, 100 µg/ml streptomycin, 0.25 µg/ml amphotericin B (Mediatech, Inc.), and 15% fetal bovine serum (Hyclone, Logan, UT).
2) CMT 64/67 cells: Spontaneous tumor in a C57BL/lcrf-at mouse, characterized as papillary adenocarcinoma of the lung (Franks et al., 1976). Cells cultures were maintained in RPMI 1640 medium (Mediatech, Inc.) adjusted to contain 1.0 mM sodium pyruvate, 0.05 mM 2-mercaptoethanol, 100 units/ml of penicillin, 100 µg/ml streptomycin, 0.25 µg/ml amphotericin B (Mediatech, Inc.), and 10% fetal bovine serum (Hyclone).

Cell cultures were incubated at a temperature of 37ºC in an atmosphere of 95% air and 5% CO_2 (ThermoForma, Mariette, OH).

Asbestos Exposure

All asbestos exposure experiments were performed using the amphibole crocidolite, which was chosen due to its high toxicity in human studies (Enterline & Henderson, 1973; Faust, 1995). Adherent LA-4 or CMT 64/67 cells were trypsinized with 2-3 ml of Trypsin/EDTA (Mediatech Inc.), counted using a Z1 Coulter Particle Counter (Beckman Coulter, Hialeah, FL), and plated 24 hours prior to exposure at 50,000 cells in a volume of 200 µl of media per well in a 96-well plate. Cell culture media was changed at exposure time. Crocidolite stock suspension (10 mg/ml) was freshly made by

mixing crocidolite obtained from Research Triangle Institute (Research Triangle Park, NC) with sterile water. The suspension was sonicated using a Sonicator Ultrasonic processor XL (Misonix, Franingdale, NY) for one minute, mixed with fresh cell culture media and added to the 96-well plate. Cells were exposed to crocidolite for 24 hours before performing any assessment unless indicated.

Cell Cytotoxicity Assays

Viability Assay: This colorimetric assay correlates with the number of viable cells in proliferation. The conversion of MTS tetrazolium into aqueous soluble formazan is accomplished by metabolically active cells. After exposure at doses described in results, a volume of 100 µl of media was removed leaving 100 µl of media in each well. Twenty µl of CellTiter96 AQueous One Solution Reagent from Promega (Madison, WI) was added into each well and incubated for 1-4 hours at 37ºC in a humidified 5% CO_2 atmosphere. Optical density (OD) was measured using a microplate reader (Molecular Devices, Sunnyvale, CA) at a wavelength of 490 and for reference at 650 nm. For normalizing, each control group (non-exposed) was considered to have 100% viability.

Cytotoxicity Assay: LDH (lactate dehydrogenase) is an enzyme, which is abundant in the cytosol. Its release correlates with loss of membrane integrity and cell death. LDH was measured using the Cytotoxicity Detection Assay (LDH) (Roche Applied Science, Indianapolis, IN), which contains a substrate that changes color in the presence of LDH. Cells were plated 24 hours before exposure as previously described. At exposure time, cell culture media was replaced with 1% FBS in order to decrease the LDH background absorbance, as recommended by manufacturer. Triton X-100 (Sigma-Aldrich Inc., St

Louis, MO) at 1% was used as a positive control. After exposure 100 µl of cell culture media was transferred to a 96-well plate, mixed with 100 µl of reaction mixture, and incubated for 30 minutes at room temperature and protected from light. OD was measured at a wavelength of 492 and 650 nm. Cytotoxicity was calculated as a percentage between minimum or 0% (non-exposed) and maximum or 100% (Triton X-100) control values.

Statistical analysis

Experiments were repeated at least three times. Results were presented as the mean and standard error of the mean (SEM) unless indicated. When required data was normalized with its respective control in order to exclude differences in background conditions such as presence of different culture media, chemical inhibitors, peptides, bronchoalveolar lavaged fluid (BALF), and blocking antibodies. Data was analyzed using student T test for independent variables, or nonparametric statistics methods as required such as Mann-Whitney U test when comparing two groups, and Kruskal-Wallis test when comparing three groups or more. Statistical analyses were performed using the software GB-Stat version 6.5.6 (Dynamic Microsystems, Inc., Silver spring, MD). Alpha error was set at $p<0.05$.

Results

In order to determine if crocidolite could induce toxicity in LA-4 and CMT 64/61 cells, a viability assay was performed using increasing doses of crocidolite. Three doses of crocidolite were used: 5, 10, and 20 $\mu g/cm^2$ and Triton X-100 (1%) for positive

control. Only LA-4 cells showed a decrease in viability following a dose response mode (Figure 2.1). In order to confirm these results, cytotoxicity assay was performed using the crocidolite dose of 20 $\mu g/cm^2$. The results showed an increase in LDH release in the exposed group, confirming the results of the viability assay (Figure 2.2). On the other hand CMT 64/61 cells were resistant to asbestos-induced toxicity at all doses used (Figure 2.1). Only LA-4 cells were cytotoxic to crocidolite, consequently crocidolite exposure experiments in Aims II and III were performed only on LA-4 cells.

Aim II. Evaluate the ability of asbestos to induce the inflammatory mediator PGI_2 (Prostacyclin)

Asbestos is known to induce lung inflammation that progresses to fibrosis. Prostacyclin release is an indicator of asbestos–induced cell activation and inflammation. Prostacyclin has diverse effects in different cells. Previous studies in fibroblast showed that exposure to prostacyclin analogues significantly inhibited contraction of extracellular matrix (Kamio et al., 2007), in colonic epithelial cells exposed to butyrate, an apoptosis inducer, prostacyclin confers an antiapoptotic effect (Cutler et al., 2003), and in macrophages prostacyclin regulates phagocytosis, bacterial killing, and cytokine generation (Aronoff et al., 2007). All these findings show the ability of prostacyclin to interact with the different cells involved in the development of ILD. In murine lung epithelial cells, the asbestos-induced prostacyclin induction has not been previously described. Therefore, this aim will determine if prostacyclin release is induced in lung epithelial cells after asbestos exposure.

Methods

6-keto Prostaglandin $F_{1\alpha}$ Detection Assay

Prostacyclin is non-enzymatically hydrated to 6-keto $PGF_{1\alpha}$, which is a more stable metabolite. In order to detect prostacyclin, experiments were directed to measure 6-keto $PGF_{1\alpha}$ as an indicator of prostacyclin production. Cells were plated at 40,000 - 50,000 cells/well in a 96-well plate. After twenty-four hours crocidolite exposure at doses

described in Results, 6-keto $PGF_{1\alpha}$ was detected using an ACE™ (acetylcholinesterase) competitive enzyme immunoassay (Cayman Chemical, Ann Arbor, MI) according to manufacturer instructions. For each condition, 50 µl of cell culture media were transferred to a pre-coated 96-well plate (mouse monoclonal anti rabbit IgG), mixed with 6-keto $PGF_{1\alpha}$ tracer and antiserum (rabbit antiserum 6-keto $PGF_{1\alpha}$) and incubated for 18 hours at 4ºC. Plates were developed using Ellman's Reagent for the detection of acetylcholinesterase, and read at a wavelength of 405 nm.

Cyclooxygenase Inhibitors

The COX-1/COX-2 inhibitor Indomethacin, and the COX-2 inhibitor Indomethacin Heptyl Ester were used at doses 10 and 100 times their respective IC_{50} (inhibitory concentration of 50% of the total activity) (Kalgutkar et al., 2000). Inhibitors were added at the same time fresh cell culture media containing crocidolite was added to the cells as previously described in *Aim I.*

Cox 2 real time polymerase chain reaction

Two to four hours after crocidolite exposure (10 µg/cm^2), LA-4 cells were lysed using Trizol reagent (Invitrogen, Carlsbad, CA) and total RNA was isolated following manufacturer's instructions. First strand reverse transcription was performed using RETROscript™ (Ambion Inc., Austin, TX) with oligo dT primers, and amplification was performed using the Platinum® Quantitative PCR SuperMix-UDG (Invitrogen) following manufacturer's recommendations. Real time probes and primers from murine Cox 2 and GAPDH (endogenous control) were obtained from TaqMan® Gene Expression Assays (Applied Biosystems, Foster City, CA). Amplification was run and signals detected using an ABI Prism 7700 Sequence Detection System (Applied

Biosystems). Ct values were recorded for each condition and Cox 2 data was analyzed relative to GAPDH.

Results

As previously described, endothelial cells release prostacyclin when exposed to asbestos. Since epithelial cells produce prostacyclin, it was important to determine if crocidolite induced/augmented prostacyclin production in LA-4 cells. Prostacyclin production through the detection of its metabolite 6-keto $PGF_{1\alpha}$ was approached in LA-4 cells after crocidolite exposure at a final concentration of 10 $\mu g/cm^2$ for 24 hours. A statistically significant increase of prostacyclin metabolite was observed in the exposed group (Figure 2.3). Prostacyclin production requires cyclooxygenase and the specific isomerase prostacyclin synthase as previously described in Figure 1.9. There are two Cox isoforms: Cox 1 (constitutively expressed) and Cox 2 (inducible). It has been shown that prostacyclin biosynthesis is highly but not absolutely Cox 2 dependent (Belton et al., 2000; Caughey et al., 2001). In order to determine which Cox isoform was involved in prostacyclin increase, the Cox inhibitors Indomethacin (a Cox 1 and 2 inhibitor) and Indomethacin heptyl ester (a specific Cox 2 inhibitor) were used. Reduction of prostacyclin biosynthesis by the Cox 2 selective inhibitor Indomethacin heptyl ester (at a dose of 10 times its respective IC_{50}) suggested that asbestos exposure might induce higher activity of Cox 2 (Figure 2.4).

Based of the previous findings using Cox inhibitors, it was necessary to determine if asbestos was inducing the expression of Cox 2 mRNA in LA-4 cells. Cox 2 mRNA was quantified using real time PCR. LA-4 cells were plated and exposed as previously

described and lysed 2 and 4 hours after crocidolite exposure. LA-4 cell expression of Cox 2 mRNA increased more than 5 fold two hours after exposure to asbestos then returning to its basal level 4 hours post exposure (Figure 2.5), suggesting a transitory increase. Further studies to determine increases in protein expression of Cox 2 and prostacyclin synthase by WB, and phospholipase A_2 activity due to crocidolite exposure did not work (data not shown), because the total amount of protein recovery in the cell lysate from the crocidolite exposed groups were very low in comparison with the non-exposed groups presumably due to the adsorption of proteins by crocidolite.

In order to determine if Cox 1/2 and prostacyclin contributed to asbestos-induced cytotoxicity, cells were treated with Cox inhibitors at increasing doses before asbestos exposure. Interestingly, after 24 hours of crocidolite exposure, Cox inhibitors did not protect LA-4 cells from asbestos-induced cytotoxicity. All groups, either with or without Cox inhibitors, showed a decrease in viability following a dose response mode with no statistically significant difference when comparing exposed groups without Cox inhibitors with exposed groups that received Cox inhibitors (Figures 2.6 and 2.7). Apparently, indomethacin at a dose of 75 µM showed some cell protection from crocidolite-induced cytotoxicity. But this effect was seen only in one of the three experiments performed. Because Cox inhibitors prevented prostacyclin release and not asbestos-induced cytotoxicity, it is possible to suggest that LA-4 cells have the ability to respond in two different ways after crocidolite exposure: A cytotoxic response, which is Cox independent, and a prostacyclin response, where the induction of Cox 2 appears to be the primary event promoting prostacyclin biosynthesis. The next aim evaluated if these different responses were receptor mediated.

Aim III. Evaluate the role of Vitronectin receptor in asbestos induced response

As previously described, asbestos after being coated with vitronectin, binds mesothelial cells through vitronectin receptor (VNR) (Boylan, Sanan et al., 1995). This aim will determine if asbestos induced-cytotoxicity and induction of Cox 2 and prostacyclin biosynthesis is mediated through lung epithelial cell VNR.

Methods

Vitronectin Receptor Expression

Three hundred thousand LA-4 cells were labeled with fluorescent murine-specific anti-αv antibody (anti-CD51, RMV-7, Armenian hamster IgG, phycoerythrin labeled) purchased from BD PharMingen (San Jose, CA). After 20 minutes incubation at 4ºC, fluorescence was detected on a FACSAria Flow cytometer using FACS Diva software (Becton Dickson, Franklin Lakes, NJ). LA-4 cells with no fluorescent antibody were used as control. In order to exclude dead cells from the analysis, Hoechst 33258 dye (Invitrogen) was added to a final concentration of 1 µg/ml. Cells uptaking the dye were considered dead cells.

Vitronectin Receptor Inhibition

RGDS peptide: The tetrapeptide Arg-Gly-Asp-Ser or RGDS (Sigma-Aldrich, St Louis, MO) was used as a competitive inhibitor of VNR binding, and the Arg-Gly-Glu-Ser or

RGES (Sigma-Aldrich) for non-specific binding control. Peptides were added at a final concentration of 10 and 100 µg/ml simultaneously with crocidolite asbestos exposure as previously described in *Aim 1*.

VNR blocking antibody (RMV-7): The blocking antibody RMV-7 was used to specifically inhibit VNRs. RMV-7 antibody was added at a final concentration of 2 µg/ml one hour before crocidolite exposure as previously described in *Aim 1*.

Bronchoalveolar lavaged fluid (BALF) isolation

BALB/c mice were obtained from our animal facility. Mice 6 to 8 weeks old were used for BALF isolation. All animal procedures were approved by the University of Montana Institutional Animal Care and Use Committee (IACUC). Five female mice were euthanized by a lethal injection of Pentobarbital 0.1 ml of a 0.65% solution. Lungs were surgically removed with the heart and lavaged one time only, in order to prevent dilution of the BALF, with 0.9 ml of cold sterile phosphate buffered saline adjusted to contain 100 units/ml of penicillin, 100 µg/ml streptomycin, 0.25 µg/ml amphotericin B (Mediatech, Inc.). All samples were mixed and centrifuged at 1,500 RPM for 10 minutes. The BALF supernatant was separated and the cell pellet discarded.

Asbestos Exposure

LA-4 cells were trypsinized and plated as previously described in Aim I. At exposure time media was changed to Opti-mem® I reduced serum medium (Mediatech, Inc.), which contains minimal protein levels. Then BALF was added to a final

concentration of 25% and also crocidolite to a final concentration of 10 and 15 μg/cm^2. Cells were incubated for 24 hours before performing any measurement.

Results

Flow cytometry was used to determine if LA-4 cells expressed a vitronectin receptor. Antibodies recognizing the alpha v (αv) subunit revealed expression of this chain on the surface of LA-4 cells. These findings verified that LA-4 cells express the alpha v (αv) subunit, which is the common subunit in all VNR (Figures 2.8 and 2.9). In order to determine if the prostacyclin production was VNR mediated, inhibitors of VNRs such as RGDS peptides and blocking antibodies were used. In the groups exposed to crocidolite (20 μg/cm^2) and treated with either RGDS peptide or VNR blocking antibody a statistically significant decrease in prostacyclin metabolite production was observed confirming VNR involvement in the prostacyclin production (Figures 2.10 and 2.11).

In all previous experiments involving VNR it was assumed that the crocidolite fibers were coated with the ECM proteins present in the fetal bovine serum of the cell culture media. ECM proteins are present in many bodily fluids and since asbestos is typically inhaled it was important to demonstrate similar effects at a physiologically relevant concentration of ECM proteins in the airway/alveolar spaces. The simple way to determine this was by harvesting BALF. LA-4 cells were exposed to crocidolite in the presence of reduced serum media and BALF. LA-4 cells when present in reduced serum media did not produce prostacyclin when exposed to crocidolite (Figure 2.12), however when BALF was added to the reduced serum media, LA-4 cells released prostacyclin when exposed to crocidolite (Figure 2.12). This finding suggests that proteins present in

BALF (and also in fetal bovine serum) are required to induce the production of prostacyclin. When viability was evaluated in the presence of reduced serum, LA-4 cells were protected from crocidolite-induced toxicity, and the addition of BALF did not increase the toxicity (Figure 2.13) suggesting that other factors (e,g, non-RGD ECM proteins) present in the fetal bovine serum, but not in BALF, are required to induce cytotoxicity of LA-4 cells when exposed to crocidolite.

As previously established, the cytotoxic response may be Cox independent. To determine if a protein containing a RGD motif or if VNR were required for asbestos-induced cytotoxicity in LA-4 cells, cell toxicity assays as previously described in Aim I were performed using RGDS peptide and VNR blocking antibody RMV-7. Neither RGDS peptide nor RMV-7 prevented crocidolite-induced cytotoxicity (10 μg/cm^2) of LA-4 cells (Figure 2.14 and 2.15).

Aims III'. Characterize asbestos exposed floating cells

It has been previously reported that asbestos promotes cell detachment of alveolar epithelial cells (Donaldson et al., 1993). In this study, it also was observed by light microscopy that LA-4 cells exposed to asbestos detach forming floating clusters composed of cells binding multiple asbestos fibers. This aim was an attempt to obtain some preliminary data about floating cell viability and the VNR involvement in the formation of these floating clusters.

Methods

Crocidolite Exposure

Cells were plated on a 25 cm^2 flask 24 hours before crocidolite exposure. RMV-7 antibody was added 1 hour before exposure at a final concentration of 1.5 µg/ml. Crocidolite final concentration used was 20 $\mu g/cm^2$. Measurements were performed 24 hours after exposure.

Cell Count

Floating cells were collected from media, and counted by hemocytometer.

Cell Viability: Trypan Blue Exclusion

Collected floating cells were stained with Trypan Blue in a 1:1 dilution. Cells excluding the dye were considered viable.

Results

In order to verify if the increase in floating cells was real, culture media was removed and cell counted. An increase in the number of floating cells was seen in the crocidolite-exposed group (Figure 2.16). The viability of floating cells in the exposed group was almost six times less than the unexposed one (Figure 2.17). In the presence of VNR blocking antibody, RMV-7, a statistically significant decrease in the number of floating cells was observed (Figures 2.18). When viability was evaluated after crocidolite exposure, a statistically significant increase was observed in the group treated with RMV-7 (Figures 2.19). Because asbestos exposure was affecting the total number of floating cells, and viability was detected in percentage, Figure 2.20 was designed combining the data from Figures 2.16, 2.17, 2.18, and 2.19 in order to visualize in absolute cell count the effect of crocidolite exposure in viability with or without RMV-7, so no statistics were performed. This figure shows that the groups exposed to crocidolite have higher numbers of floating dead cells in comparison with the non-exposed groups, also that RMV-7 by itself apparently did not increase the number of floating cells by blocking VNR, and finally that RMV-7 decreased the number or floating dead cells in the crocidolite-exposed group.

Summary

LA-4 cells when exposed to crocidolite activate a pathway characterized by the release of prostacyclin, which is Cox-2 and VNR mediated. Simultaneously a cytotoxic pathway, which is Cox independent, is activated. Crocidolite induces cell detachment of LA-4 cells, which seems to be VNR mediated. In addition, it seems that VNR plays a role in the cytotoxic pathway of these floating cells.

Discussion

Asbestos is known to induce lung inflammation that progresses to fibrosis. It has been postulated that ILD develops in an inflammatory environment with altered repair mechanisms. Crocidolite-induced direct damage to alveolar cells such as macrophages, alveolar type I, or type II cells may generate the conditions required for ILD development. Moreover, it is possible that alveolar type II cells independently could play an important role, because they secrete pulmonary surfactant (in order to prevent alveolar collapse) and replace the damaged type I cells by acting as a stem cell (Finkelstein & Barrett, 2000). Direct damage to alveolar type II cells could create an inflammatory environment and interference with the repair mechanisms related to type I cells replacement, the conditions required for ILD development. This study compared two immortalized murine lung epithelial cell lines in order to determine which one could be a better model for the study of asbestos-induced responses. Results showed that crocidolite-induced toxicity is cell type specific, because LA-4 cells were susceptible to crocidolite-induced toxicity, while CMT 64/67 cells were resistant despite the high doses of crocidolite used. So, it is possible that some receptors required for crocidolite interaction be present in LA-4 cells and not in CMT 64/67 cells. LA-4 cells have been characterized as alveolar type II cells (Stoner, Kikkawa et al., 1975), the same alveolar cell type that plays an important role in ILD development. Consequently LA-4 cells were used in all further crocidolite-exposure experiments in the present study

Prostacyclin release is an indicator of asbestos–induced cell activation and inflammation (Garcia, Dodson et al., 1989; Garcia, Gray et al., 1988). Prostacyclin is a product of arachidonic acid metabolism. Its production requires cyclooxygenase and the

specific isomerase prostacyclin synthase as previously described in Figure 1.9. Due to its instability, it is non-enzymatically hydrated to 6-keto $PGF_{1\alpha}$, a more stable metabolite. In this study 6-keto $PGF_{1\alpha}$ production was considered an indicator of prostacyclin synthesis. Prostacyclin has diverse effects in different cells such as endothelial cells, epithelial cells, macrophages, and fibroblasts as previously described. Curiously all these different cells also could be playing a role in the development of ILD. This study has shown that murine type II cells produce prostacyclin after asbestos exposure. This finding allows us to propose that asbestos-induced prostacyclin release is a mechanism in which type II cells could regulate the activity of different cell populations in the alveolar space and be directly or indirectly involved in the development of ILD.

Prostacyclin synthesis requires Cyclooxygenase (Cox). There are two Cox isoforms: Cox 1 (constitutively expressed) and Cox 2 (inducible). Several studies have shown that prostacyclin biosynthesis is highly Cox 2 dependent, but this is not absolute (Belton, Byrne et al., 2000; Caughey, Cleland et al., 2001). Lovgren et al. reported that Cox 2 dependent prostacyclin production played an important role in the development of lung fibrosis in the bleomycin-induced pulmonary fibrosis mouse model (Lovgren et al., 2006). Murakami et al. reported that repeated administration of a long-acting prostacyclin agonist attenuated the development of bleomycin-induced pulmonary fibrosis and also improved survival in these mice (Murakami et al., 2006). The present study showed that prostacyclin production, induced by crocidolite exposure, was prevented in the presence of Cox 2 inhibitors, suggesting that prostacyclin production was Cox 2 dependent. Moreover, a two-hour crocidolite exposure increased the expression of Cox 2 mRNA five-fold in LA-4 cells. This increase was transitory, and probably adequate enough to

maintain prostacyclin synthesis for a minimum of 24 hours. Based on the cited reports and our findings it is possible to postulate that exposure of type II cells to crocidolite induces Cox 2 and prostacyclin synthesis, which is Cox 2 dependent. This increase in prostacyclin production could be a protective mechanism against the development of crocidolite-induced pulmonary fibrosis. Unfortunately this effect is short-lived relative to the direct toxicity of crocidolite on LA-4 cells. In this study, Cox inhibitors did not protect LA-4 cells from asbestos-induced cytotoxicity. Since the use of the same Cox inhibitors prevented prostacyclin release and did not protect the cells from asbestos-induced cytotoxicity, I propose that LA-4 cells respond in two different ways after crocidolite exposure: A prostacyclin response, where the induction of Cox 2 appears to be the primary event promoting prostacyclin biosynthesis, and cytotoxic response, which is Cox independent.

As previously described, coating crocidolite asbestos with vitronectin enhances its internalization via the alpha V integrin vitronectin receptor $\alpha v\beta 5$ in mesothelial cells (Boylan, Sanan et al., 1995). Vitronectin receptor (VNR) is a group of integrins sharing a common αv subunit. Murphy et al. reported that engagement of the VNR $\alpha v\beta 3$ induces Cox 1 and Cox 2 expression in endothelial cells (J. F. Murphy et al., 2003). The present study showed that LA-4 cells expressed the αv subunit, present in all vitronectin receptors.

VNR and some other integrins recognize the Arg-Gly-Asp (RGD) motif present in a variety of ligands such as vitronectin. RGD peptides have been previously used as competitive inhibitors for receptors that recognized RGD domain (Roberts, Yokoyama et al., 1991; Ruoslahti, 2003). Because VNR recognizes the RGD domain, this study used

RGD peptides for the inhibition of VNR ligand binding. The use of RGD peptides decreased prostacyclin production, after crocidolite exposure, more than 20%. Although the decrease is statistically significant, it also suggests that other mechanisms, which do not depend on the RGD domain recognition, are responsible for prostacyclin production after crocidolite exposure.

The important role of TGFβ in healing and fibrosis and ILD has been well established (Gross & Hunninghake, 2001; Pittet et al., 2001; Toews, 2000; Wang, Scabilloni et al., 2005). As previously described, there are five different types of VNRs (based on their β subunit): αvβ1, αvβ3, αvβ5, αvβ6, and αvβ8. It has been described that VNRs αvβ6 and αvβ8 bind the TGFβ latency-associated peptide (LAP) inducing activation of TGFβ in lung and skin, and that the β6 null mice are protected from bleomycin-induced pulmonary fibrosis (Munger et al., 1999; Pittet, Griffiths et al., 2001). In addition, VNRs αvβ1 and αvβ5 also bind directly to LAP, but without TGFβ activation (Sheppard, 2005). So it is possible that VNRs involvement in asbestos-induced ILD be through TGFβ activation. It was previously described that VNR αvβ5 enhances internalization of vitronectin coated crocidolite fibers by mesothelial cells (Boylan, Sanan et al., 1995; Pande, Mosleh et al., 2006). Because VNR αvβ5 also binds LAP, it is possible to postulate that vitronectin-coated crocidolite fibers compete with LAP for VNR αvβ5 binding. This competition might affect the amount of free LAP that potentially could be activated to TGβ by other VNRs such as αvβ6 or αvβ8.

In this study, when VNRs were specifically blocked with an antibody, the prostacyclin production after crocidolite exposure decreased more than 20%. Curiously, this finding, which is consistent with the decrease found when RGD peptides were used,

favors the idea of VNR involvement in prostacyclin production after crocidolite exposure. VNR inhibitors (RGD peptides and blocking antibody) induced only a 20% decrease in the crocidolite-induced prostacyclin release. Because the 6-keto $PGF_{1\alpha}$ assay is an estimate of the total prostacyclin released in the last 24 hours after crocidolite exposure, it would have been interesting to determine the effect of VNR inhibitors in the trend of prostacyclin release over crocidolite exposure time in order to detect a further decrease in crocidolite-induced prostacyclin release.

Vitronectin is a multifunctional protein with an RGD motif that is recognized by different members of the integrin family including VNR (McKusick, 1989; Schvartz, Seger et al., 1999; Takagi, 2004). Vitronectin coats asbestos fibers enhancing cell internalization. It is a multifunctional adhesive protein present in large concentrations in blood serum (Schvartz, Seger et al., 1999). It diffuses into the extravascular tissue where it could bind some other proteins (Hayman et al., 1983). It has been found in bronchoalveolar lavaged fluid (BALF) and pleural liquid, and in higher concentrations during inflammatory states (Boylan, Sanan et al., 1995). In all previous asbestos exposure experiments, it was assumed that the crocidolite fibers were coated with the ECM proteins present in the fetal bovine serum of the cell culture media. Because most of the asbestos exposure is typically by inhalation, it was important to demonstrate similar effects at a physiologically relevant concentration of ECM proteins in the BALF. In this study, when LA-4 cells were exposed to crocidolite in the presence of reduced serum culture media, prostacyclin production was prevented; and when BALF was added, prostacyclin production was rescued. These findings suggest that one or more factors present in BALF (and in fetal bovine serum) are necessary to induce prostacyclin release

in LA-4 cells exposed to crocidolite. Although this study did not look for the presence of vitronectin in the BALF or fetal bovine serum our findings suggest some factor or factors coats crocidolite fibers, favoring cell interaction and prostacyclin release. Surprisingly, crocidolite cytotoxicity was prevented in the presence of reduced serum culture media, and the addition of BALF did not rescue the cytotoxicity. This finding favors the rationale that a factor or factors present in fetal bovine serum (e.g. ECM proteins) and not in BALF is required to induce cytotoxicity. It is also possible that the same factor is present in very low amounts in BALF, but during lung injury and inflammatory states, the factor levels increase allowing crocidolite-induced cytotoxicity. Unexpectedly, when RGD peptides or VNR blocking antibody were used in the presence of fetal bovine serum in order to prevent crocidolite-induced cytotoxicity, LA-4 cells were not protected from cytotoxicity. Since RGD peptides are expected to compete with any ECM protein containing a RGD domain, it is possible to postulate that the RGD domain is not the only one recognized by integrin (e.g. CS-1 domain), or that the RGD domain of some ECM involved in cytotoxicity have higher affinity for the receptor than the RGD peptides, reducing their competition ability.

The findings that VNR inhibitors did not prevent crocidolite-induced cytotoxicity, strengthen the idea that LA-4 cells respond in two different pathways after crocidolite exposure: A prostacyclin response, which is Cox 2 and VNR dependent, and cytotoxic response, which is Cox and VNR independent. Both pathways could be associated with the development of lung fibrosis, because they could be affecting the balance of bound and free LAP. The prostacyclin pathway, which is VNR dependent, could promote LAP release by competition as previously described, and the cytotoxic pathway decreases the

number of cells binding LAP. In either pathway, free LAP is able to bind others VNRs (such as αvβ6 or αvβ8) expressed in type II cells or other alveolar cells, inducing TGFβ activation and promoting healing and/or fibrosis.

The findings with floating LA-4 cells raised additional issues: Do LA-4 cells bind and grow on crocidolite fibers, detach from the bottom, and once floating they die; or do the cells die first, detach, and form clumps with floating crocidolite fibers? The decrease in floating cell number when crocidolite with VNR inhibitor was used favors the idea that VNR interaction with asbestos is an early event before cell detachment, and allows to postulate that LA-4 cells first bind crocidolite fibers through the VNR before detaching. This statistically significant 20% decrease in floating cells number is consistent with other experiments using VNR inhibitors. However a decrease of only 20% also suggest that VNR is not the only receptor involved. Unexpectedly, cell viability increased more than 50% in floating cells when VNR inhibitor was used. This finding apparently contradicts the idea that cytotoxicity is VNR independent, but favors the idea that LA-4 cells initially bind crocidolite fibers through VNR (and/or by gravity as observed by light microscopy that fibers do not float), then grow on the fibers, and finally detach. Once cells start floating, gravity no longer plays a role keeping the fibers in contact with the cells, but VNR role might be more important keeping crocidolite fibers in close contact with the cell membrane and this way indirectly inducing cytotoxicity.

Figure 2.21 shows a proposed model for the alveolar type II cell response after crocidolite exposure. First, an RGD protein present in fetal bovine serum and BALF coats crocidolite. This RGD protein is a ligand for VNR. This interaction will induce Cox 2 expression and activity promoting prostacyclin release. Second, crocidolite also induces

cytotoxicity independently from RGD protein, VNR, Cox 1 or Cox 2. And third, cells bind RGD coated crocidolite fibers through VNR and detach from the bottom of the flask forming floating clusters of cells attached to crocidolite fibers. Then, floating cells become cytotoxic and die.

Figure 2.1

Crocidolite-Induced Cytotoxicity in Lung Epithelial Cells Dose Response (N=3-6)

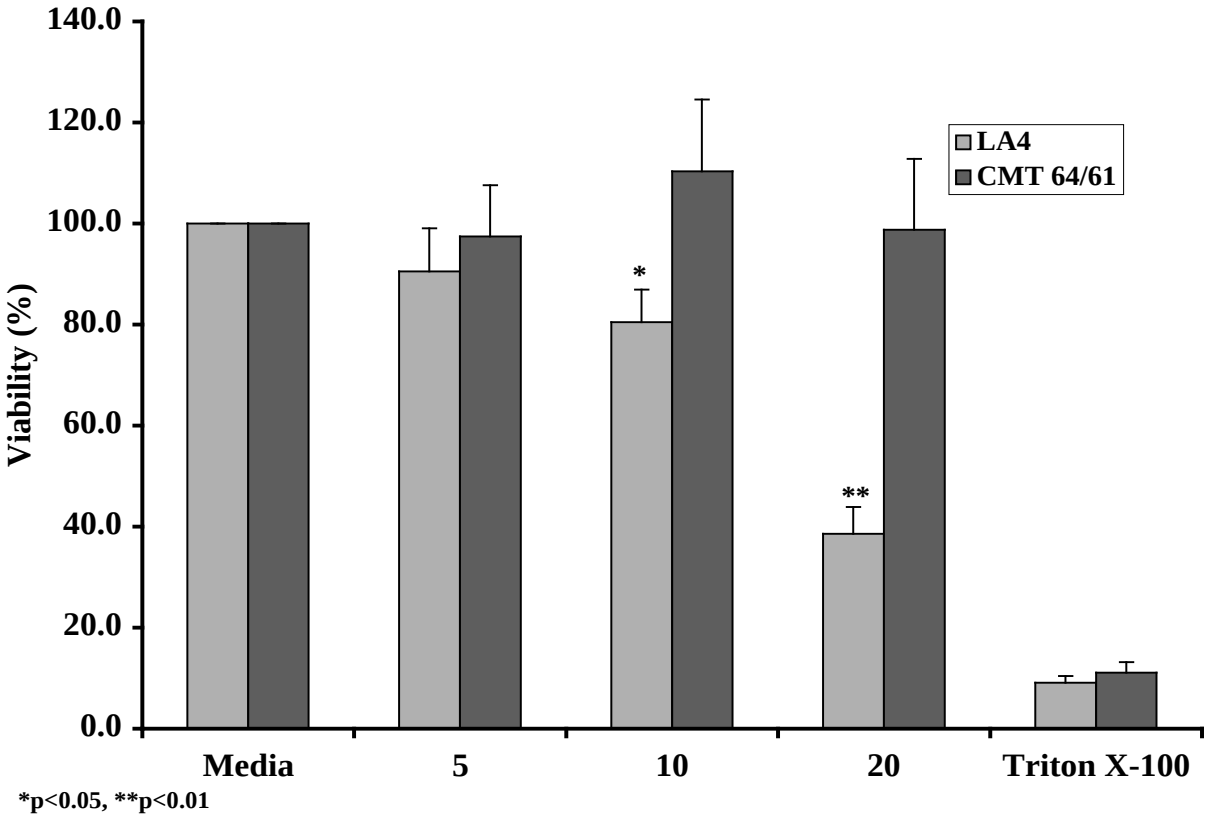

Cells were trypsinized and plated 24 hours prior to exposure at 50,000 cells in a 96-well plate. Crocidolite was added to a final dose of 5, 10, or 20 µg/cm^2 per well. After 24 hours of exposure, viability was measured using CellTiter96 Aqueous One Solution Reagent (Promega) as described in Methods section. Values were normalized considering that cells exposed to media only have 100% of viability.

Figure 2.2

LA-4 cells Lactate Dehydrogenase (LDH) Release after Crocidolite Exposure (N=3)

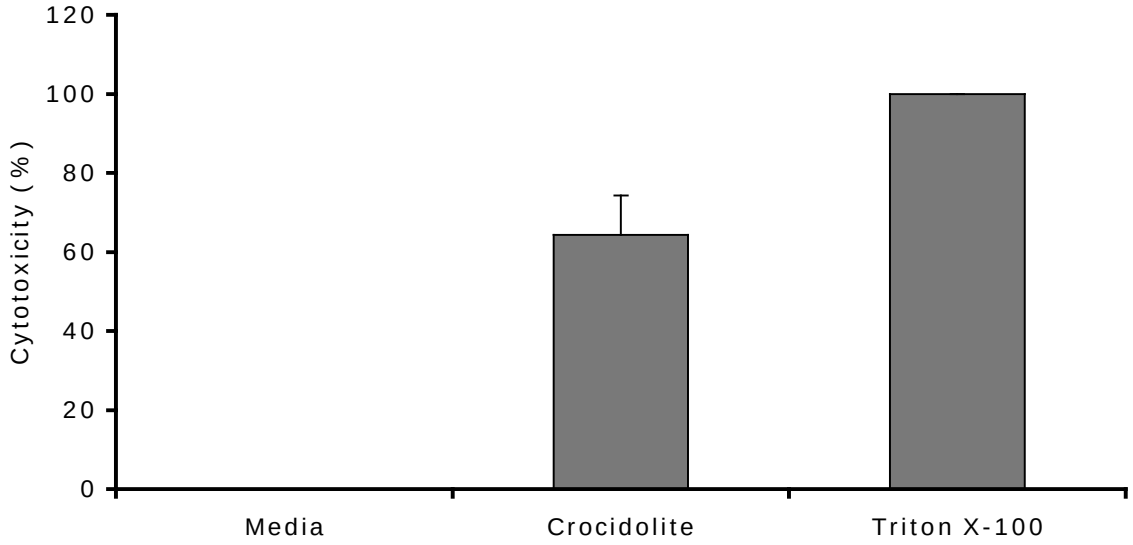

Treatment Groups

Cells were trypsinized and plated 24 hours prior to exposure at 50,000 cells in a 96-well plate. Crocidolite was added to a final dose of 20 μg/cm^2 per well. After 24 hours of exposure, cytotoxicity was approached detecting LDH release using Cytotoxic Detection Assay (LDH) (Roche Applied Sciences) as described in Methods section. Values were normalized considering that cells exposed to media only have no LDH release and cells exposed to Triton X-100 have 100% of LDH release.

Figure 2.3

6-keto $PGF_{1\alpha}$ Production in LA-4 Cells After Crocidolite Exposure (N=3)

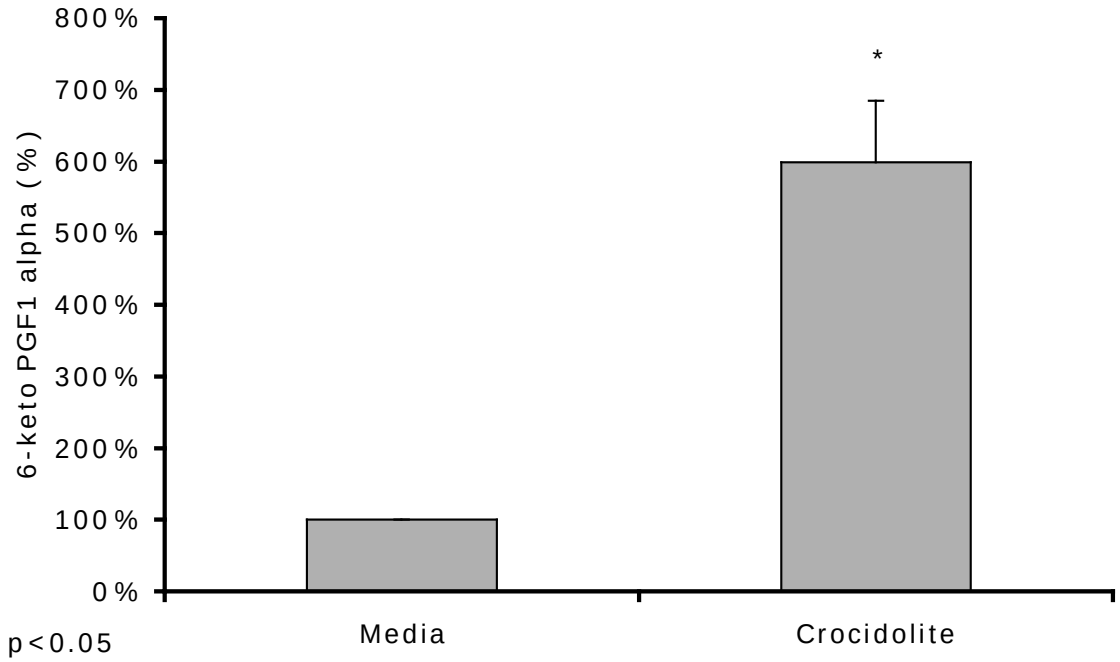

Cells were trypsinized and plated 24 hours prior to exposure at 50,000 cells in a 96-well plate. Crocidolite was added to a final dose 10 μg/cm^2 per well. After 24 hours of exposure, 6-keto $PGF_{1\alpha}$ release was measured using ACE Competitive Enzyme Immunoassay (Cayman Chemical) as described in Methods section. Values were normalized considering that cells exposed to media only have 100% of 6-keto $PGF_{1\alpha}$ release.

Figure 2.4

6-keto $PGF_{1\alpha}$ Production in LA-4 Cells After Crocidolite Exposure (10 $\mu g/cm^2$) in the Presence of COX inhibitors (N=2-3)

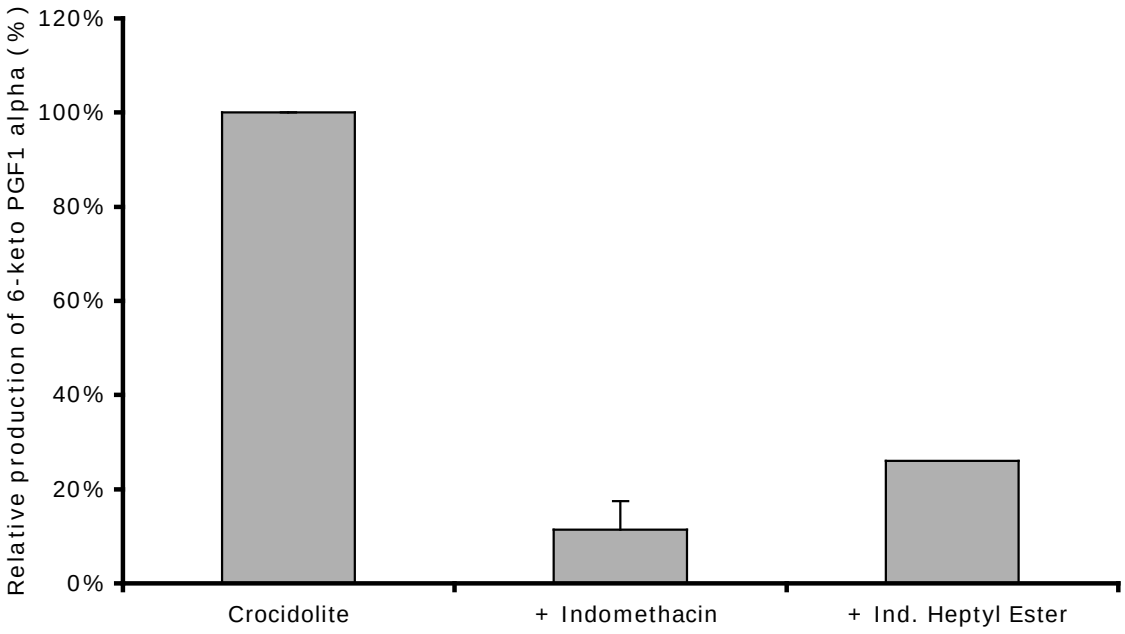

Treatment Groups

Cells were trypsinized and plated 24 hours prior to exposure at 50,000 cells in a 96-well plate. The Cox 1/2 inhibitor Indomethacin and the specific Cox 2 inhibitor Indomethacin heptyl ester were added at a dose 10 times their respective IC_{50} (inhibitory concentration of 50% of the total activity) simultaneously with crocidolite (10 $\mu g/cm^2$ per well). After 24 hours of exposure, 6-keto $PGF_{1\alpha}$ release was measured using ACE Competitive Enzyme Immunoassay (Cayman Chemical) as described in Methods section. Values were normalized considering that cells exposed to media only have 100% of 6-keto $PGF_{1\alpha}$ release.

Figure 2.5

Cyclooxygenase 2 mRNA Expression After Crocidolite Exposure (10 µg/cm^2) (N=3)

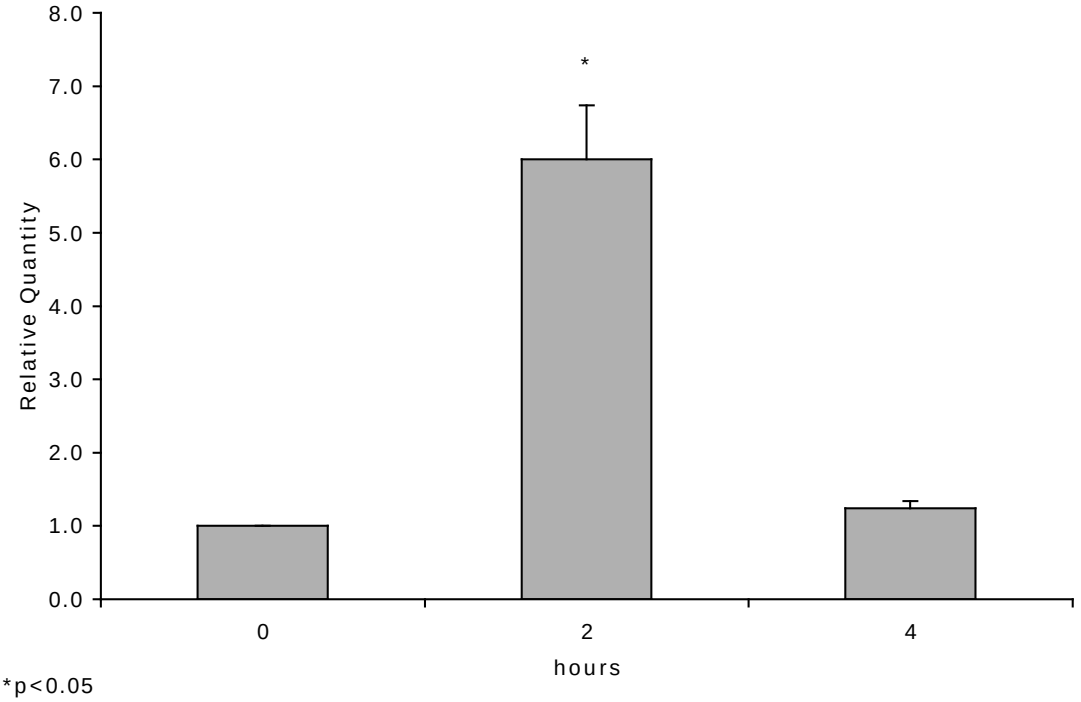

Hours After Crocidolite Exposure

Cells were trypsinized and plated 24 hours prior to exposure at 50,000 cells in a 96-well plate. Crocidolite was added to a final dose 10 µg/cm^2 per well. After 2 and 4 hours of crocidolite exposure, cells were lysed and total RNA isolated using Trizol reagent (Invitrogen). First strand reverse transcription was performed with oligo dT and amplification done using Platinum Quantitative PCR SuperMix-UDG (Invitrogen). C_t values were recorded and Cox 2 data analyzed relative to GAPDH.

Figure 2.6

Crocidolite-Induced Cytotoxicity in the Presence of the COX 1/2 Inhibitor Indomethacin
(N=3)

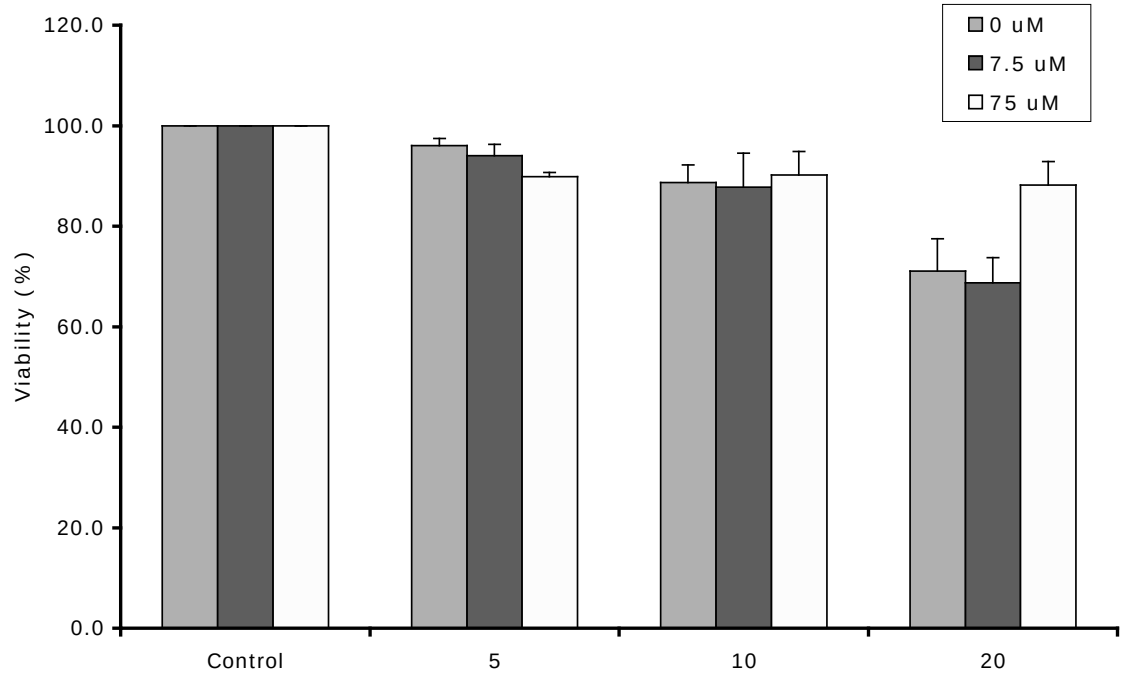

Cells were trypsinized and plated 24 hours prior to exposure at 50,000 cells in a 96-well plate. The Cox 1/2 inhibitor Indomethacin was added at doses 10 and 100 times its IC_{50} simultaneously with crocidolite (5, 10, 20 µg/cm^2 per well). After 24 hours of exposure, viability was measured using CellTiter96 Aqueous One Solution Reagent (Promega) as described in Methods section. Values were normalized. Media only exposed cells were considered to have 100% of viability.

Figure 2.7

Crocidolite-Induced Cytotoxicity in the Presence of the COX 2 Inhibitor Indomethacin Heptyl Ester
(N=3)

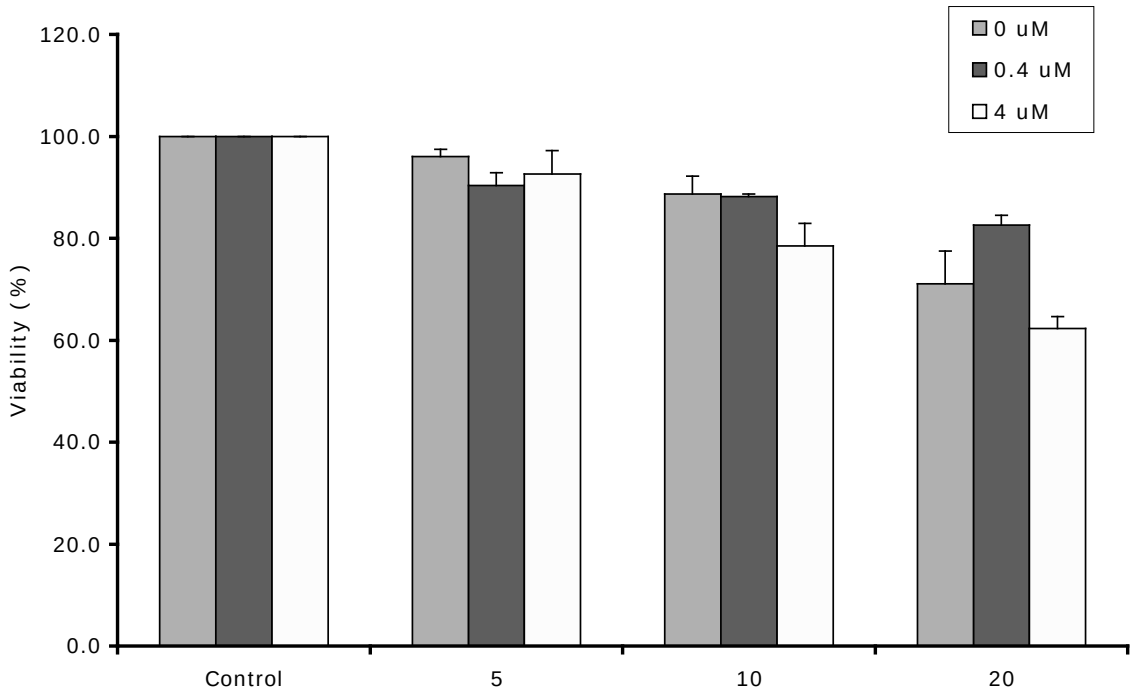

Cells were trypsinized and plated 24 hours prior to exposure at 50,000 cells in a 96-well plate. The specific Cox 2 inhibitor Indomethacin heptyl ester was added at doses 10 and 100 times its IC_{50} simultaneously with crocidolite (5, 10, 20 µg/cm^2 per well). After 24 hours of exposure, viability was measured using CellTiter96 Aqueous One Solution Reagent (Promega) as described in Methods section. Values were normalized. Media only exposed cells were considered to have 100% of viability.

Figure 2.8

Integrin Vitronectin Receptor Expression in LA-4 cells

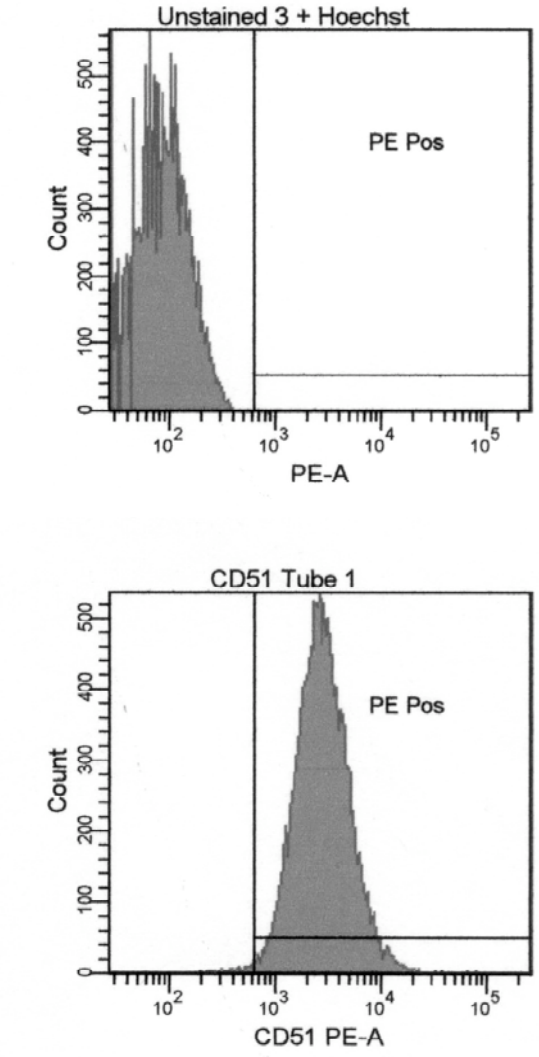

Three hundred thousand LA-4 cells were labeled with anti-alpha-v (CD51) fluorescent labeled antibody. After 20 minutes incubation at 4ºC, fluorescence was detected on a FACs Aria Flow cytometer using FACs Diva software (Becton Dickson). Hoechst 33258 dye (Invitrogen) was added to a final concentration of 1 µg/ml in order to exclude dead cells. Results shown are representative of three experiments.

Figure 2.9

Integrin Vitronectin Receptor in LA-4 cells
(N=3)

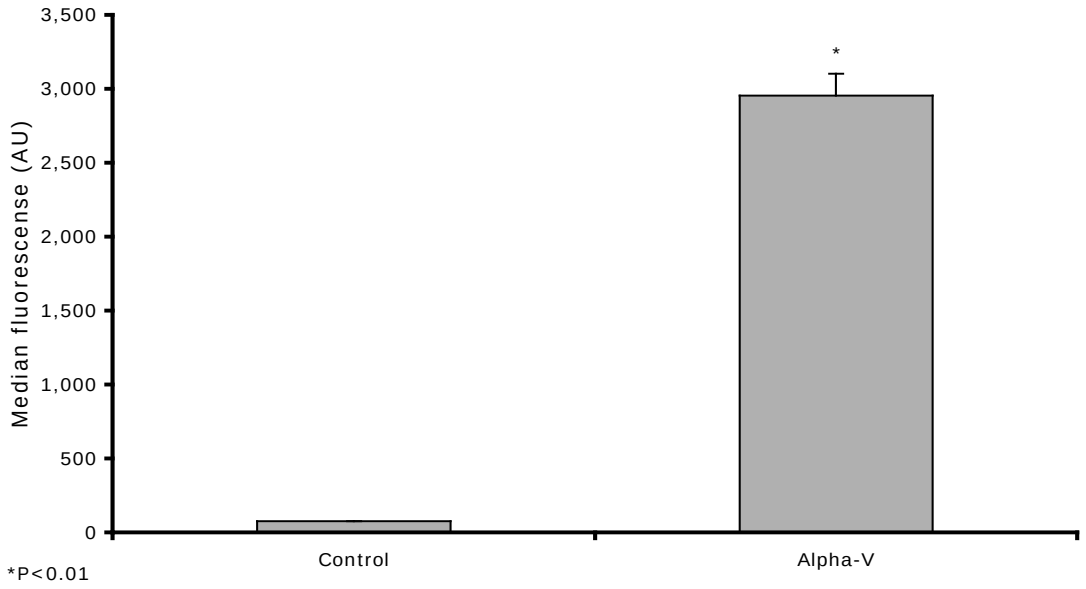

Antibody (Type of Receptor)

Three hundred thousand LA-4 cells were labeled with anti-alpha-v fluorescent labeled antibody. After 20 minutes incubation at 4ºC, fluorescence was detected on a FACs Aria Flow cytometer using FACs Diva software (Becton Dickson). Hoechst 33258 dye (Invitrogen) was added to a final concentration of 1 µg/ml in order to exclude dead cells.

Figure 2.10

6-keto $PGF_{1\alpha}$ Production in LA-4 Cells After Crocidolite Exposure (20 µg/cm^2) in the Presence of RGDS peptide inhibitor (N=3)

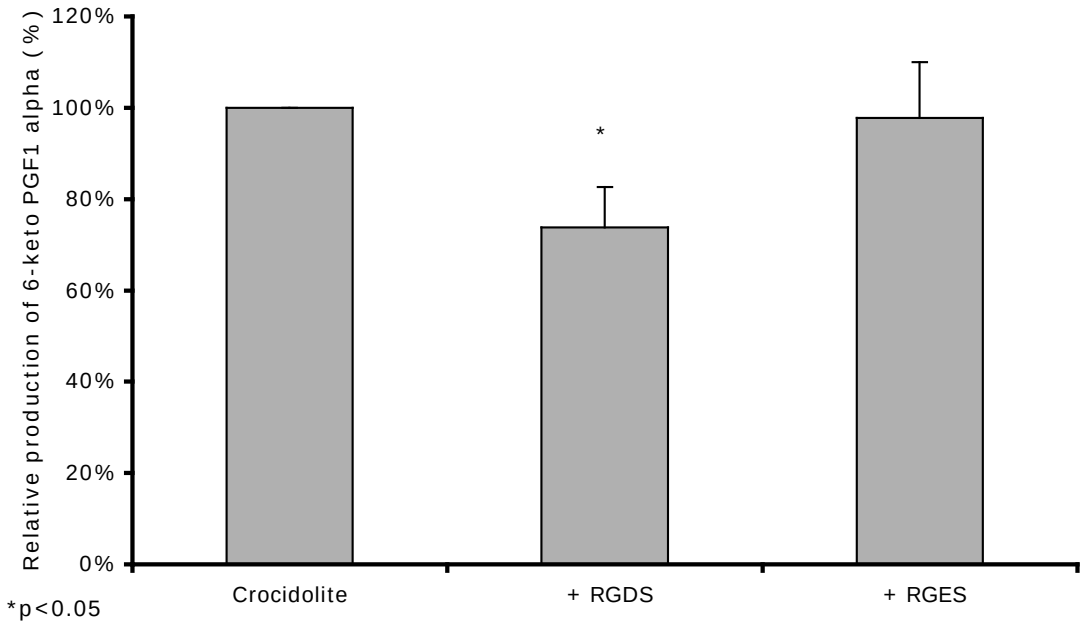

Cells were trypsinized and plated 24 hours prior to exposure at 50,000 cells in a 96-well plate. RGDS peptide (a VNR inhibitor) or RGES peptide (non-specific binding control) at a final dose of 10 µg/ml were added simultaneously with crocidolite (20 µg/cm^2 per well). After 24 hours of exposure, 6-keto $PGF_{1\alpha}$ release was measured using ACE Competitive Enzyme Immunoassay (Cayman Chemical) as described in Methods section. Values were normalized considering that cells exposed to crocidolite with no inhibitor have 100% of 6-keto $PGF_{1\alpha}$ release.

Figure 2.11

6-keto $PGF_{1\alpha}$ Production in LA-4 Cells After Crocidolite Exposure (20 $\mu g/cm^2$) in the Presence of RMV-7 VNR inhibitor (N=3)

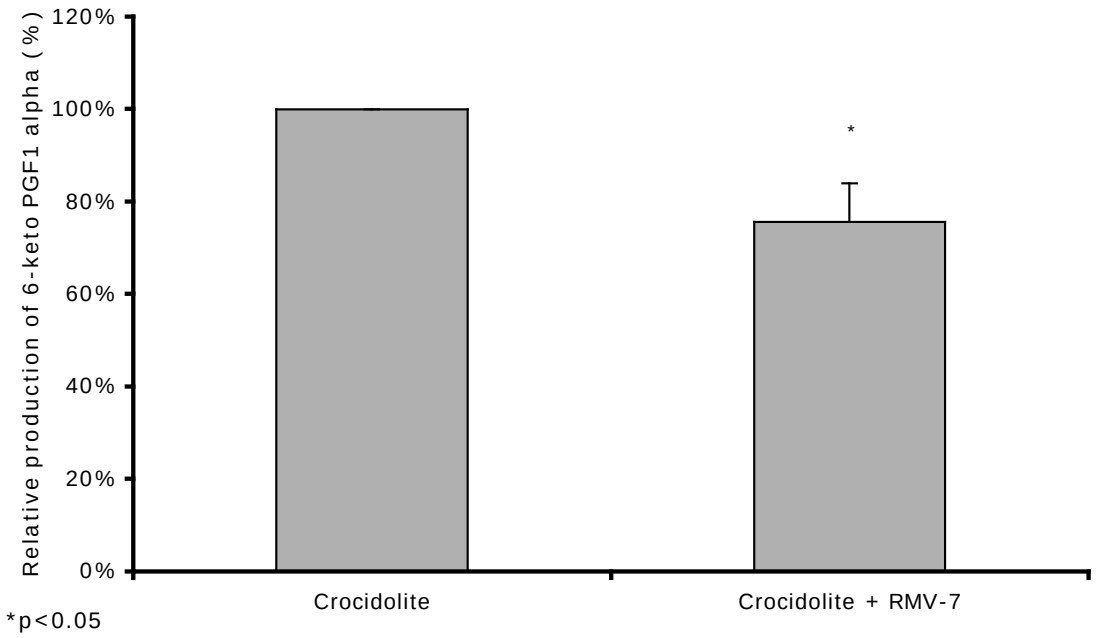

Cells were trypsinized and plated 24 hours prior to exposure at 50,000 cells in a 96-well plate. RMV-7 blocking antibody (anti-alpha-v) was added at a final dose of 2 µg/ml one hour before crocidolite exposure (20 $\mu g/cm^2$ per well). After 24 hours of exposure, 6-keto $PGF_{1\alpha}$ release was measured using ACE Competitive Enzyme Immunoassay (Cayman Chemical) as described in Methods section. Values were normalized considering that cells exposed to crocidolite with no inhibitor have 100% of 6-keto $PGF_{1\alpha}$ release.

Figure 2.12

6-keto $PGF_{1\alpha}$ Production in LA-4 Cells After Crocidolite Exposure in the Presence of BALF
(N=3)

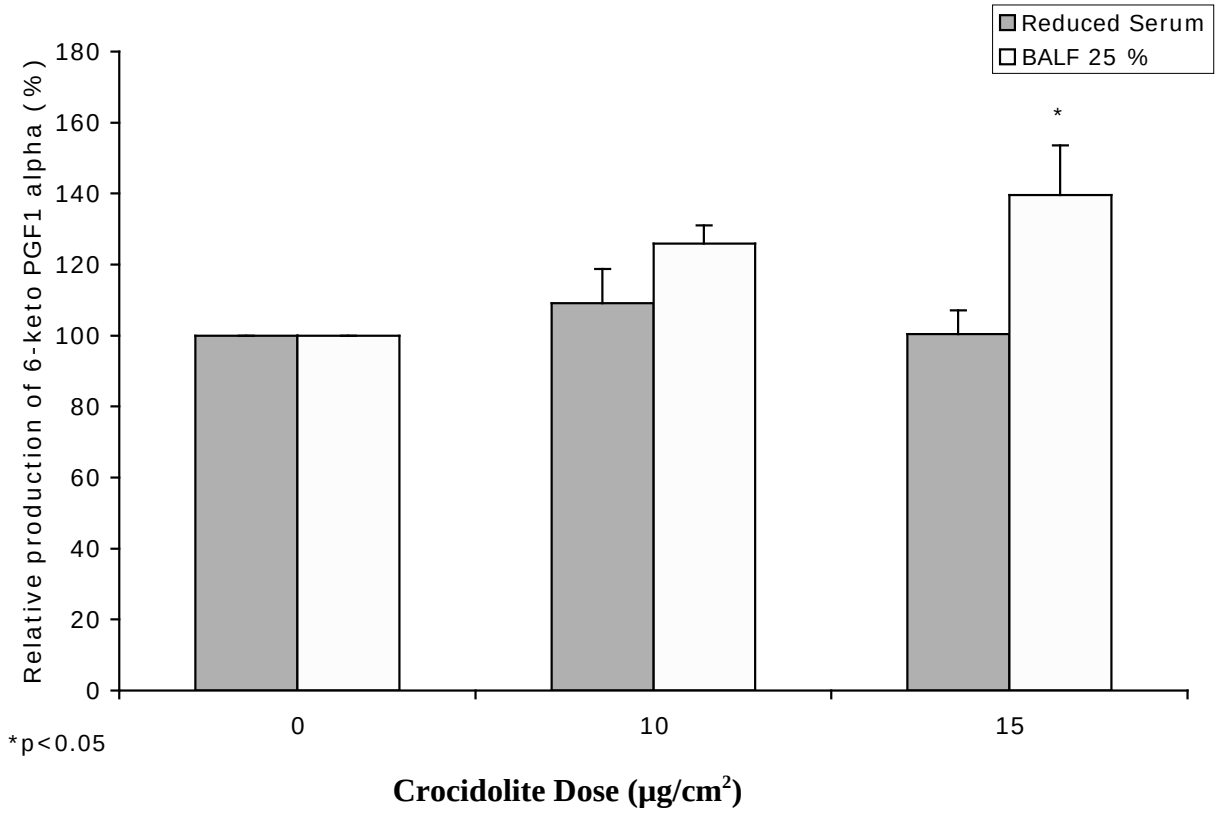

Cells were trypsinized and plated 24 hours prior to exposure at 50,000 cells in a 96-well plate. Then media was changed for Opti-mem I reduced serum medium (Mediatech Inc.) and BALF added to a final concentration of 25% with crocidolite (10 and 15 µg/cm^2 per well). After 24 hours of exposure, 6-keto $PGF_{1\alpha}$ release was measured using ACE Competitive Enzyme Immunoassay (Cayman Chemical) as described in Methods section. Values were normalized considering that cells no exposed to crocidolite have 100% of 6-keto $PGF_{1\alpha}$ release.

Figure 2.13

Crocidolite-Induced Cytotoxicity in the Presence of Reduced Serum Media and BALF
(N=3)

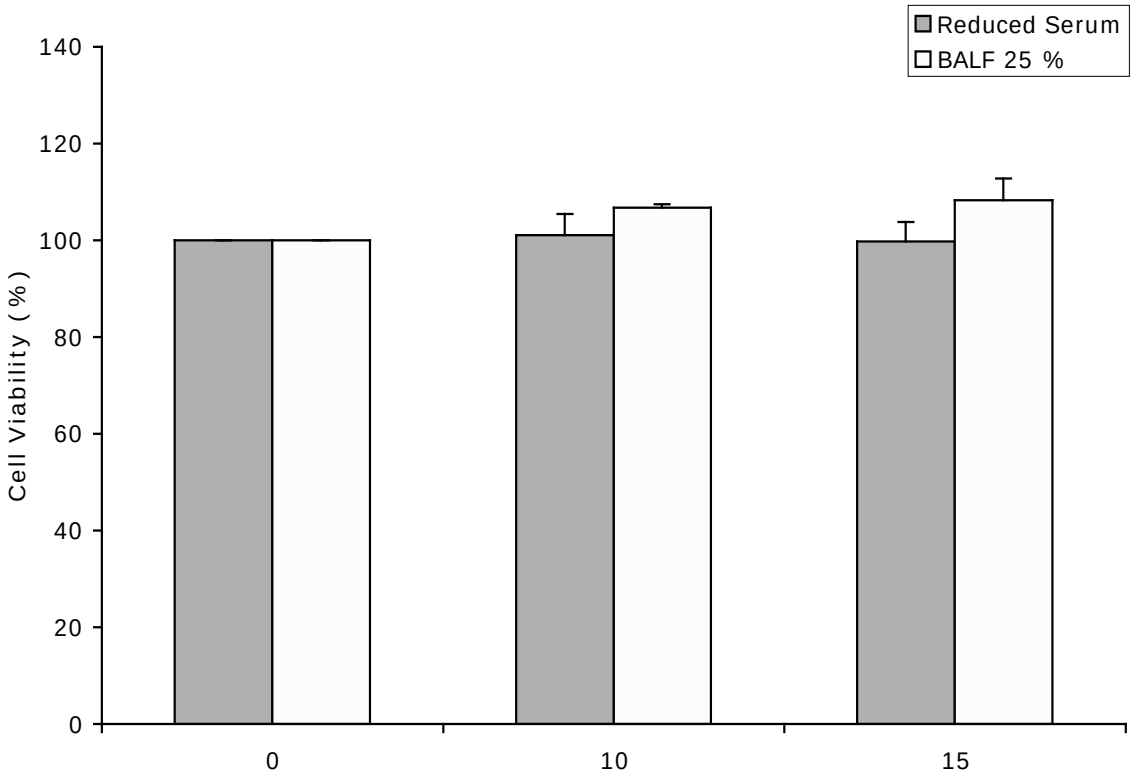

Crocidolite Dose (µg/cm^2)

Cells were trypsinized and plated 24 hours prior to exposure at 50,000 cells in a 96-well plate. Then media was changed for Opti-mem I reduced serum medium (Mediatech Inc.) and BALF added to a final concentration of 25% with crocidolite (10 and 15 µg/cm^2 per well). After 24 hours of exposure, viability was measured using CellTiter96 Aqueous One Solution Reagent (Promega) as described in Methods section. Values were normalized considering that cells exposed to media only have 100% of viability.

Figure 2.14

Crocidolite-Induced Cytotoxicity in the Presence of RGDS Peptide Inhibitor (N=3)

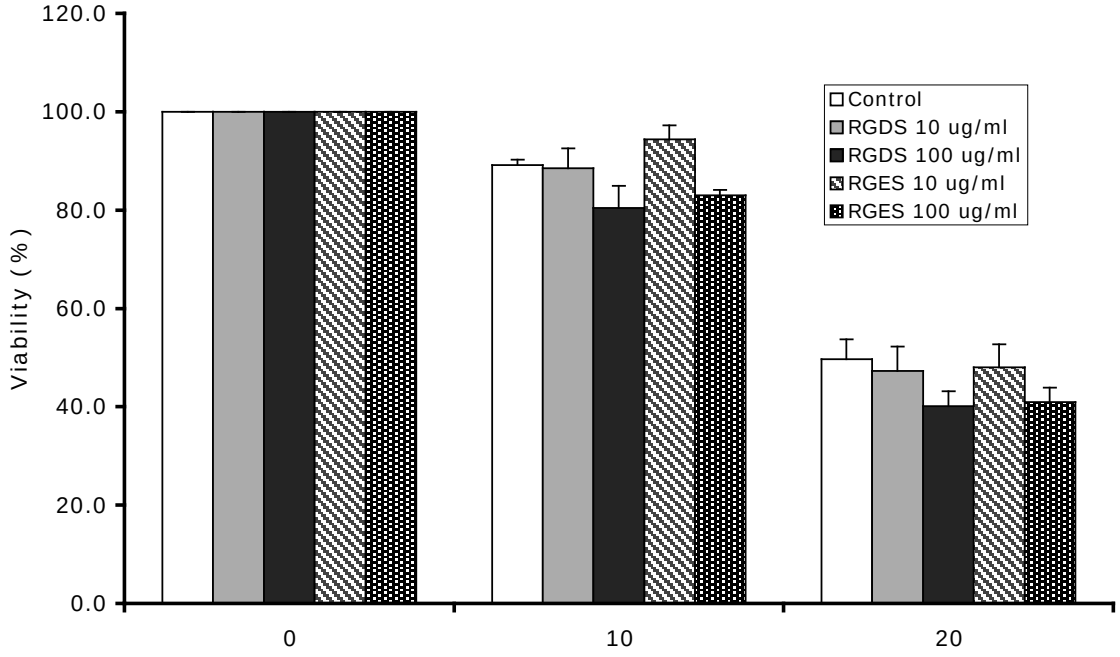

Crocidolite Dose (µg/cm^2)

Cells were trypsinized and plated 24 hours prior to exposure at 50,000 cells in a 96-well plate. RGDS peptide (a VNR inhibitor) or RGES peptide (non-specific binding control) at a final dose of 10 and 100 µg/ml were added simultaneously with crocidolite (5, 10, 20 µg/cm^2 per well). After 24 hours of exposure, viability was measured using CellTiter96 Aqueous One Solution Reagent (Promega) as described in Methods section. Values were normalized considering that cells exposed to media only have 100% of viability.

Figure 2.15

LA-4 cells LDH Release after Crocidolite Exposure (20 µg/cm^2) in the Presence of RMV-7 VNR Inhibitor (N=3)

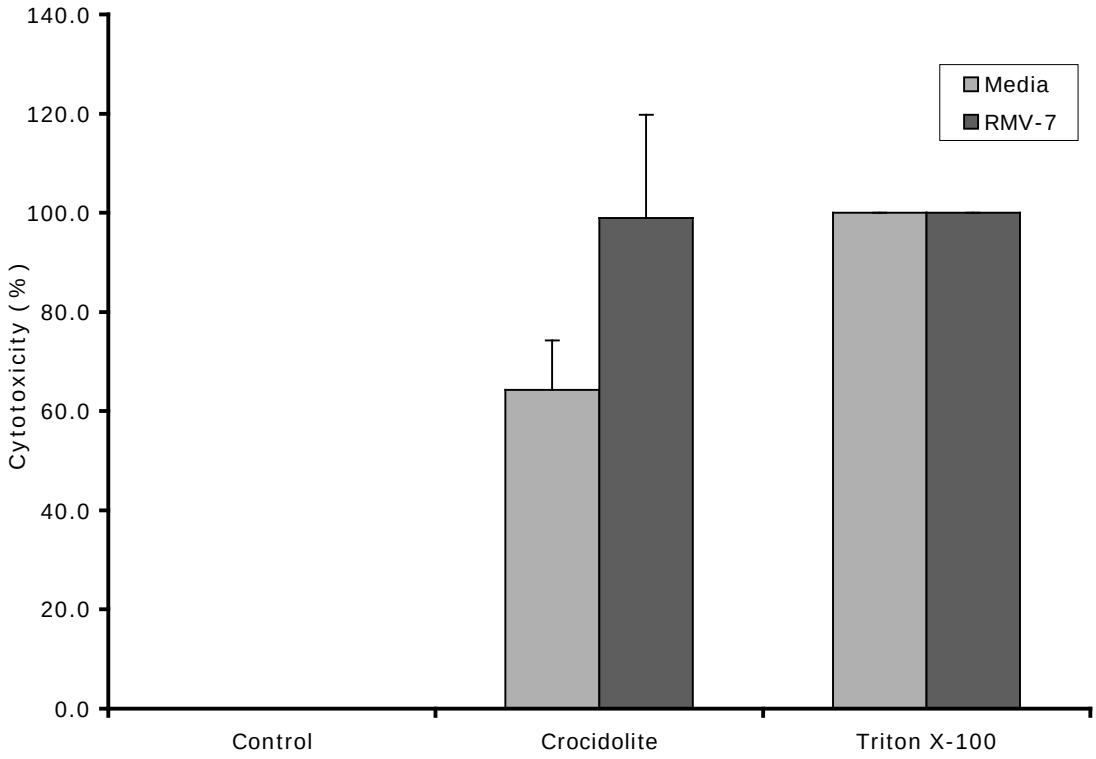

Cells were trypsinized and plated 24 hours prior to exposure at 50,000 cells in a 96-well plate. RMV-7 blocking antibody (anti-alpha-v) was added at a final dose of 2 µg/ml one hour before crocidolite exposure (20 µg/cm^2 per well). After 24 hours of exposure, cytotoxicity was approached detecting LDH release using Cytotoxic Detection Assay (LDH) (Roche Applied Sciences) as described in Methods section. Values were normalized considering that cells exposed to media only have no LDH release and cells exposed to Triton X-100 have 100% of LDH release.

Figure 2.16

Floating LA-4 Cells After Crocidolite Exposure (20 µg/cm^2) (N=3)

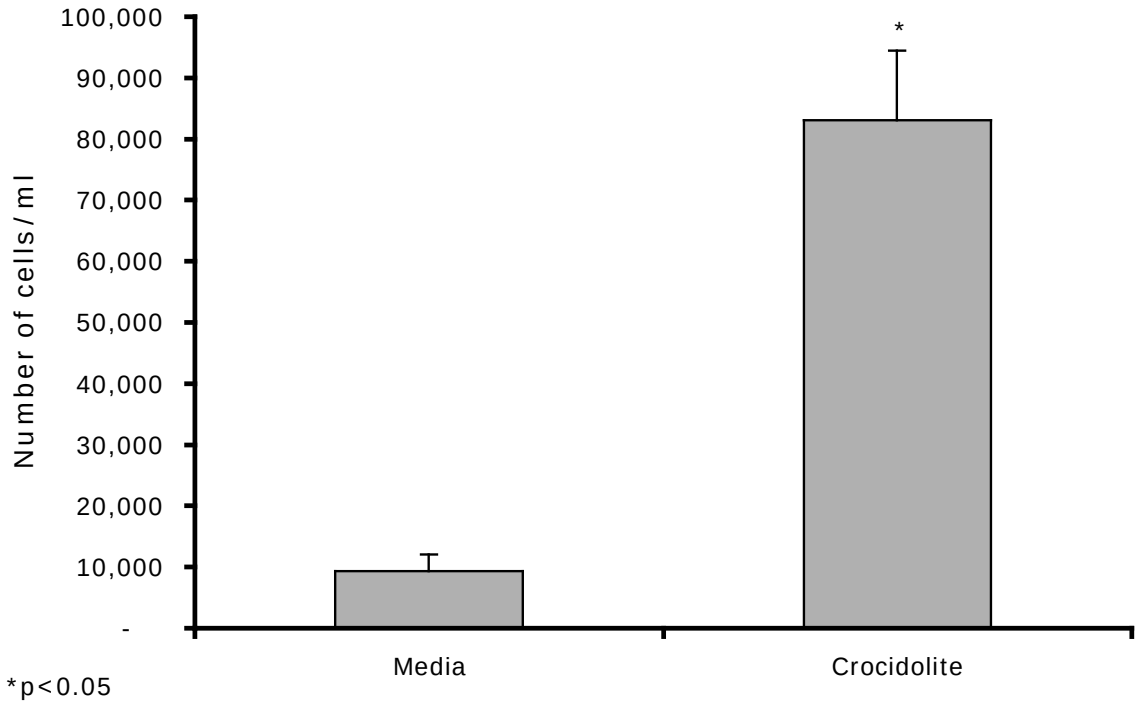

Cells were trypsinized and plated 24 hours prior to exposure at one million cells in a 25 cm^2 flask. Then Crocidolite was added to a final dose of 20 µg/cm^2. After 24 hours of exposure, floating cells were collected from media, and counted by hemocytometer.

Figure 2.17

Floating LA-4 Cells Viability After Crocidolite Exposure (20 µg/cm^2) (N=3)

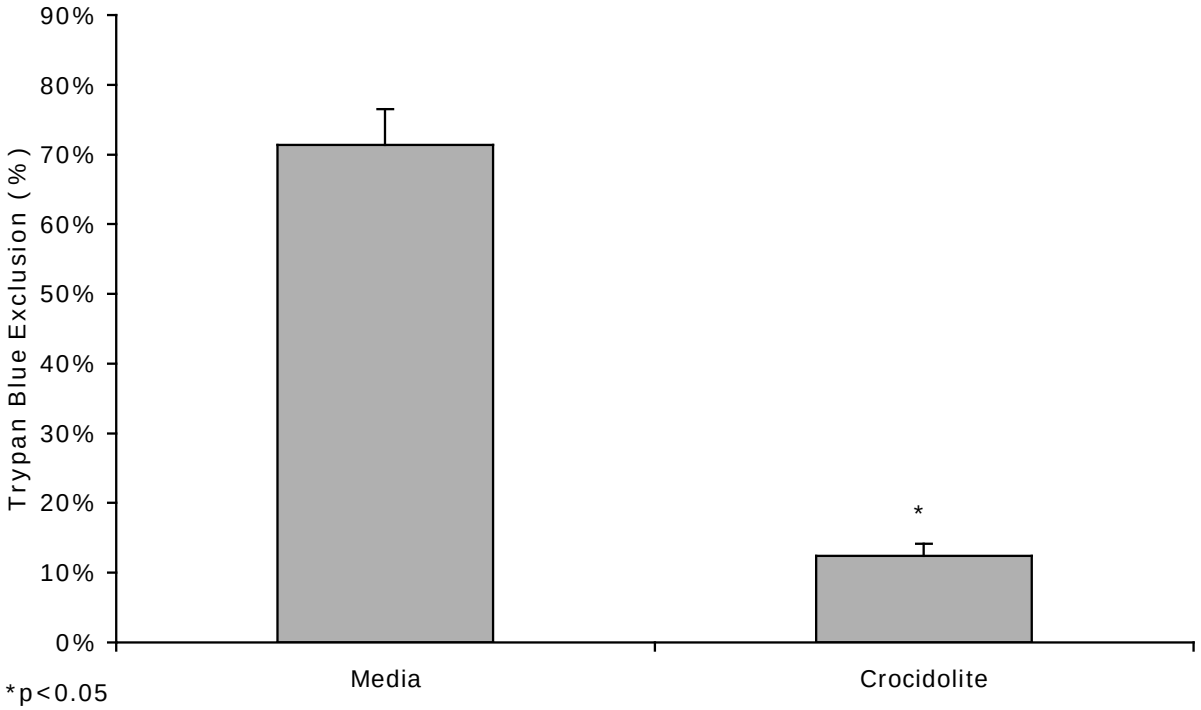

Cells were trypsinized and plated 24 hours prior to exposure at one million cells in a 25 cm^2 flask. Then Crocidolite was added to a final dose of 20 µg/cm^2. After 24 hours of exposure, floating cells were collected from media. Then, a sample from each group was taken and stained with Trypan Blue in a 1:1 dilution. Cells excluding the dye were considered viable.

Figure 2.18

Floating LA-4 Cell Count After Crocidolite Exposure (20 µg/cm^2) in the Presence of RMV-7 VNR Inhibitor (N=3)

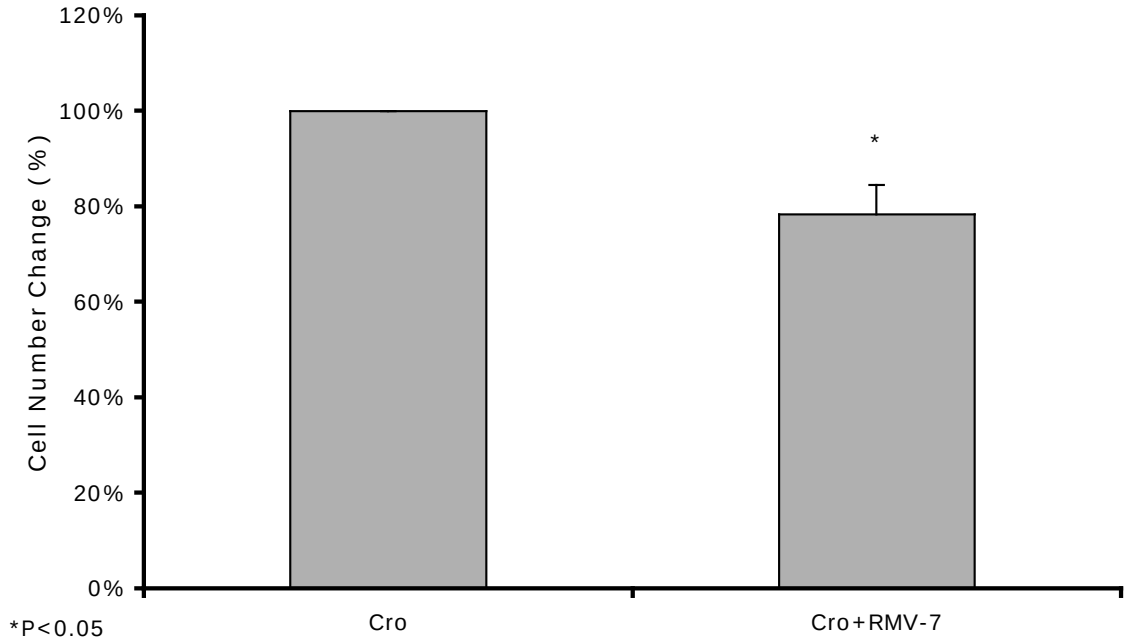

Cells were trypsinized and plated 24 hours prior to exposure at one million cells in a 25 cm^2 flask. One hour before exposure RMV-7 antibody was added at a final concentration of 1.5 µg/ml. Then Crocidolite was added to a final dose of 20 µg/cm^2. After 24 hours of exposure, floating cells were collected from media, and counted by hemocytometer. Values were normalized with their respective control (media only, and media with RMV-7). The group exposed to crocidolite without RMV-7 was considered to have 100% of floating cells.

Figure 2.19

Floating LA-4 Cells Viability After Crocidolite Exposure (20 µg/cm^2) in the Presence of RMV-7 VNR inhibitor (N=3)

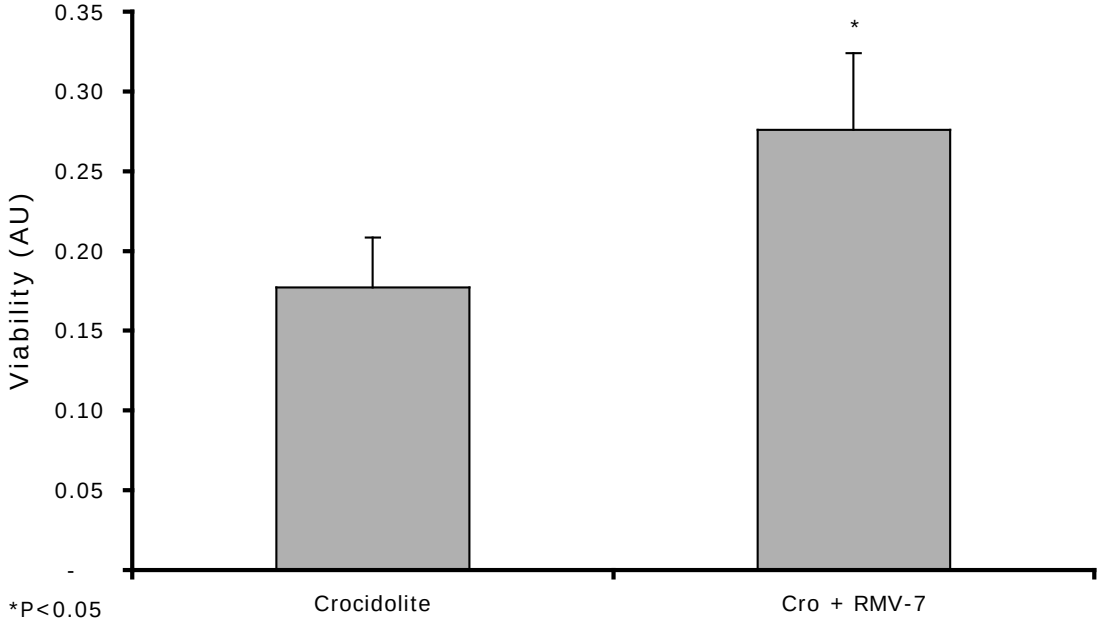

Cells were trypsinized and plated 24 hours prior to exposure at one million cells in a 25 cm^2 flask. One hour before exposure RMV-7 antibody was added at a final concentration of 1.5 µg/ml. Then Crocidolite was added to a final dose of 20 µg/cm^2. After 24 hours of exposure, floating cells were collected from media. Then, a sample from each group was taken and stained with Trypan Blue in a 1:1 dilution. Cells excluding the dye were considered viable. Ratios were calculated with their respective control (media only, and media with RMV-7).

Figure 2.20

Floating LA-4 Cells Absolute Numbers and Viability After Crocidolite Exposure (20 µg/cm^2)
(N=3)

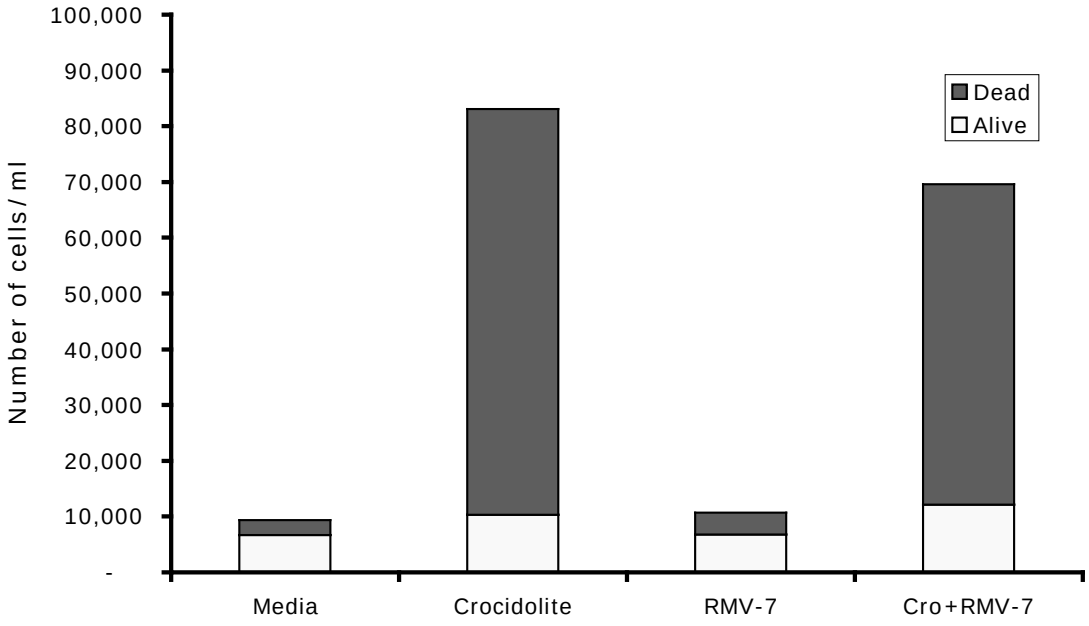

Treatment Group

Cells were trypsinized and plated 24 hours prior to exposure at one million cells in a 25 cm^2 flask. One hour before exposure RMV-7 antibody was added at a final concentration of 1.5 µg/ml. Then Crocidolite was added to a final dose of 20 µg/cm^2. After 24 hours of exposure, floating cells were collected from media, and counted by hemocytometer. Then, a sample from each group was taken and stained with Trypan Blue in a 1:1 dilution. Cells excluding the dye were considered viable. Absolute cell count numbers were calculated using total cell count number and percentage of viable cells.

Figure 2.21

Proposed Model for Crocidolite Induced Response in Alveolar Type II Cells

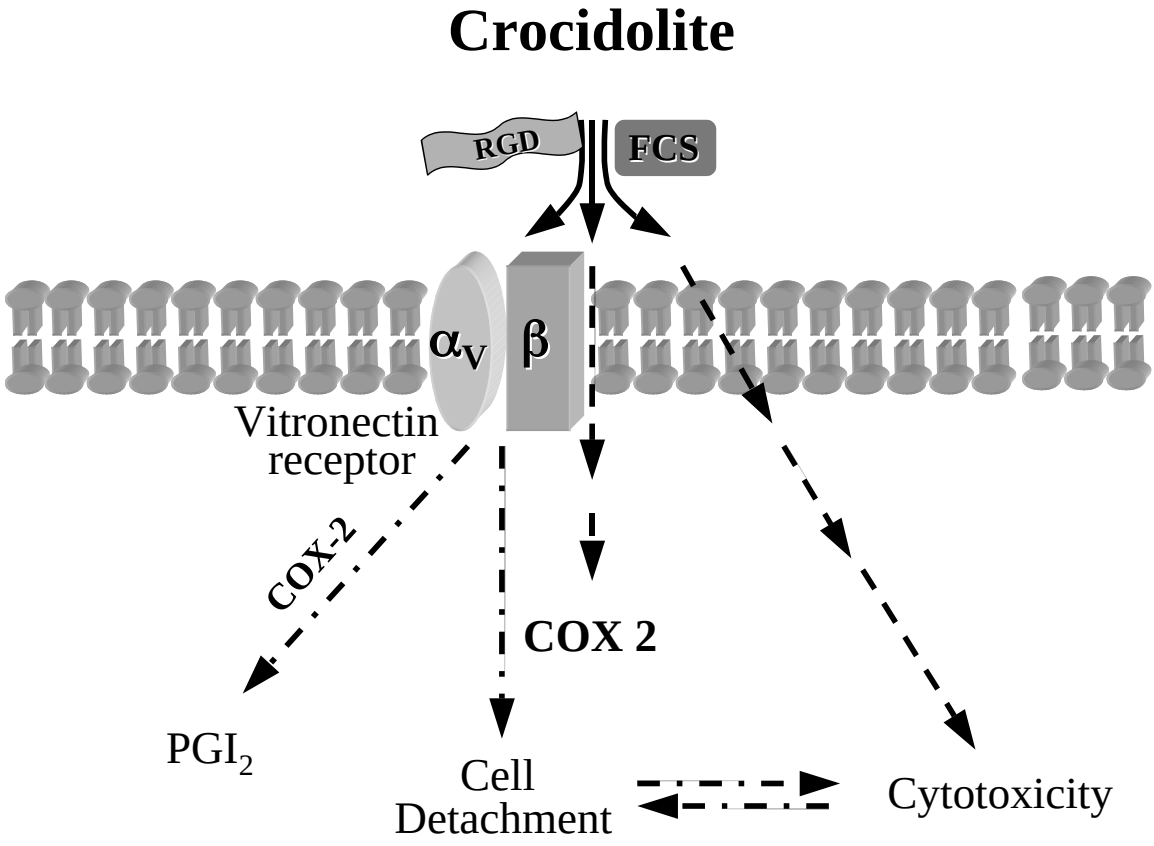

First, an RGD protein present in fetal bovine serum and BALF coats crocidolite and binds VNR. This interaction will induce Cox 2 expression and activity promoting prostacyclin biosynthesis. Second, crocidolite also induces cytotoxicity independently from RGD protein, VNR, Cox 1 or Cox 2. And third, cells bind RGD coated crocidolite fibers through VNR and detach from the bottom of the flask forming floating clusters of cells attached to crocidolite fibers. Then, floating cells become cytotoxic and die

Chapter 3

Role of Scavenger Receptors in Silica Binding and Apoptosis

Silicosis is the ILD produced by the inhalation of silica particles. ILD are a large and heterogeneous group of lower respiratory tract disorders, also known as “Interstitital pulmonary fibrosis” or “Diffuse parenchymal lung disease.” Silica particles, after reaching the alveoli, are phagocytosed by the resident alveolar macrophages (AM). Macrophages containing silica undergo apoptosis releasing the particles that will be taken up by other AMs. This permanent cycle of phagocytosis-apoptosis contributes to the induction of ILD (Wang, Antonini et al., 2003; Wang, Scabilloni et al., 2005). The macrophage scavenger receptor A (SR-A or CD204) is a pattern recognition receptor able to interact with multiple ligands with different levels of affinity. It has been reported that SR-A has an important role in the process of silica-induced apoptosis, but the mechanism is still unknown (Chao, Hamilton et al., 2001; R. F. Hamilton, de Villiers et al., 2000; R. F. Hamilton, Iyer et al., 1996; Iyer, Hamilton et al., 1996)

Structurally SR-AII is a trimeric transmembrane protein that contains five domains: 1) cytoplasmic, 2) transmembrane domain, 3) spacer, 4) α-helical coiled-coiled, and 5) collagenous domain. SR-AI contains an additional 6th domain called cysteine-rich (SRCR) (Kodama, Freeman et al., 1990). The role of the cytoplasmic domain in surface expression and modified LDL internalization had been previously described (Kosswig, Rice et al., 2003; Morimoto, Wada et al., 1999). The cytoplasmic region of SR-AI and II contains twelve amino acids that could be phosphorylated (Ser and Thr). Four of these

amino acids are common in the SR-A sequence of five different mammalian species. These amino acids correspond to Ser25, Ser32, Ser53, and Thr34 in the SR-A mouse sequence. Based on this information, it is possible that these four amino acids play an important role in SR-A signaling.

As mentioned above, the key difference between SR-AI and SR-AII is that SR-AI contains a SRCR. Previous studies comparing SR-AI and SR-AII binding properties were performed using modified LDL as ligands, showing no difference in polyanion binding specificity between both SR-As. Since there are no studies evaluating the role of the SR-A cytoplasmic domain in the silica-induced apoptosis or comparing binding properties between SR-AI and SR-AII using silica as a particulate ligand, we generated the following general hypothesis:

Hypothesis

"Silica binding to SR-A results in an induction of apoptosis mediated by a signal transduction mechanism beginning at specific cytoplasmic domains, and the presence of the SCRC domain in SR-AI increases the binding efficiency of silica."

Aims

I. Evaluate the effect of transfected wild type CD204 in CHO cells (null for CD204).

II. Identify which amino acids (Ser or Thr) in the cytoplasmic domain of CD204 are responsible for the induction of apoptosis.

III. Evaluate the role of SRCR domain by comparing SR-AI and SR-AII containing clones in their response to silica.

Aim I. Evaluate the effect of transfected wild type CD204 in CHO cells (null for CD204)

It has been previously described that CHO cells normally null for SR-AII become apoptotic after silica exposure when they express SR-AII (R. F. Hamilton, de Villiers et al., 2000). In this aim a SR-AII construct was developed and CHO cells were stably transfected in order to generate CHO cells expressing SR-AII as previously described in the Hamilton et al. paper. Stably SR-AII transfected cells were used as a positive control in further studies to evaluate silica-induced apoptosis. After generating the stably SR-AII CHO transfected cell line their functionality was examined by measuring binding and uptake of AcLDL, and apoptosis following silica exposure

a. Induce expression of CD204 in CHO cells.

b. Evaluate functionality of the CHO-CD204 transfected cells.

c. Determine apoptosis induced by silica in CHO-CD204 transfected cells.

Aim I.a. Induce expression of CD204 in CHO cells.

After generating the SR-A constructs, stable CHO cell lines expressing SR-AII were developed by transfecting CHO cells with the constructs.

Methods

Cell Culture

Chinese Hamster Ovarian cells CHO-K1 cells (ATCC, Manassas, VA) were maintained in Ham's F12K medium (Mediatech, Inc.) supplemented with 2 mM L-glutamine adjusted to contain 100 units/ml of penicillin, 100 µg/ml streptomycin, 0.25 µg/ml amphotericin B (Mediatech, Inc.), and 10% fetal bovine serum (Hyclone). Cell cultures were incubated at a temperature of 37ºC in an atmosphere of 95% air and 5% CO_2 (ThermoForma).

Plasmid Constructs

Mammalian expression vectors pcDNA3.1(+) Hygro and pcDNA3.1/myc-His-A (Figure 3.1) were purchased from Invitrogen. The murine SR-AII cDNA used was obtained from Invitrogen NIH Mammalian Gene Collection full-length (IRAV), clone ID 3594142 Mus musculus macrophage scavenger receptor 1 cDNA, which was inserted into a pCMV-SPORT6 vector. The following procedures were performed in order to subclone the SR-AII cDNA into the pcDNA3.1(+) Hygro vector. The restriction sites KpnI and XbaI were identified in the SR-AII cDNA at the 5’ and 3’ terminus respectively. In order to use the pcDNA3.1/myc-His-A vector, a mutation of the stop codon was required to achieve the expression of the myc epitope and 6X His tag

contained in the vector. The forward primer containing a KpnI restriction site 5'-GCT GCT GGT ACC ACG CGT CCG ATA AAT CAG TGC TGT-3', and the reverse primer containing an XbaI restriction site and a mutation of the stop codon 5'-GCT GCT TCT AGA GGG TAC TGA TCT TGA TCC GCC TAC-3' were used. PCR was run using these primers and Pfu DNA polymerase from Stratagene (La Jolla, CA). PCR products and vectors were digested with KpnI and XbaI, and ligated with T4 DNA Ligase from Promega (Madison, WI). All constructs were verified by restriction map and sequencing. Sequences were compared with the GenBank Mus musculus macrophage scavenger receptor 1, mRNA (cDNA clone MGC:6140 IMAGE:3594142), accession number BC003814.1.

Transfection

The following constructs were transfected in CHO cells separately: EVh (pcDNA3.1(+) Hygro), EVn (pcDNA3.1/myc-His-A), SRA-IIh (pcDNA3.1(+) Hygro + SR-AII), and SR-AIIn (pcDNA3.1/myc-His-A + SR-AII). Lipofectamine 2000 Transfection Reagent (Invitrogen) was used for CHO cell transfection following manufacturer's instructions. Briefly, 24 hours before transfection CHO cells were plated in 24-well plates at 1.2 x 10^5 cell per well in 0.5 ml of antibiotic free medium. Then 0.8 μg of vector DNA and 2.5 μl of transfection reagent were diluted in separate tubes with 50 μl of Opti-mem I reduced serum medium (Invitrogen). After five minutes of incubation at room temperature both solutions were combined and re-incubated at room temperature for 20 additional minutes. The combined solution was then added directly to the well containing CHO cells and mixed. Cells were incubated at the conditions

previously mentioned and growth medium was changed after 4 hours. Forty-eight hours after transfection, Geneticin or Hygromycin antibiotic (Invitrogen) was added at a final concentration of 500 or 700 μg/ml respectively, for antibiotic selection of transfected cells. Successful clones were isolated and characterized.

Confirmation of Genomic Incorporation

Genomic DNA was isolated from one to two million transfected cells with the DNeasy Blood & Tissue Kit from Qiagen Inc. (Valencia, CA). Isolated genomic DNA was amplified using T7 as sense primer (present only in the vector) and as antisense the SR-AII primer 5'-CCT CCA TGT CCT TCA TGT GTG- 3'. PCR was run using Pfu DNA polymerase from Stratagene.

Immunoprecipitation and Western Blot

Cells were cultured on 75 cm^2 flasks. After scraping, ten million cells were incubated on ice for 30 min in 200 μl of lysis buffer as previously described (R. F. Hamilton, de Villiers et al., 2000). Rat anti mouse CD204 antibody (2F8) from Serotec (Oxford, UK) was added to reach a final dilution of 1:40, and incubated overnight at 4°C in an end-over-end rotator. Thereafter 30 μl of Protein G-agarose from Roche Applied Science (Indianapolis, IN) was added and incubated under the same conditions overnight. The lysate containing the antibodies and protein G-agarose was washed three times and 30 μl of Laemmli sample buffer containing 5% beta mercaptoethanol was added. CD204 immunoprecipitated cell lysate was incubated at 70°C for ten minutes, loaded in a 4-15% linear gradient Ready Gel Tris-HCl gel from Bio-Rad (Hercules, CA), and

electrophoresed for 1 hour at 100 volts. Proteins were electrophoretically transferred to a Trans-Blot Transfer medium nitrocellulose membrane (Bio-Rad) for 1.5 hrs at 100 volts and blocked for 1 hour at room temperature with buffer containing non-fat milk dry 5%. Primary monoclonal anti-6X His tag antibody from Abcam (Cambridge, MA) was added to reach at a final dilution of 1:5000, and incubated overnight at 4°C. Nitrocellulose membranes were washed 3 times for 5 minutes each and exposed to horseradish peroxidase conjugated anti-rabbit IgG antibody from Cell Signaling Technology (Danvers, MA) for 1h at room temperature. Enhanced chemiluminescence (ECL) development was performed with ECL western blotting detection reagents from Amersham Biosciences (Piscataway, NJ) according to manufacturer's instructions. Images were taken using a Versadoc Imaging System 3000 (Bio-Rad).

Results

In order to establish a transfection control for future comparisons, constructs containing the mammalian expression vectors pcDNA3.1(+) Hygro or pcDNA3.1/myc-His-A only were used and named empty vector (EV) EVh or EVn respectively. Constructs generated with SR-AII were named SR-AIIh or SR-AIIn as for EVs. Restriction mapping was performed with the enzyme Sca I on both constructs to verify the final product containing SR-AII. Figures 3.2 and 3.3 show the presence of the SR-AII in both constructs. Sequence results were confirmatory of SR-AII cDNA sequence (data not shown). After transfection, SR-AIIh incorporation in CHO cell genome was verified by the presence of a PCR product of around 500 base pairs (Figure 3.4). Protein expression was confirmed in cells transfected with SR-AIIn by IP and WB due to the

presence of 6X-His tag (Figure 3.5). SRA-IIn monomer has a molecular weight of approximately 75 kDa, the MW of the band shown in Figure 3.5. Also a band of approximately 60 kDa could be seen in each of the different groups of cells. This band could be the result of some non-specific binding by the heavy chain of the anti-CD204 IgG used for IP. The presence of the 75 kDa band not only confirmed the expression of SRA-II, but also demonstrated that the full length of the SRA-II including the 6X His tag was expressed. After verifying SR-AII protein expression, SR-AII surface functionality was evaluated in the SR-AII transfected CHO cells.

Aim I.b. Evaluate functionality of CD204 in CHO transfected cells.

Total SR-A expression was verified previously by IP, but not SR-A expression on the cell surface. This aim looked for a better approach of determining SR-A functionality on the surface of transfected CHO cells using different techniques such as AcLDL uptake and silica binding in order to verify SR-A surface expression.

Methods

Acetylated Low Density Lipoproteins (AcLDL) Uptake

Cells were plated in a Lab-Tek II eight-well chamber slide from Nalge Nunc International (Rochester, NY) at $5x10^4$ cells per well 24 hours before exposure. When SR blocking ligands were used, cells were pre-treated with Polyinosinic acid (PolyI) from Sigma-Aldrich (St. Louis, MO) at 100 μg/ml or anti CD204 blocking antibody 2F8 (Serotec) at 1 μg/ml for 30 minutes as previously reported (Obot et al., 2002). Alexa Fluor 488 conjugated AcLDL (Invitrogen) was then added to the cells at a final concentration of 10 μg/ml and incubated for 90 minutes at 37ºC. After incubation medium was removed, cells were fixed with 3% paraformaldehyde in PBS, incubated for 20 minutes at room temperature, and washed four times with PBS as reported by DiDonato et al., for the study of lipid droplets (DiDonato & Brasaemle, 2003). Nuclei staining with propidium iodide (PI) was performed for cell detection. PI was added at a final concentration of 500 ng/ml, incubated for 5 min at room temperature and washed three times with PBS. Images were taken at 400x magnification with a Zeiss Axioskop

Fluorescence Microscope using a FITC/GFP filter (blue light) for Alexa Fluor 488 and Rhodamine/Texas Red filter (green light) for PI. Confocal microscopy pictures were taken at 1000x magnification with a Radiance 2000 Laser Scanning System (BioRad) attached to a Nikon Eclipse TE300 microscope. Images were processed with Adobe Photoshop version 7.0.1 and ImageJ version 1.35q. For fluorescence quantification, slides were scanned using a Laser Scanning Cytometer (LSC) with a 20x objective. Cells were detected by contouring around nucleic acid PI stain and data was analyzed with WinCyte LSC software V3.6 from CompuCyte Corporation.

Silica Exposure

Crystalline silica (min-U-sil-5) 1-5 µm diameter from Pennsylvania Sand Glass Corp. (Pittsburgh, PA) was initially acid washed in 1M HCl at 100ºC, washed in sterile water three times and dried at 200ºC. Silica suspension (40 mg/ml) was freshly made by mixing in pure water. The suspension was sonicated using a Sonicator Ultrasonic processor XL (Misonix) for one minute, mixed with fresh cell culture media and added to the cell cultures.

Quantification of Silica Binding and/or Uptake

One million cells were exposed to silica at a concentration of 150 µg/ml in an end-over-end rotator for 90 minutes at 37ºC. Silica binding/uptake was quantified by evaluating cell granularity as measured by flow cytometric right angle scatter (RAS), which correlates with particle binding/uptake (Palecanda & Kobzik, 2000).

Statistical Analysis

Results were presented as the mean and SEM unless indicated. When required data was normalized with its respective control in order to exclude differences in background conditions. Data was analyzed using Student T test for independent variables, paired T test, ANOVA, or nonparametric statistics (Mann-Whitney U test was used when comparing two groups, and Kruskal-Wallis test when comparing three groups or more). Statistics analyses were performed using the software GB-Stat version 6.5.6. Alpha error was set at $p<0.05$.

Results

In order to verify functional surface expression of SR-AII on CHO transfected cells fluorescent microscopy studies were performed. Cells transfected with each construct (SR-AIIh or SR-AIIn) internalized fluorescent labeled AcLDL. This was verified by co-localization of the Alexa488 labeled AcLDL with the PI labeled cells using the fluorescence microscope (Figures 3.6 and 3.7). Fluorescence quantification of the Alexa488 labeled AcLDL in the cells using the LSC confirmed the observations of the fluorescence microscope due to an increase in fluorescence in the cells transfected with SR-AII. Because AcLDL have been internalized by SR-AII receptors and SR-AII receptors needed to be on the cell surface in order to bind and internalize AcLDL, these results strongly support the idea that functional SR-AIIh and SR-AIIn are expressed on the cell surface. (Figures 3.8 and 3.9). In order to verify if the increase of AcLDL uptake was specific for SR-AII expression, SR-AII blocking ligands 2F8 (CD204 specific) and PolyI (broad unspecific scavenger receptor ligand) were used in each transfected SR-AII

construct. Figures 3.10 and 3.11 show the results of these experiments in percentage. Fluorescence values within each experiment were very different, but the blocking antibody 2F8 decreased the uptake of AcLDL in every experiment. Due to the difference in fluorescence among experiments, paired T tests were performed between the group with AcLDL and each groups with inhibitors. A statistically significant decrease in AcLDL uptake was found in each group that received SR-AII inhibitors. This indicated that AcLDL uptake was SR-AII specific. After verifying SR-A functionality, some preliminary silica binding studies were performed. Several attempts were performed in order to detect silica binding/uptake by side scatter (granularity) in SR-AII transfected CHO cells. Figures 3.12, 3.13, and 3.14 show these results with each construct (SR-AIIh and SR-AIIn). In every experiment run, side scatter apparently was higher in the control groups (EVh or EVn) than in the SR-AII transfected groups. All these finding show that SR-AII is functional on the cell surface of transfected CHO cells due to the increase in AcLDL uptake. Unfortunately the same transfectants did not bind/uptake silica (evaluated by side scatter) in any of the three experiments run. On the contrary SR-AII transfectants exposed to silica showed less granularity than exposed controls. Because silica interaction with SR-AII induces apoptosis (R. F. Hamilton, de Villiers et al., 2000) the next aim evaluated silica SR-AII interaction by apoptosis detection.

Aim I.c. Determine apoptosis induced by silica in CHO-CD204 transfected cells.

Stable transfected CHO cells expressing functional SR-A were exposed to silica in order to induce apoptosis as previously reported. Apoptosis detection was performed using different methods previously reported (Lecoeur, 2002; Lovborg et al., 2005; Plaetzer et al., 2005).

Methods

Apoptosis Assays

TiterTACS: Apoptosis detection was performed by in situ detection of DNA fragmentation in immobilized cells. TiterTACS (R&D systems, Minneapolis, MN) labels fragmented DNA allowing colorimetric detection of apoptotic cells. Cells were scraped and plated 24 hours prior to exposure at 2 $x10^5$ cell in a volume of 200 µl per well in a 96 well plate. Cell culture media was changed at exposure time. Silica was added to a final concentration of 66.7 µg/cm^2. Cells were exposed to silica for 24 hours before performing any assessment. After fixing the cells, TiterTACS was used to detect DNA fragmentation according to manufacturer's assay protocol. Absorbance at 450 nm was measured.

Caspase-3 Activity Assay for High Throughput Screening (HTS): Caspase 3 is a terminal caspase activated during apoptosis and can serve as an assay for undergoing apoptosis. After apoptotic stimuli cells activate Caspase-3. Activated Caspase-3 specifically cleaves after the aspartate residues in the DEVD peptide sequence. Detection of the cleavage of a fluorescent labeled DEVD containing substrate can be achieved by monitoring the shift in fluorescence. Caspase-3 Activity Assay for HTS was purchased from Calbiochem (EMD,

San Diego, CA). Cells were scraped and plated 24 hours prior to exposure at 2 x10^5 cell in a volume of 100 µl per well in a 96 well plate. Cell culture media was changed at exposure time. Silica was added to a final concentration of 50 µg/cm^2 and cells were exposed to silica for 24 hours before performing any assessment. Caspase-3 activity was detected according to manufacturer's assay protocol. Fluorescence was detected at an excitation wavelength of 400 nm and emission wavelength of 505 nm.

Tunel Assay (Terminal Deoxynucleotide Transferase dUTP Nick End Labeling): As previously described, apoptotic cells degrade their nuclear DNA into fragments, and its detection allows the identification of apoptotic cells. Cells were scraped and 1.5 x 10^6 cells were transfered to 25 cm^2 flasks and preincubated for 48 hours. Silica was added at a final concentration of 50 µg/cm^2. After 24 hour-exposure cells were trypsinized, washed and transferred to fresh tubes for DNA labeling. APO-BrdU TUNEL Assay Kit from Invitrogen was purchased. Cells were fixed and stained following manufacturer's assay protocol. Samples were analyzed by flow cytometry.

Cell Cytotoxicity Assays

Viability Assay: Cells were scraped and plated 24 hours prior to exposure at 50,000 cells in a volume of 200 µl per well in a 96 well plate. Cell culture media was changed at exposure time. Silica was added to final concentrations of 25, 50, and 100 µg/cm^2. Cells were exposed to silica for 24 hours before performing any assessment. After exposure, a volume of 100 µl of media was removed leaving 100 µl of media in each well. Twenty µl of CellTiter96 AQueous One Solution Reagent from Promega (Madison, WI) was added into each well and incubated for 1-4 hours at 37ºC in a humidified 5% CO_2 atmosphere.

Optical density (OD) was measured using a microplate reader (Molecular Devices, Sunnyvale, CA) at a wavelength of 490 and for reference at 650 nm. For normalizing, each control group (non-exposed) was considered to have 100% viability.

Cytotoxicity Assay: LDH release was measured using the Cytotoxicity Detection Assay (LDH) (Roche Applied Science, Indianapolis, IN). Cells were scraped and plated 24 hours before exposure as previously described. At exposure time, cell culture media was replaced with 1% FBS in order to decrease the LDH background absorbance, as recommended by manufacturer. Triton X-100 (Sigma-Aldrich Inc., St Louis, MO) at 1% was used as a positive control. After exposure 100 µl of cell culture media was transferred to a 96-well plate, mixed with 100 µl of reaction mixture, and incubated for 30 minutes at room temperature protected from light. OD was measured at a wavelength of 492 and 650 nm. Cytotoxicity was calculated as a percentage between minimum or 0% (non-exposed) and maximum or 100% (Triton X-100) control values.

Data was analyzed as previously described in Aim I.b.

Results

DNA fragmentation, a marker of apoptosis, was approximated using TiterTACS in SR-AIIn transfected cells exposed to 66.7 µg/cm^2 of silica. A slight, but not statistically significant increase in DNA fragmentation was observed (Figure 3.15). Caspase-3 activity, a second different method for the detection of apoptosis, was used. Silica exposure of at a dose of 50 µg/cm^2 did not increase caspase-3 activity in SR-AIIn transfected CHO cells in comparison with its transfected EVn control (Figure 3.16).

TUNEL assay detected by flow cytometry was performed in SR-AIIh transfected CHO cells after being exposed to silica 50 μg/cm^2. No difference was found between SR-AIIh and its respective transfected control (Figure 3.17).

Because apoptosis could not be consistently detected using several known techniques, cell cytotoxicity assays were performed in order to verify if silica is toxic to CHO transfected cells. CHO cells transfected with either SR-AIIh or SR-AIIn constructs did not show significant differences in LDH release in comparison with its respective transfection control when increasing silica doses of 25, 50, and 100 μg/cm^2 were used (Figures 3.18 and 3.19). Viability of CHO cells transfected with SR-AIIh was not different from its respective control when exposed to the same increasing silica doses of 25, 50, and 100 (Figure 3.20). However, it was observed that increasing doses of silica were similarly toxic in SR-AII and their respective transfection control. In order to determine if any kind of SR could be responsible for this silica-induced toxicity, SR-AII inhibitors were preincubated for 30 minutes before adding a silica dose of 50 μg/cm^2. The use of SR-A inhibitors 2F8 and PolyI did not decrease the release of LDH after silica exposure in any of the CHO transfected cells groups suggesting no SR-A involvement in silica-induced cytotoxicity (Figure 3.21).

Aim II. Identify which amino acids (Ser or Thr) in the cytoplasmic domain of CD204 are responsible for the induction of apoptosis.

The cytoplasmic region of SR-AI and II contains twelve amino acids that could be phosphorylated (Ser and Thr). Four of these amino acids are common in the SR-A sequence of five different mammal species. These amino acids correspond to Ser25, Ser32, Ser53, and Thr34 in the SR-A mouse sequence. In this study, this aim was carried out simultaneously with aim I evaluating the role of different constructs in silica-induced apoptosis.

a. Induce mutations in phosphorylation sites Ser 25, Ser 32, Thr 34, and Ser 53.

b. Induce apoptosis with silica in CHO cells transfected with each mutated CD204, and evaluate if apoptosis is inhibited or increased with each specific mutation.

Aim II.a. Induce mutations in potential phosphorylation sites Ser 25, Ser 32, Thr 34, and Ser 53.

SR-AI/II cDNA sequences corresponding to the cytoplasmic domain of five different species (human, mouse, bovine, dog, and rabbit) were aligned and a consensus of four Ser/Thr amino acids was found. Separate constructs expressing mutations in these cytoplasmic Ser/Thr. A fifth mutation affecting the extracellular lysine cluster, which is necessary for AcLDL binding (Andersson & Freeman, 1998; Doi, Higashino et al., 1993), was generated in order to verify if the lysine cluster was also necessary for silica binding.

Methods

Mutations

Mutations of the SR-AII Serines 25, 32, 53, Threonine 34, and Lysines 339-342 were performed separately. The constructs SR-AIIh and SR-AIIn were mutated using the QuikChange site-directed mutagenesis kit (Stratagene) following manufacturer's recommendations. The following primers (5' to 3') were designed to introduce those mutations:

1) S25A
    a. sense TGA CTG CAG TTC AGA AGC CGT GAA ATT TGA CGC AC
    b. antisense GTG CGT CAA ATT TCA CGG CTT CTG AAC TGC AGT CA
2) S32A
    a. sense TGA AAT TTG ACG CAC GTG CCA TGA CAG CAT CCC TTC C
    b. antisense GGA AGG GAT GCT GTC ATG GCA CGT GCG TCA AAT TTC A

3) S53A

   a. sense GGA GAA GTT GAA GGC CTT CAA GGC TGC CC

   b. antisense GGG CAG CCT TGA AGG CCT TCA ACT TCT CC

4) T34A

   a. sense CGC ACG TTC AAT GGC AGC ATC CCT TCC TC

   b. antisense GAG GAA GGG ATG CTG CCA TTG AAC GTG CG.

5) K-E

   a. sense GGA TCT CCT GGA CCT GAA GGA CAA GAG GGA GAG AAG G

   b. antisense CCT TCT CTC CCT CTT GTC CTT CAG GTC CAG GAG ATC C.

Once each mutated SR-AII was generated, DH5α cells (Invitrogen) were transformed with each mutated construct. After verifying each mutated construct by DNA sequencing, CHO cells were transfected with each construct separately using Lipofectamine 2000 Transfection Reagent (Invitrogen) as previously described in *Aim I.a*. Forty-eight hours after transfection Geneticin or Hygromycin antibiotic (Invitrogen) was added at a final concentration of 500 and 700 μg/ml respectively, for antibiotic selection of transfected cells for 15 days. Successful clones were isolated and characterized. Protein expression was confirmed by IP as described in *Aim I.a.*, and functionality by AcLDL uptake as described in *Aim I.b*.

Data was analyzed and presented as previously described in *Aim 1.b*.

Results

Constructs expressing mutated CD204 were isolated and verified by DNA sequencing (Figure 3.22). Protein expression of mutated CD204 were evaluated by IP and WB, which showed a band of approximately 75 kDa confirming the expression of the mutated SRA-II proteins (Figure 3.23). A second IP and WB was performed 4 weeks after the first one. Results were non consistent with previous findings showing increase or decrease on protein expression in the different mutations after 4 weeks (data not shown). In addition, it was not possible to determine surface expression of SR-AII due to the low affinity of the SR-AI/II antibody.

AcLDL uptake was quantified as previously described in *Aim I.b.* using the LSC (Figure 3.24). All of the transfectants expressing mutated cytoplasmic domain were able to internalize AcLDL, with no statistical difference between any of them and normal SR-AII. As expected, the K-En mutant did not bind AcLDL due to the lack of lysine cluster necessary for this function.

Aim II.b. Induce apoptosis with silica in CHO cells transfected with each mutated CD204, and evaluate if apoptosis is inhibited or increased with each specific mutation.

After verifying mutated SR-AII constructs expression and functionality by AcLDL uptake, silica-induced apoptosis was evaluated in all constructs to determine their role inducing apoptosis.

Methods

TiterTACS: Apoptosis detection was performed by in situ detection of DNA fragmentation in immobilized cells. TiterTACS (R&D systems, Minneapolis, MN) labels fragmented DNA allowing colorimetric detection of apoptotic cells. Cells were scraped and plated 24 hours prior to exposure at 2 $x10^5$ cell in a volume of 200 µl per well in a 96 well plate. Cell culture media was changed at exposure time. Silica was added to a final concentration of 66.7 µg/cm^2. Cells were exposed to silica for 24 hours before performing any assessment. After fixing the cells, TiterTACS was used to detect DNA fragmentation according to manufacturer's assay protocol. Absorbance at 450 nm was measured.

Caspase-3 Activity Assay for High Throughput Screening (HTS): Caspase-3 Activity was detected with the Assay for HTS purchased from Calbiochem (EMD). Cells were scraped and plated 24 hours prior to exposure at 2 $x10^5$ cell in a volume of 100 µl per well in a 96 well plate. Cell culture media was changed at exposure time. Silica was added to a final concentration of 50 µg/cm^2 and cells were exposed to silica for 24 hours before performing any assessment. Caspase-3 activity was detected according to manufacturer's

assay protocol. Fluorescence was detected at an excitation wavelength of 400 nm and emission wavelength of 505 nm using a plate reader.

Data was analyzed and presented as previously described in *Aim 1.b*.

Results

CHO cells transfected with SR-AIIn were exposed to 50 µg/cm^2 of silica for 24 hours. DNA fragmentation and Caspase-3 activity were evaluated and no statistically significant differences could be found between the mutated constructs and CHO cells transfected with SR-AIIn or the transfection control (Figures 3.25, and 3.26).

Hamilton et al reported that MARCO (another SR-A) can interact with silica and induce apoptosis in MARCO transfected CHO cells (R. F. Hamilton, Jr. et al., 2006). MARCO has a extracellular cysteine rich domain, which is also present in the SR-AI and not in SR-AII. Therefore the next aim was designed determine whether if the presence of the extracellular cysteine rich domain in SR-AI could confer functional differences in comparison with SR-AII.

Aim III. Evaluate the role of SRCR domain by comparing SR-AI and SR-AII containing clones in their response to silica.

In this study, all previous experiments have been performed using SR-AII. As previously described the structural difference between SR-AI and SR-AII is the presence of the cysteine region (SRCR) at the end of the extracellular region in SR-AI. Previous studies comparing SR-AI and SR-AII binding to modified LDL showed no functional difference between both receptors. Because it is unknown if silica binds both receptors with the same affinity, the present study look for silica binding differences between SR-AI and SR-AII. This aim evaluated whether there were any functional differences between SR-AI and SR-AII transfected cells by examining AcLDL uptake, silica binding, and silica-induced apoptosis.

Methods

The murine SR-AI cDNA used was obtained from pXmSRI-28 through a kind gift from Dr. Monty Krieger (Biology Department, MIT, MA). The procedure performed to subclone the SR-AI cDNA into the vector pcDNA3.1(+) Hygro (Invitrogen) was the same described in *Aim 1.a.* for SR-AII. After verifying the DNA sequence of the constructs, CHO cells were transfected. Measurement of the uptake of AcLDL and silica binding were performed as previously described in *Aim I.b.*, and apoptosis as previously described in *Aim I.c*. Data was analyzed and presented as previously described in *Aim 1.b.*

Results

After transfecting CHO cells and selecting them by antibiotic resistance, genomic incorporation of constructs was verified as previously described (Figure 3.27). The next step was to determine if both receptors were functional using AcLDL uptake as previously done. Both receptors were able to internalize AcLDL in amounts that were statistically significant. In all experiments CHO cells transfected with SR-AII internalized more AcLDL than SR-AI, but without a statistically significant difference (Figure 3.28). These results confirmed the functionality of SR-AI and SR-AII in CHO transfected cells. In order to verify the direct role of SR-A protein expression in the increase of AcLDL uptake, the specific SR-AI/II blocking antibody 2F8 and the unspecific PolyI inhibitor, were added 30 minutes before AcLDL exposure. Both inhibitors in all six experiments performed decreased AcLDL uptake in CHO cells transfected with SR-AI or SR-AII (Figure 3.29). When data was analyzed (paired T test), 2F8 blocking antibody did not decrease statistically significantly the AcLDL uptake in SR-AI transfected cells. However, because it was expected to induce only a decrease in uptake, statistical analysis using one-tail test was performed (instead of 2-tail test). Results showed a $p<0.05$ in the decrease of AcLDL in SR-AI transfectants when 2F8 was used. However, neither silica binding (detected by flow cytometric right angle scatter) nor apoptosis (detected by TUNEL assay) was different among control EVh, SR-AIh or SR-AIIh transfected cells (Figure 3.30 and 3.31). In order to verify if silica was able to induce toxicity in CHO transfected cells, cell cytotoxicity assays were performed. None of the SR-A transfected cells showed differences in LDH release (Figure 3.32) or viability (Figure 3.33) at increasing silica doses of 25, 50, and 100 $\mu g/cm^2$ in comparison

with EVh control. There was no functional difference between SR-AI and SR-AII when AcLDL was used. When silica studies were performed comparing SR-AI and SR-AII transfectants, no difference could be established.

Summary

Two different mammalian expression vectors pcDNA3.1(+) Hygro and pcDNA3.1/myc-His-were used in order to induce murine SR-AII expression in CHO cells. After transfection and antibiotic selection, it was verified that the constructs were incorporated into the genome. Cells transfected with SR-AII internalized AcLDL in statistically significant amounts. In addition, the AcLDL internalization was blocked the SR-A I/II inhibitors: 2F8 antibody and PolyI, confirming SR-AI/II involvement in AcLDL uptake. Silica binding of transfected CHO cells was not significantly different from transfected controls. Silica-induced apoptosis was approached by different methods such as TUNEL, and Caspase 3 activity. None of these methods found a statistically significant increase in apoptosis after silica exposure compared to their respective transfected controls. In addition Viability and LDH release were not statistically significant different between SR-AII and their respective transfected controls. Mutated cytoplasmic Ser or Thr constructs (S25, S32, S53, and T34) or mutated extracellular lysine cluster (K-E) constructs were generated in the mammalian expression vector pcDNA3.1/myc-His-A. All except K-E mutation internalized AcLDL as expected. None of the constructs produce any change in silica binding or apoptosis. SR-AI construct was generated and CHO cells were transfected with it. No statistically significant difference was found between SR-AI and SR-AII in AcLDL uptake, silica binding, silica-induced apoptosis, viability, and LDH release.

Discussion

Scavenger receptors are members of a family of membrane receptors, initially described as a binding site on macrophages that mediate uptake and degradation of AcLDL (Goldstein, Ho et al., 1979). Today, it is well recognized that scavenger receptors are a growing family of glycoproteins, implicated as pattern recognition receptors, that not only have a broad ligand binding ability to polyanions, but also are expressed in different cell types (Peiser & Gordon, 2001). The scavenger receptors class A (SRA) are expressed in macrophages and have the ability to bind ligands such as mLDL, negatively charged particles, silica (Chao, Hamilton et al., 2001; R. F. Hamilton, de Villiers et al., 2000; Iyer, Hamilton et al., 1996), asbestos (Resnick, Freedman et al., 1993), and LPS (Hampton et al., 1991). SRAs also have an important role mediating cell adhesion (I. Fraser, Hughes et al., 1993). There are six members of the SRA family: I, II, III, MARCO (Macrophage Receptor with Collagenous structure) (Arredouani & Kobzik, 2004), SRCL (SR with C-type lectin) (K. Nakamura et al., 2001), and SCARA5 (Jiang et al., 2006). SRA-I, SRA-II, and SRA-III are three alternative splice variants of the same gene. SRA-III is not functional and stays in the endoplasmic reticulum (J. E. Murphy et al., 2005).

The present study confirmed some previous findings reported about SR-A I/II binding AcLDL (modified LDL). Two different mammalian expression pcDNA3.1 vectors were designed, and transfected in CHO cells. Both transfectants were tested for AcLDL uptake. Fluorescent microscopy and fluorescence quantification confirmed that CHO cells expressing SR-AI or SR-AII bind and uptake AcLDL. Moreover, the use of

the specific SR-AI/II inhibitor 2F8 and non-specific SR inhibitor PolyI confirmed that the AcLDL uptake seen was SR-AI/II dependent.

The role of the SR-AI/II cytoplasmic domain in surface expression and modified LDL internalization has been previously studied (Kosswig, Rice et al., 2003; Morimoto, Wada et al., 1999). The mouse amino acid sequence of cytoplasmic SRA-II contains twelve amino acids that could be phosphorylated, and four of these are common in the SR-A sequence of five species as previously shown in Figure 1.13. These amino acids correspond to Ser25, Ser32, Ser53, and Thr34 in the SR-A I/II mouse sequence. Fong et al. reported, working with murine SR-AI/II, that only Serines were phosphorylated and that phosphorylation happened 2.5 and 5 minutes after AcLDL exposure of mouse peritoneal macrophages (Fong & Le, 1999). In addition, this same study reported that CHO cells expressing mutated murine SR-AI Ser25Ala had higher number of AcLDL binding sites in comparison with non-mutated SR-AI suggestive of an increase in receptor expression, but unfortunately no statistics were reported.

This present study generated five mutated constructs expressing S25A, S32A, S53A, T34A (all four Ser/Thr are common in five mammalian species), or K339-342E. The K339-342E mutation affects the extracellular lysine cluster, which is necessary for AcLDL binding (Andersson & Freeman, 1998; Doi, Higashino et al., 1993). Each mutated SR-AII transfectant was exposed to AcLDL. All transfectants incorporated AcLDL similarly with no statistically significant difference between mutated and normal SR-AII except the K-E mutant, which failed to uptake AcLDL uptake when compared with normal SR-AII. The K-E mutant lacks the lysine cluster required for AcLDL, so it was expected that this mutated SR-AII would not bind AcLDL. In addition, this study

found that mutated SR-AII behaved as previously reported for mutated SR-AI (Fong & Le, 1999), except for the Ser25Ala mutation. In the present study the Ser25Ala mutation showed no difference in AcLDL uptake. The differences between both studies are that this study used fluorescent-labeled AcLDL, quantification was performed by LSC, incubation was at 37ºC, and the mutated construct was a SR-AII version, and Fong et al. study used radiolabeled AcLDL, detection was performed by measuring cell-associated radioactivity, incubation was at 4ºC, and the mutated construct was a SR-AI version. Each difference could be a contributor for the difference seen. First, since there are no studies comparing LSC vs. radioactivity for the quantification of AcLDL, it is not possible to speculate about the accuracy of each method because the way data is collected, analyzed and presented is very different. Second, it has been previously described that when cells are incubated at 4ºC the binding properties of SR-AII are different than incubated at 37ºC (Andersson & Freeman, 1998; Doi, Higashino et al., 1993). And third, it has been previously reported that SR-AI and SR-AII have the same binding affinity for modified LDL (Ashkenas, Penman et al., 1993). Incubation temperature difference could be a major factor contributing to the different outcome between both studies, but another important factor to consider is the lack of statistics in Fong et al. results establishing that the increase in expression was statistically significant (or not). After verifying SR-AI or SRAII functionality by AcLDL uptake, silica binding studies determined by cell granularity were evaluated using flow cytometric right angle scatter (RAS), which correlates with particle binding/uptake (Palecanda & Kobzik, 2000). Unfortunately it was not possible to detect silica binding in any of the SR-AII constructs.

The next step was to evaluate silica-induced apoptosis in SR-AII transfectants. Apoptosis, also known as “programmed cell death”, has been initially described based on morphological criteria such as nuclear and cytoplasmic condensation, nuclear fragmentation, and formation of apoptotic bodies with intact plasma membrane (Kerr et al., 1972). Today some biochemical processes such as caspases induction have been described associated with the apoptotic process (Thornberry & Lazebnik, 1998). Different kinds of assay have been developed in order to detect and quantify apoptosis (Lecoeur, 2002; Plaetzer, Kiesslich et al., 2005). Unfortunately there is no consensus about which assay or marker is paramount for apoptosis detection. Apoptosis without caspase activation has been reported (Lovborg, Gullbo et al., 2005), and also DNA damage (TUNEL assay) with caspase precursor induction, but with no caspase activity or apoptosis (X. Liu et al., 2005).

TUNEL assay and caspase 3 activity have been previously tested in CHO cells (Yun et al., 2001) (Abdalah et al., 2006; Tannock & Lee, 2001). In the present study three assay were used: TiterTACS for DNA fragmentation in adherent cells, TUNEL assay, and caspase 3 activity. Unfortunately, none of these assays were able to detect a statistically significant increase in apoptosis in the SR-A I/II transfected group after silica exposure. Simultaneously TUNEL and Caspase 3 activity assays were evaluated in the SR-AII mutated transfectants after silica exposure, but no difference was found between each mutated SR-AII and normal SR-AII.

LDH release correlates with cell lysis as final outcome of cell death and also correlates with neuronal apoptosis (Lobner, 2000). Since, in the present study, it was not possible to detect a significant increase in silica-induce apoptosis in any of the SR-AI/II

transfectants, cell cytotoxicity assays were performed in order to detect any cell toxicity induced by silica exposure to the transfectants. In the present study no statistically significant difference in LDH release was found in the SR-A I/II transfected group after silica exposure. Because LDH release was observed in every silica-exposed group (including transfection control) SR-A inhibitors were used in order to verify if SR-AI/II or another SR were involved in silica induced LDH release. Unfortunately, no change was observed when SR-A inhibitors were used. When viability was detected after exposing the transfectants to silica, no changes between groups were also observed. A decrease in cell viability was observed in every group exposed to silica, but with no statistical difference when SR-AI/II transfectants were compared with their transfected control group.

The present study was not able to reproduce some of the findings previously reported by Hamilton et al. such as the silica-induced apoptosis of SR-AII transfected CHO cells (R. F. Hamilton, de Villiers et al., 2000) or the increase in AcLDL uptake in the mutated S25A-SR-AII transfected CHO cells (Fong & Le, 1999). The differences between this study and the one using a S25A-SR-AI mutant had been previously discussed. The most important differences between this study and the Hamilton et al study are discussed. The present study used CHO cells, an empty vector for transfection control, TUNEL assay and caspase activity for apoptosis detection, and LDH and MTS Viability assays. Hamilton et al. study used CHO ldl-A7 cells, an untransfected groups as control, histone-bound DNA fragments detection and Sub G_0 population for apoptosis detection, and Trypan blue exclusion for viability. Because each difference could be a contributor for the different outcomes, they will be discussed separately: First, the most

important difference between CHO cells and mutant ldl-A7 cells is that ldl-A7 cells are more susceptible because they cannot uptake LDL directly from the culture media so they need to synthesize their own LDL in order to survive. It is possible that the interaction of silica with SR-AII transfected cells interferes with the intrinsic LDL synthetic pathway, inducing apoptosis only in the ldl-A7 cells since it cannot uptake LDL from the cell culture media. Second, in both studies antibiotic selection of transfected clones with hygromycin or G418 was used. Because the insertion of a construct in the transfected cell followed by the addition of toxic antibiotic in the cell culture media could modify the normal cell behavior, it is recommended to use an empty vector control, in order to correct for changes in cell behavior as was done in the present study. Third, as previously discussed the use of one technique is not sufficient/recommended to establish apoptosis. The present study used two different assays to detect DNA fragmentation, and one for caspase 3 activity. Hamilton et al. used two different assays in order to detect DNA fragments and/or fragmentation. Because none of these assays were common to both studies, and the final outcome was similar in each study despite using different techniques, it is not possible to make a conclusion regarding which methods worked better. Fourth, viability and toxicity assay were also different between both studies. Hamilton et al. performed only one assay (viability), whose results correlated with the apoptosis studies. The present study performed cytotoxicity and a different viability assay, whose results also correlated with the apoptotic assessments of this study, unfortunately with opposite outcome. The results of the present study only allow to conclude that further studies are required in order to determine the role of silica in SR-AI/II mediated apoptosis and cytotoxicity in this model.

Figure 3.1

pcDNA 3.1 (+) Hygro and pcDNA 3.1/myc-HisA Mammal Expression Vector©

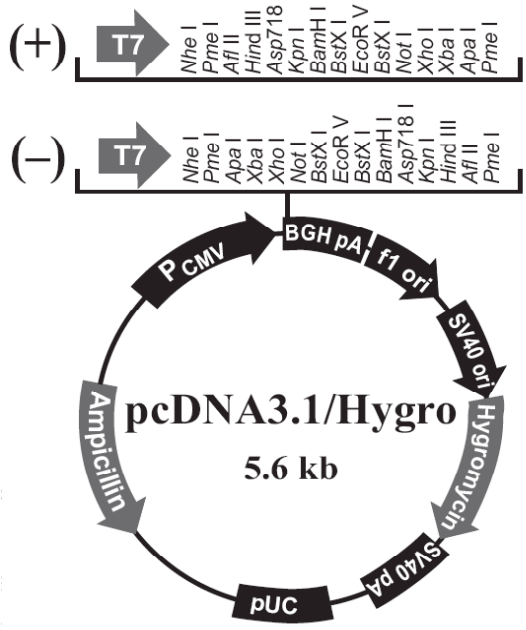

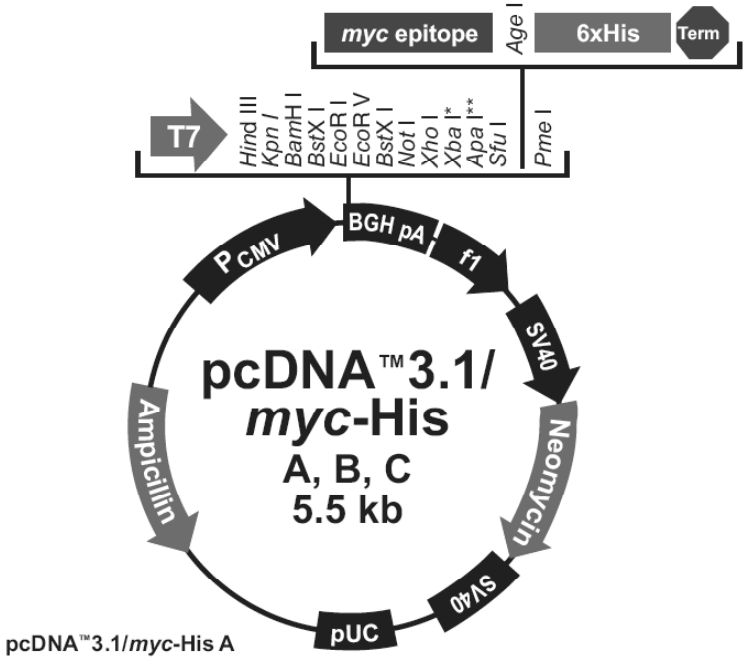

Figure 3.2

Sca I Restriction Map of SR-AIIh Construct

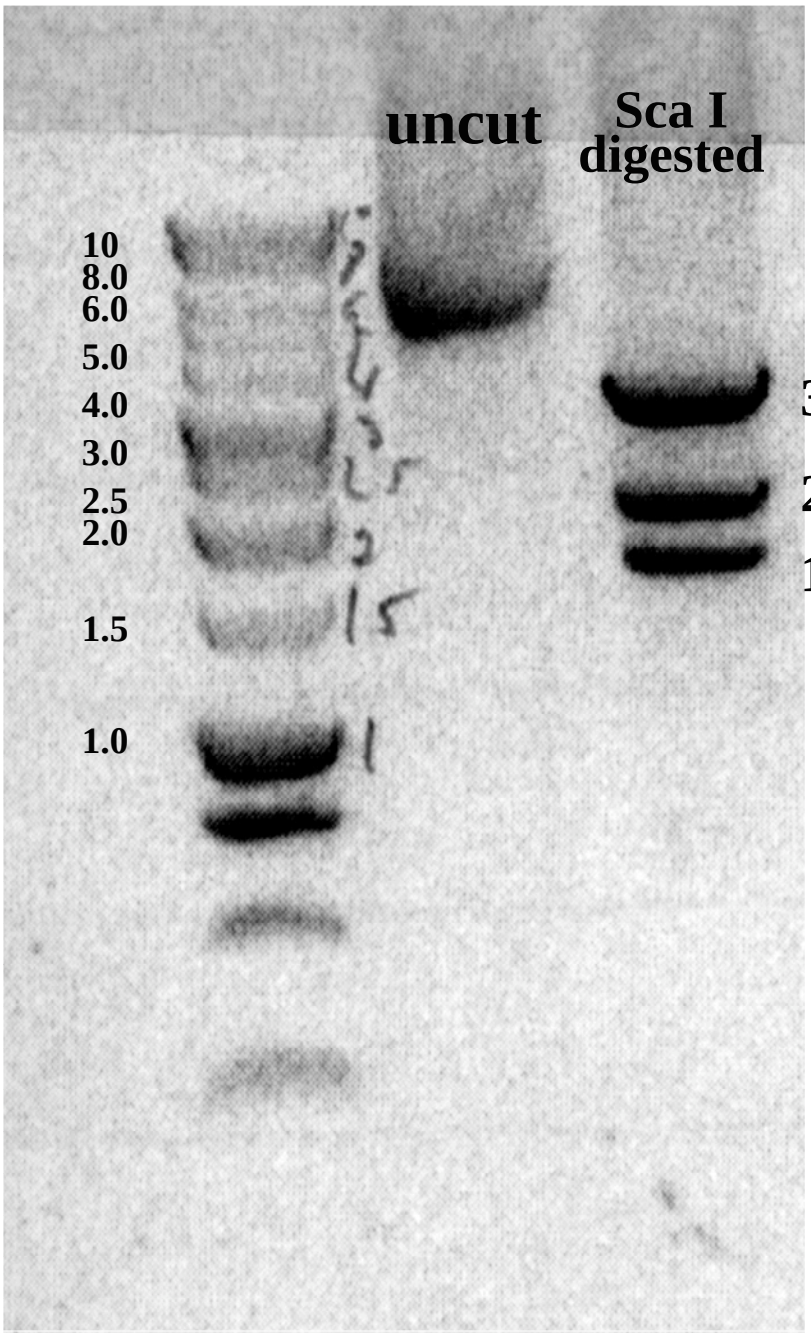

SR-AIIh constructs generated using pcDNA3.1 vectors were digested with the restriction enzyme ScaI for 3 hours at 37ºC. Then digested DNA was run in an 0.8% agarose gel. Bands in the digested construct show the presence of the construct containing SR-AII.

Figure 3.3

Sca I Restriction Map of SR-AIIn Construct

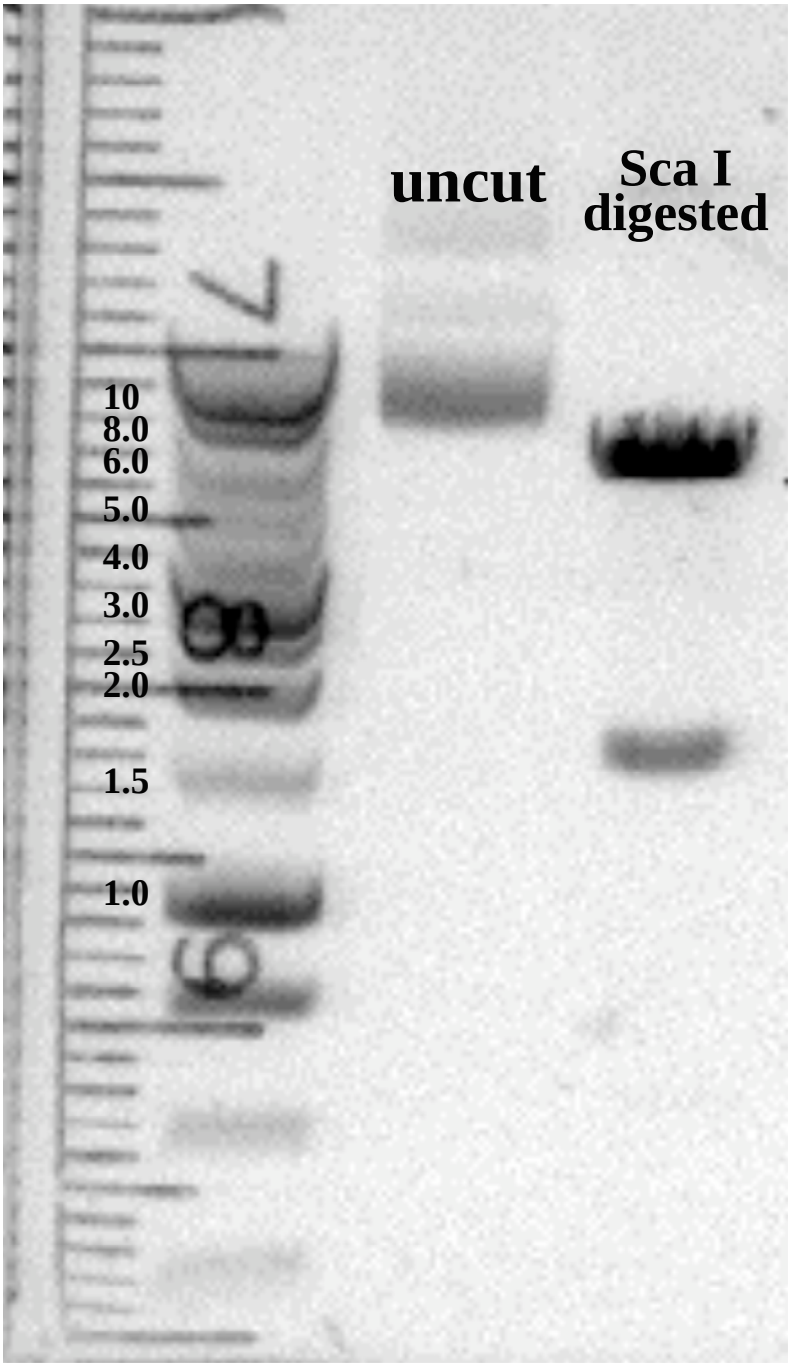

SR-AIIn constructs generated using pcDNA3.1 vectors were digested with the restriction enzyme ScaI for 3 hours at 37ºC. Then digested DNA was run in a 0.8% agarose gel. Bands in the digested construct show the presence of the construct containing SR-AII.

Figure 3.4

PCR Product Confirmatory of SR-AIIh Incorporation into Genomic CHO cells

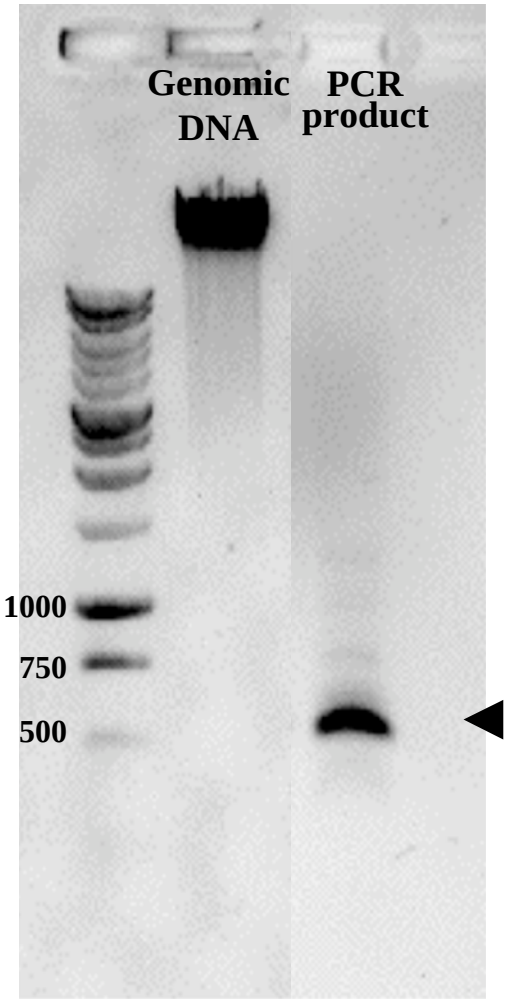

Genomic DNA was isolated from 1-2 million transfected CHO cells. DNA was amplified by PCR using a T7 primer corresponding to vector sequence, and a SR-AII primer. Then PCR product was run in a 0.8% agarose gel. Arrowhead shows PCR product band.

Figure 3.5

IP and WB of SRAIIn expressed in Transfected CHO Cells

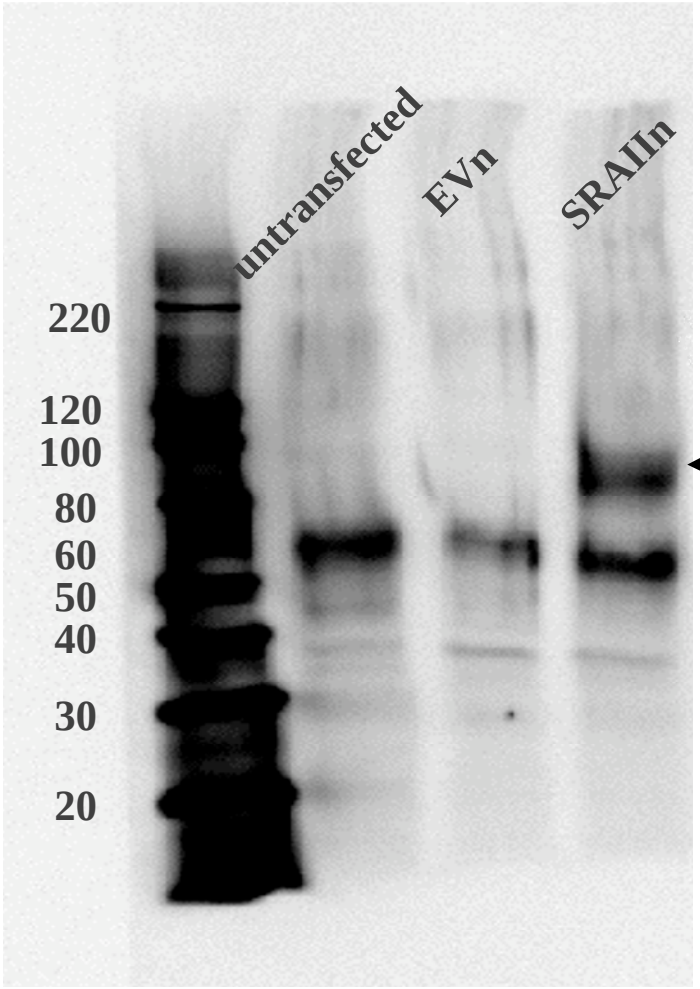

Ten million cells were lysed and IP with 2F8 antibody and protein G agarose. IP cell lysate was electhrophoresed and transferred to a nitrocellulose membrane for WB with monoclonal antibody anti-6X His tag. Bands were detected by enhanced chemiluminescence (ECL).

Figure 3.6

Uptake of AcLDL by SR-AIIh Transfected CHO Cells

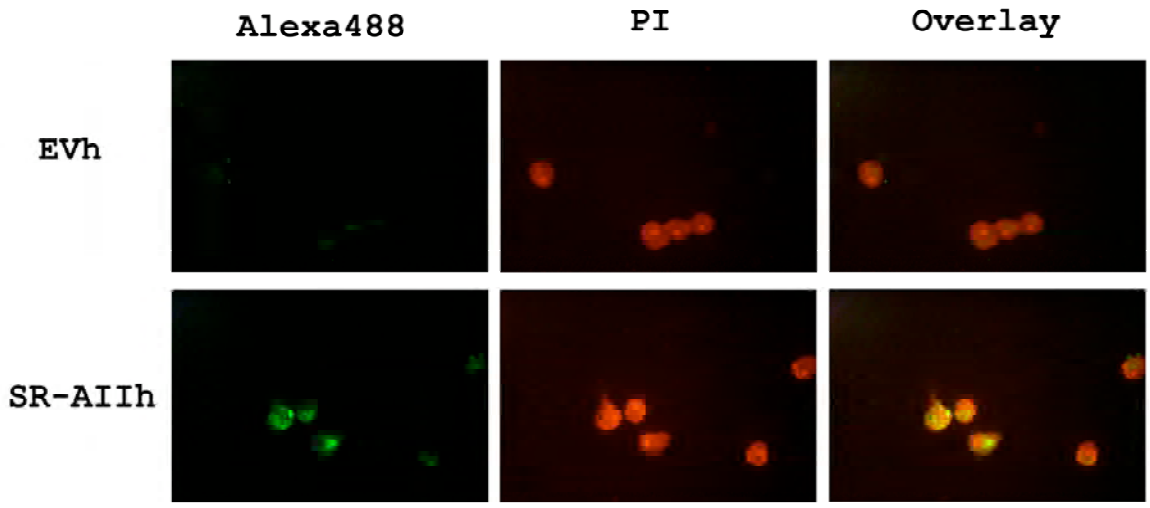

Uptake of AcLDL by transfected CHO cells with empty vector (EVh) and SRA-IIh. Cells were exposed to fluorescence labeled AcLDL for 90 minutes. Pictures were taken at 400x magnification using a FITC/GFP filter (blue light) for Alexa Fluor 488 (first column) and Rhodamine/Texas Red filter (green light) for propidium iodide (second column). The overlay at the third column shows co-localization between AcLDL and cells. 400x magnification with a Zeiss Axioskop Fluorescence Microscope

Figure 3.7

Uptake of AcLDL by SR-AIIn Transfected CHO Cells

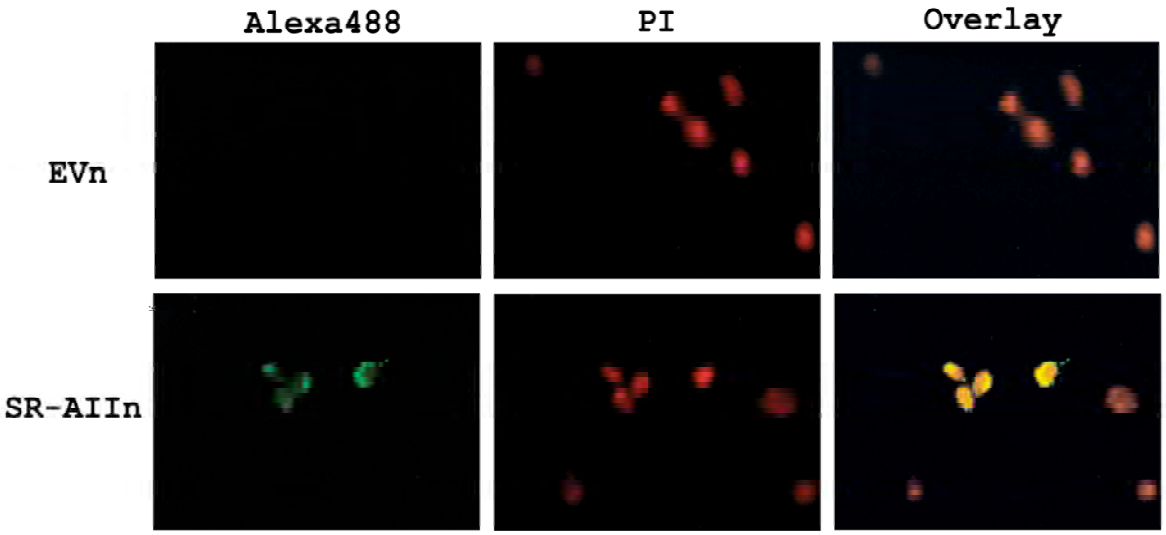

Uptake of AcLDL by transfected CHO cells with empty vector (EVn) and SRA-IIn. Cells were exposed to fluorescence labeled AcLDL for 90 minutes. Pictures were taken at 400x magnification using a FITC/GFP filter (blue light) for Alexa Fluor 488 (first column) and Rhodamine/Texas Red filter (green light) for propidium iodide (second column). The overlay at the third column shows co-localization between AcLDL and cells. 400x magnification with a Zeiss Axioskop Fluorescence Microscope

Figure 3.8

Uptake of AcLDL by SR-AIIh Transfected CHO Cells (N=6)

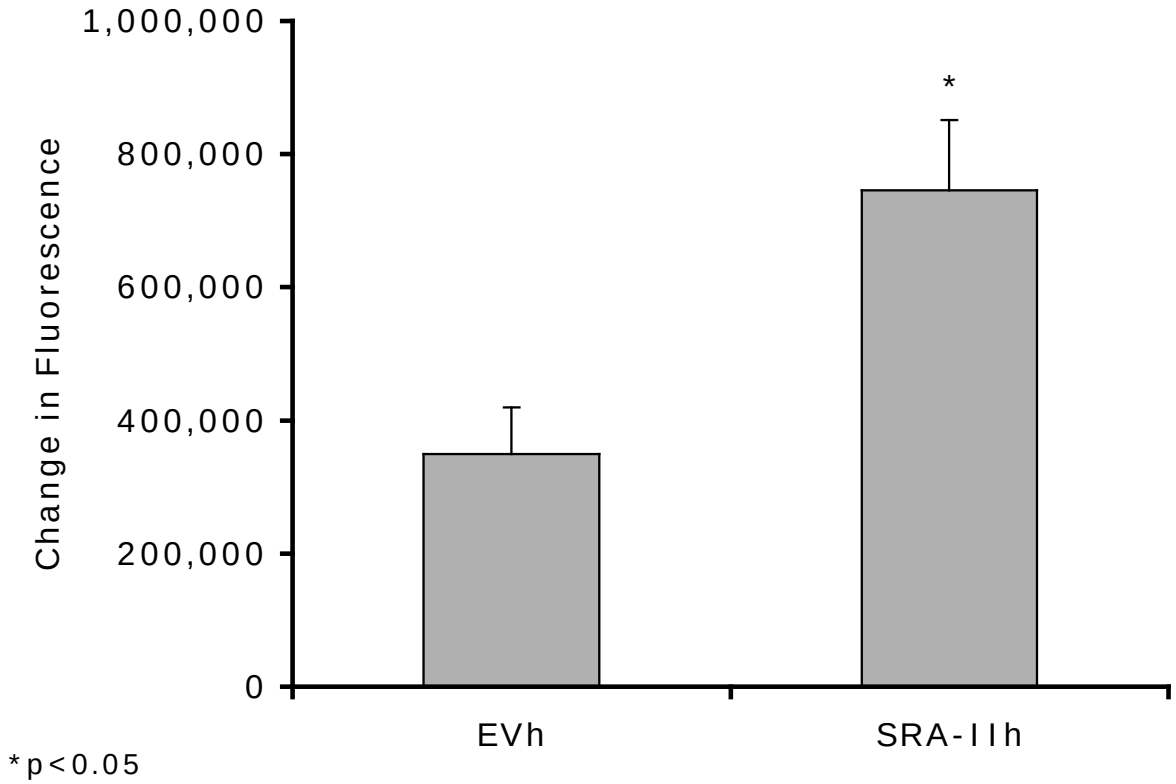

Uptake of AcLDL by CHO cells transfected with SRA-IIh Cells were exposed to fluorescence labeled AcLDL for 90 minutes. Quantification was performed using a Laser Scan Cytometer. Differences with its respective unexposed control were analyzed.

Figure 3.9

Uptake of AcLDL by SR-AIIn Transfected CHO Cells (N=5)

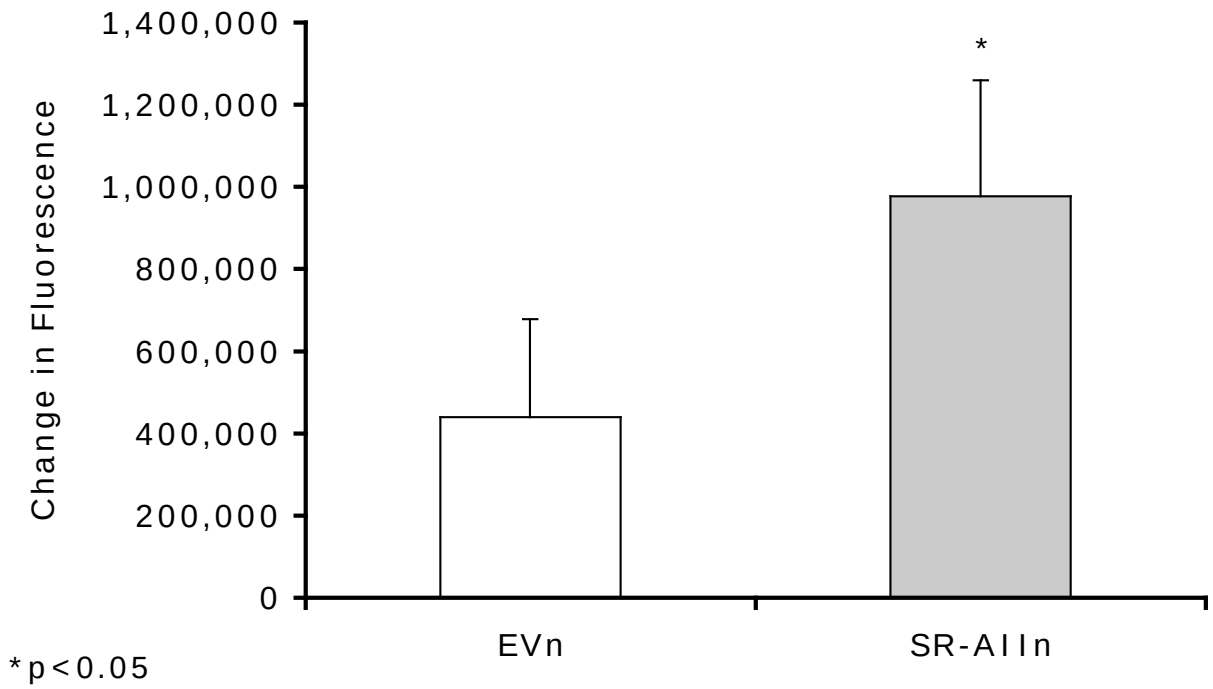

Uptake of AcLDL by CHO cells transfected with SRA-IIn Cells were exposed to fluorescence labeled AcLDL for 90 minutes. Quantification was performed using a Laser Scan Cytometer. Differences with its respective unexposed control were analyzed.

Figure 3.10

Inhibition of AcLDL Uptake in SR-AIIh Transfected Cells (N=6)

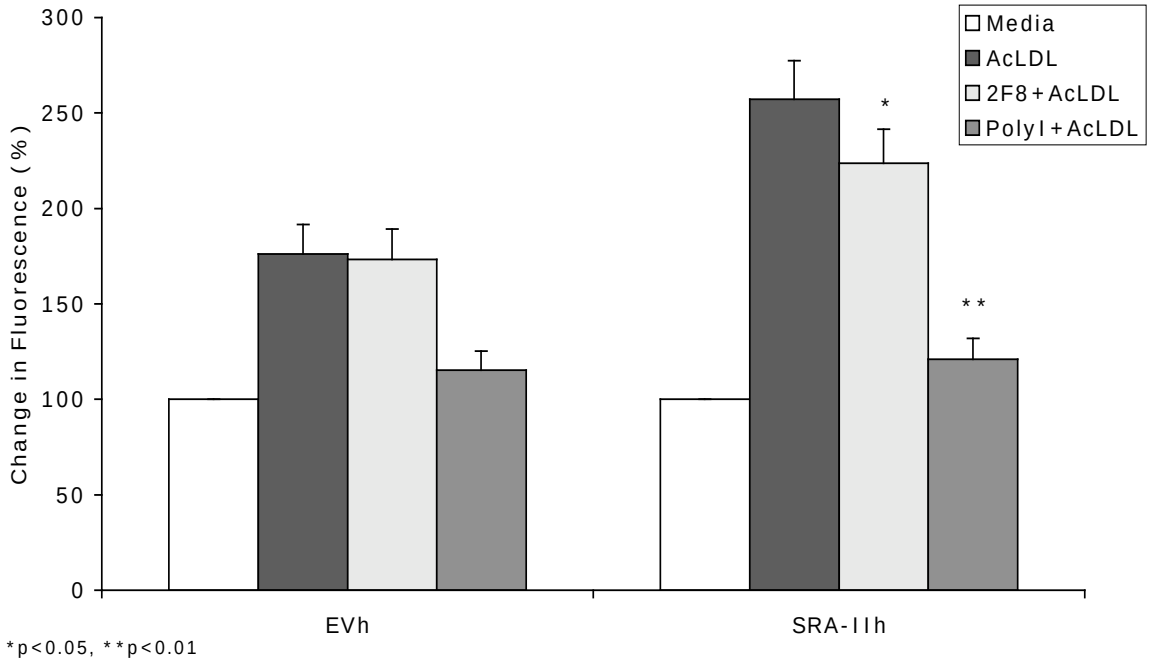

Uptake of AcLDL by transfected CHO cells with SRA-IIh when exposed to the SR-A inhibitors (ligands in a competition assay). 2F8 a specific SRA-I/II ligand (blocking antibody) and poly I a nonspecific ligand were used. Cells were pre-incubated 30 minutes with SR-A inhibitors before being exposed to fluorescence labeled AcLDL for 90 minutes. Quantification was performed using a Laser Scan Cytometer. Ratios with its respective unexposed control were analyzed and normalized to 100% for the control non-exposed group.

Figure 3.11

Inhibition of AcLDL Uptake in SR-AIIn Transfected Cells (N=2)

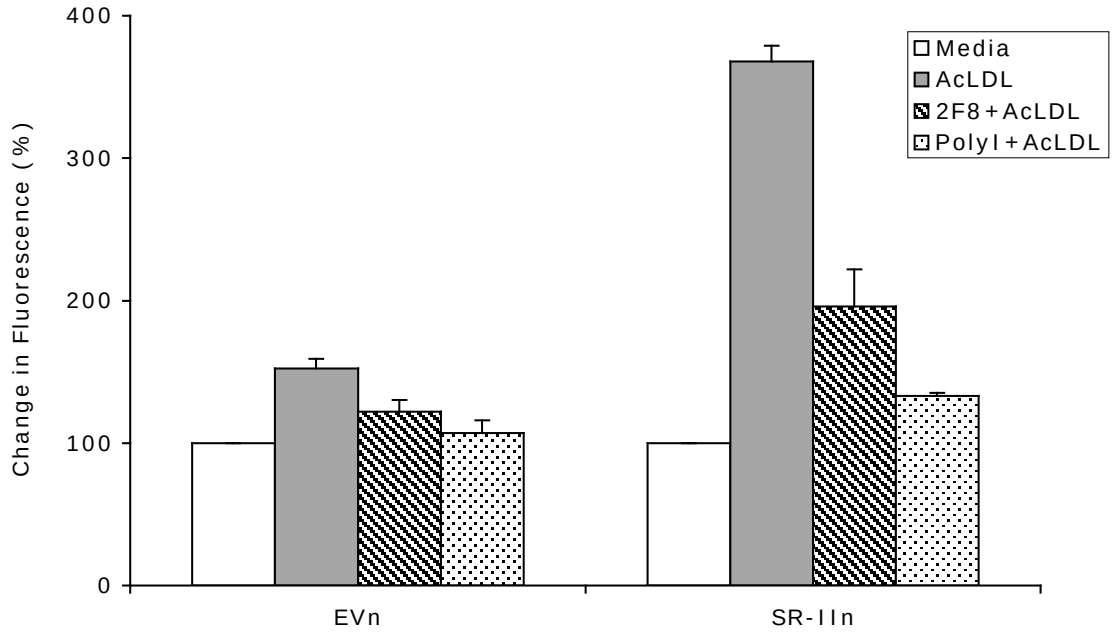

Uptake of AcLDL by transfected CHO cells with SRA-IIn when exposed to the SR-A inhibitors (ligands in a competition assay). 2F8 a specific SRA-I/II ligand (blocking antibody) and poly I a nonspecific ligand were used. Cells were pre-incubated 30 minutes with SR-A inhibitors before being exposed to fluorescence labeled AcLDL for 90 minutes. Quantification was performed using a Laser Scan Cytometer. Ratios with its respective unexposed control were analyzed and normalized to 100% for the control non-exposed group.

Figure 3.12

Change in Side Scatter in SR-AIIh Transfected Cells After Silica Exposure (N=2)

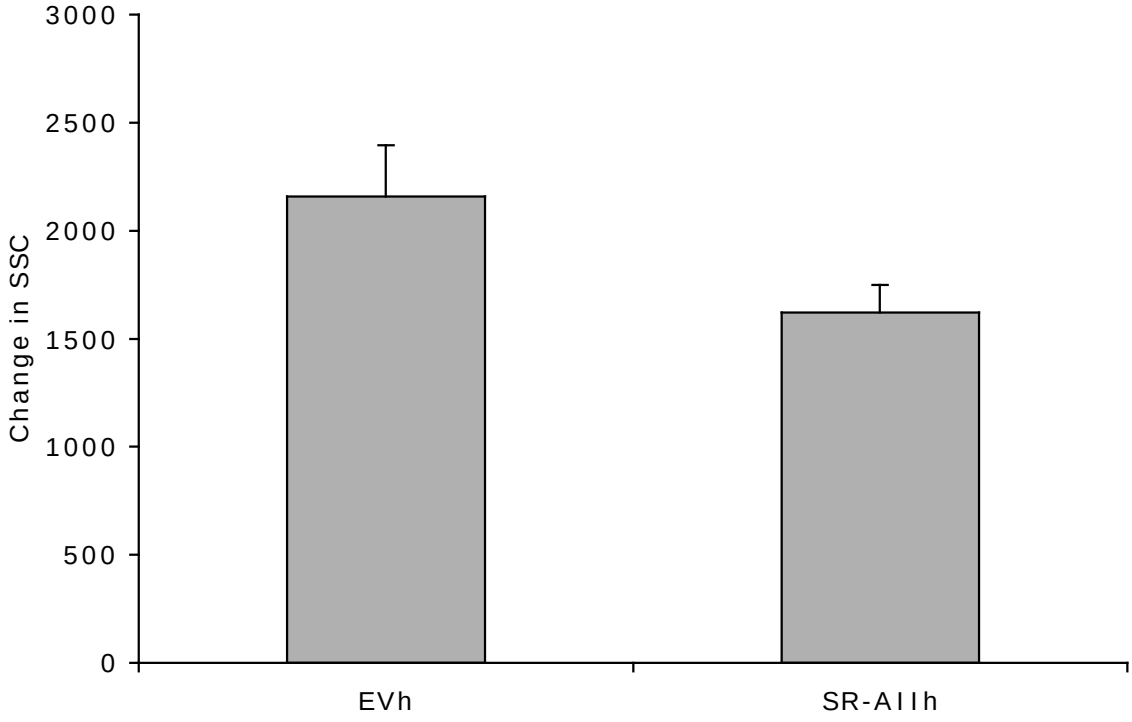

One million cells were exposed to silica at a concentration of 150 µg/ml in an end-over-end rotator for 90 minutes at 37ºC. Silica binding/uptake was quantified evaluating cell granularity by flow cytometric right angle scatter (RAS). Differences with its respective unexposed control were analyzed.

Figure 3.13

Change in Side Scatter in SR-AIIn Transfected Cells After Silica Exposure

EVn

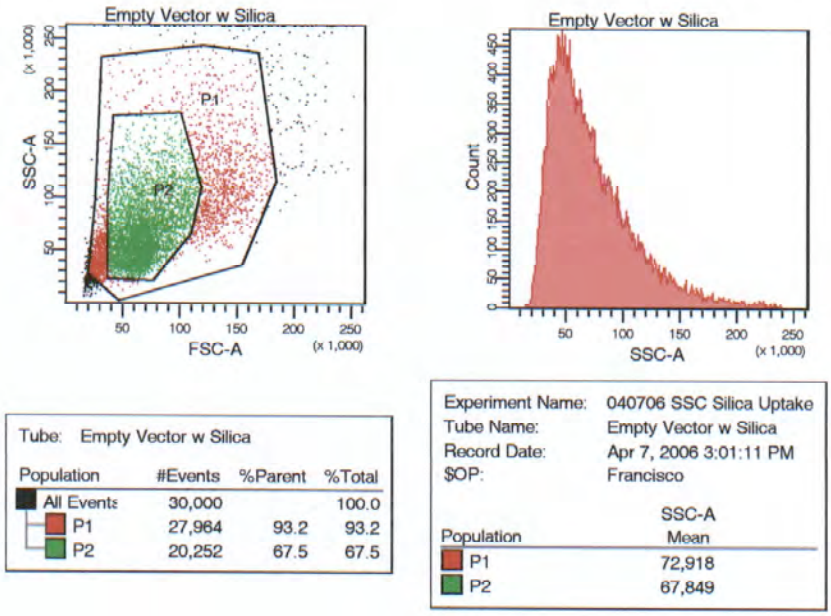

Tube: Empty Vector w Silica			
Population	#Events	%Parent	%Total
All Events	30,000		100.0
P1	27,964	93.2	93.2
P2	20,252	67.5	67.5

Experiment Name:	040706 SSC Silica Uptake
Tube Name:	Empty Vector w Silica
Record Date:	Apr 7, 2006 3:01:11 PM
$OP:	Francisco

Population	SSC-A Mean
P1	72,918
P2	67,849

SR-AIIn

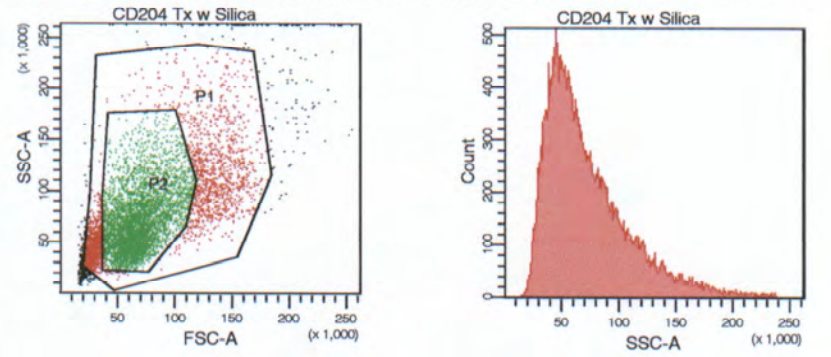

Tube: CD204 Tx w Silica			
Population	#Events	%Parent	%Total
All Events	30,000		100.0
P1	27,828	92.8	92.8
P2	19,506	65.0	65.0

Experiment Name:	040706 SSC Silica Uptake
Tube Name:	CD204 Tx w Silica
Record Date:	Apr 7, 2006 3:06:07 PM
$OP:	Francisco

Population	SSC-A Mean
P1	73,155
P2	68,916

Figure 3.14

Change in Side Scatter in SR-AIIn Transfected Cells After Silica Exposure (N=1)

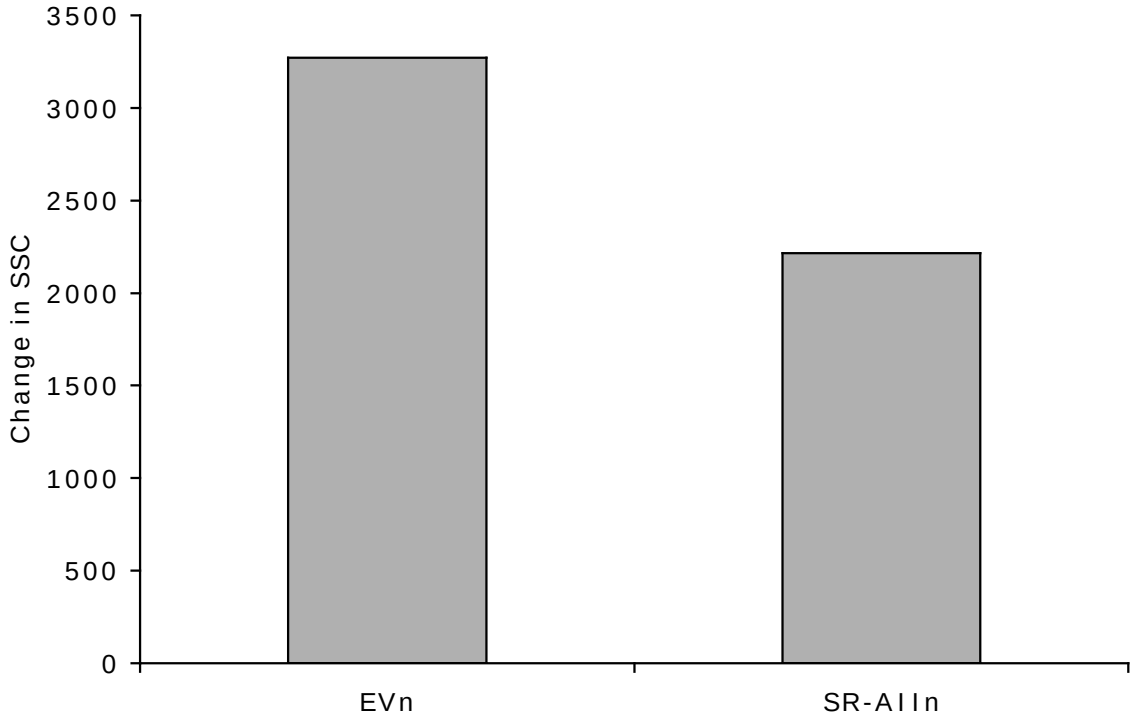

One million cells were exposed to silica at a concentration of 150 µg/ml in an end-over-end rotator for 90 minutes at 37ºC. Silica binding/uptake was quantified evaluating cell granularity by flow cytometric right angle scatter (RAS). Differences with its respective unexposed control were analyzed.

Figure 3.15

DNA Fragmentation Detected by TiterTACS in SR-AIIn Transfected Cells After Silica Exposure (N=3-4)

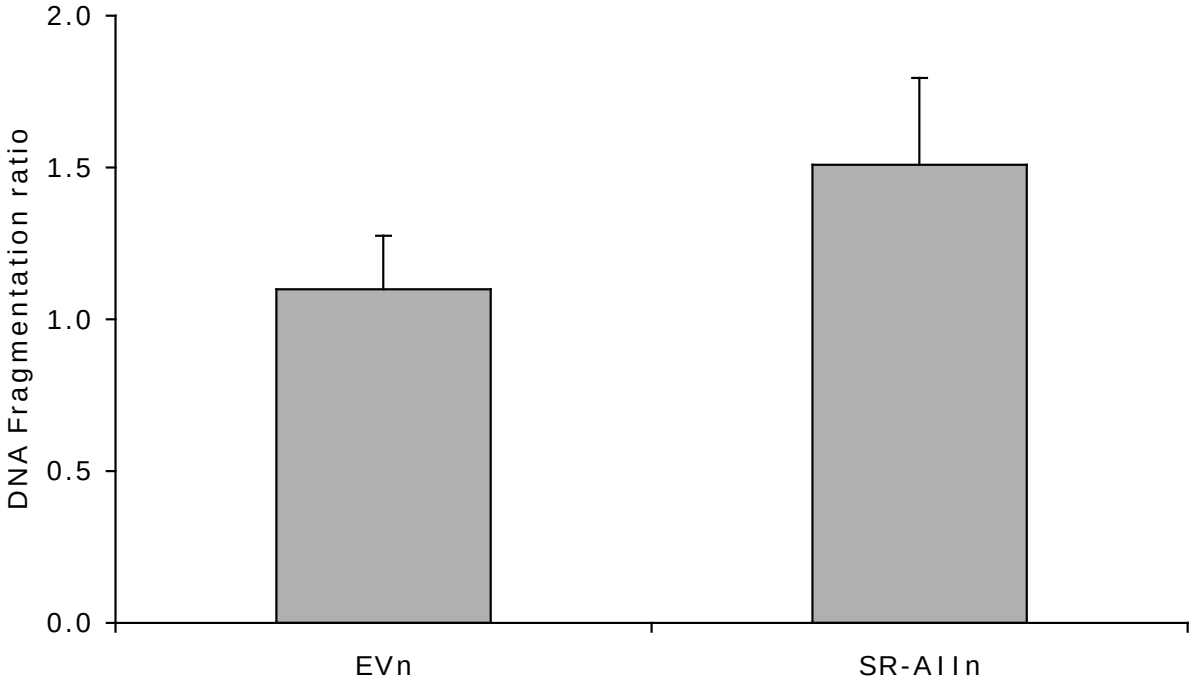

Cells were scraped and plated 24 hours prior to exposure at 2 $x10^5$ cell in a volume of 200 µl per well in a 96 well plate. Then culture media was changed and silica added to a final concentration of 66.7 µg/cm^2. Cells were exposed to silica for 24 hours. TiterTACS was used to detect in situ DNA fragmentation. Absorbance was measured. at 450 nm. Ratios with its respective unexposed control were analyzed and normalized. to 1.0 for the control non-exposed group.

Figure 3.16

Caspase-3 Activity in SR-AIIn Transfected Cells After Silica Exposure (N=2)

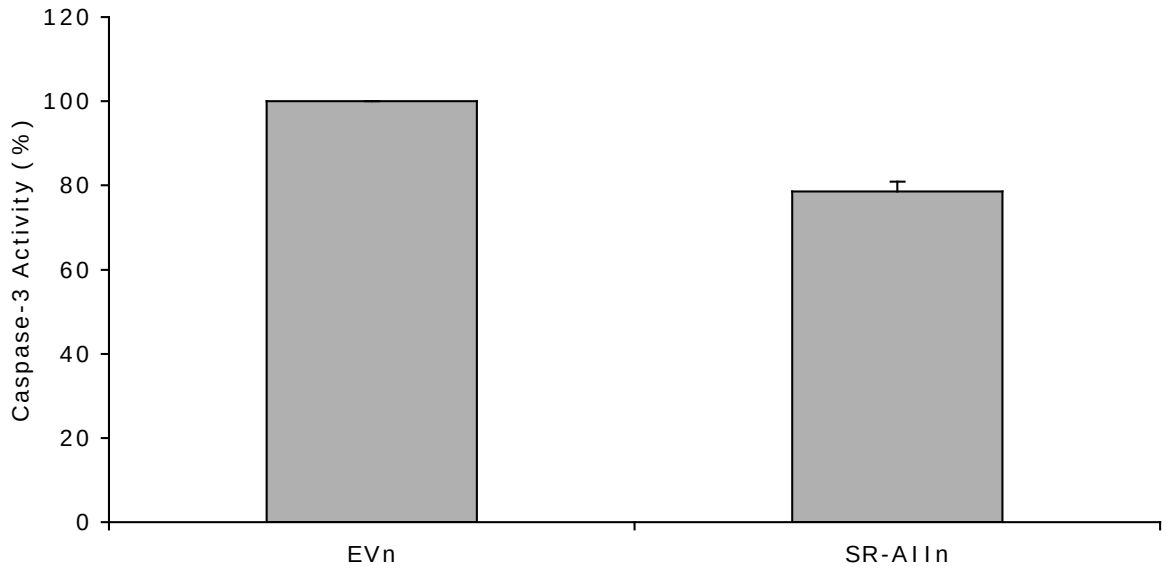

Cells were scraped and plated 24 hours prior to exposure at 2 $x10^5$ cell in a volume of 100 µl per well in a 96 well plate. Cell culture media was changed at exposure time. Silica was added to a final concentration of 50 $\mu g/cm^2$ and cells were exposed to silica for 24 hours before performing any assessment. Caspase-3 activity was detected using the Caspase-3 Activity Assay for High Throughput Screening. Fluorescence was detected at an excitation wavelength of 400 nm and emission wavelength of 505 nm. Ratios with its respective unexposed control were analyzed and normalized to 100% for the transfection control.

Figure 3.17

TUNEL Assay in Transfected Cells Exposed to Silica (N=4)

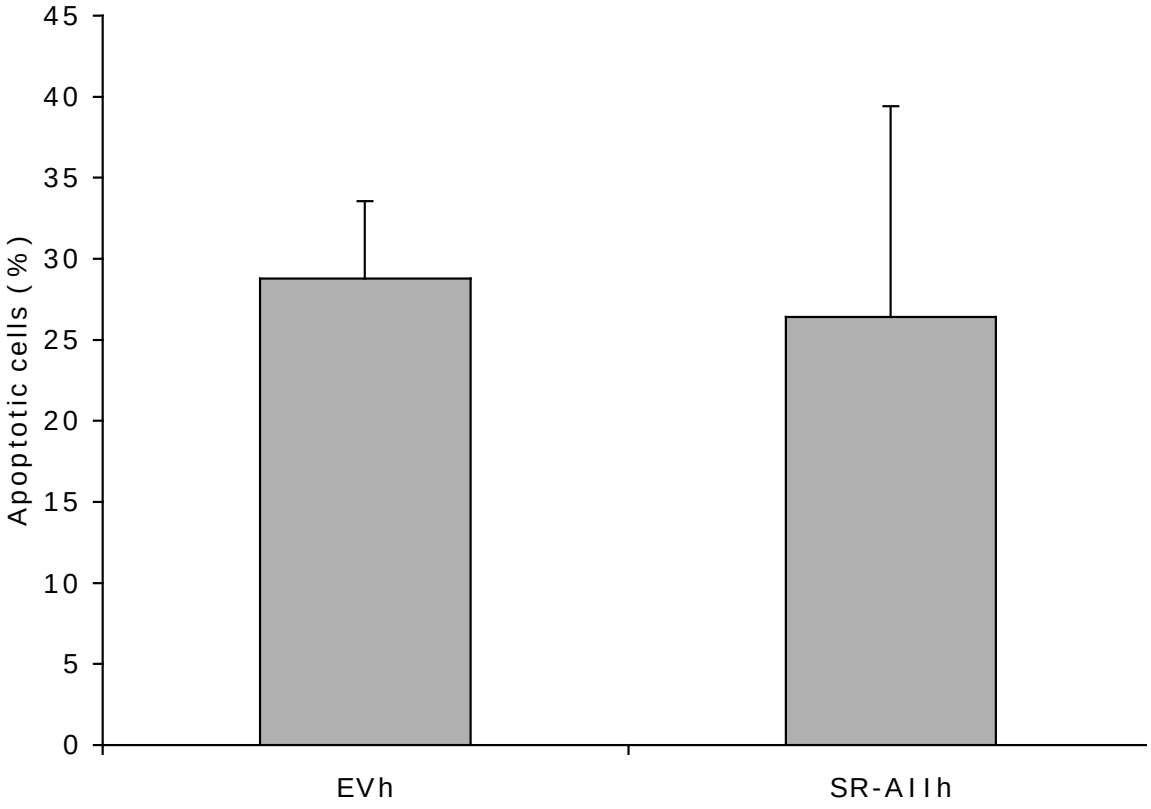

Transfected Construct

Cells were scraped and 1.5 x 10^6 cells were transfered to 25 cm^2 flasks and preincubated for 48 hours. Silica was added at a final concentration of 50 µg/cm^2. After 24 hour-exposure cells were trypsinized, washed and transferred to fresh tubes for DNA labeling using the APO-BrdU TUNEL Assay Kit. Cells were fixed, stained, and analyzed by flow cytometry. Differences in percentage with its respective unexposed control were analyzed

Figure 3.18

LDH Release by SR-AIIh Transfected Cells After Silica Exposure (N=8)

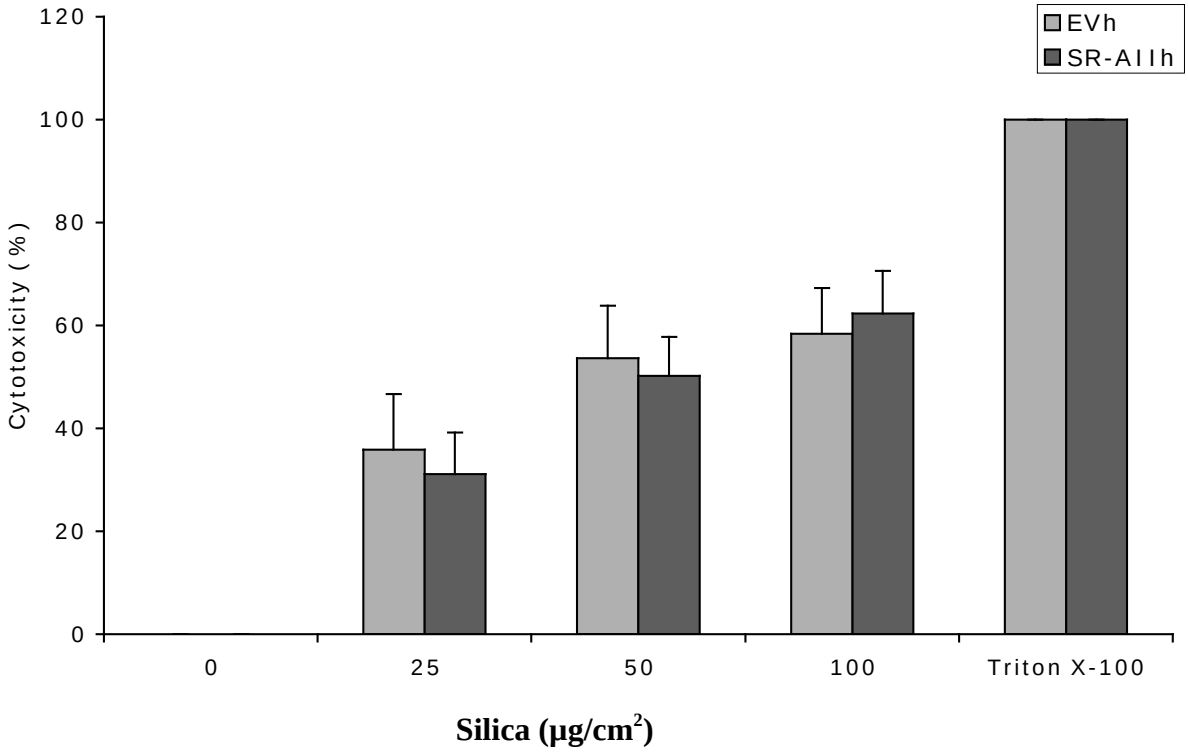

Cells were trypsinized and plated 24 hours prior to exposure at 50,000 cells in a 96-well plate. Silica was added to a final dose of 25, 50 and 100 µg/cm^2 per well. After 24 hours of exposure, cytotoxicity was approached detecting LDH release using Cytotoxic Detection Assay (LDH). Values were normalized considering that cells exposed to media only have no LDH release and cells exposed to Triton X-100 1% have 100% of LDH release.

Figure 3.19

LDH Release by SR-AIIn Transfected Cells After Silica Exposure (N=4)

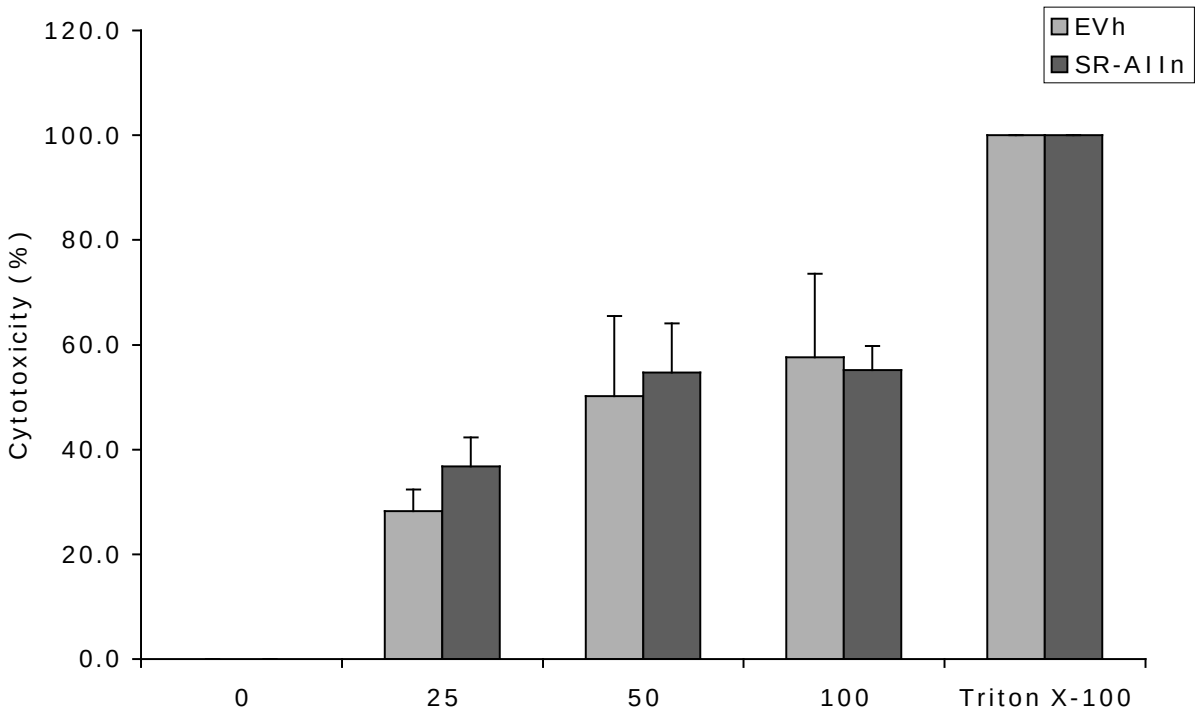

Cells were trypsinized and plated 24 hours prior to exposure at 50,000 cells in a 96-well plate. Silica was added to a final dose of 25, 50 and 100 µg/cm^2 per well. After 24 hours of exposure, cytotoxicity was approached detecting LDH release using Cytotoxic Detection Assay (LDH). Values were normalized considering that cells exposed to media only have no LDH release and cells exposed to Triton X-100 1% have 100% of LDH release.

Figure 3.20

Silica Induced Cytotoxicity in SR-AIIh Transfected Cells (N=3)

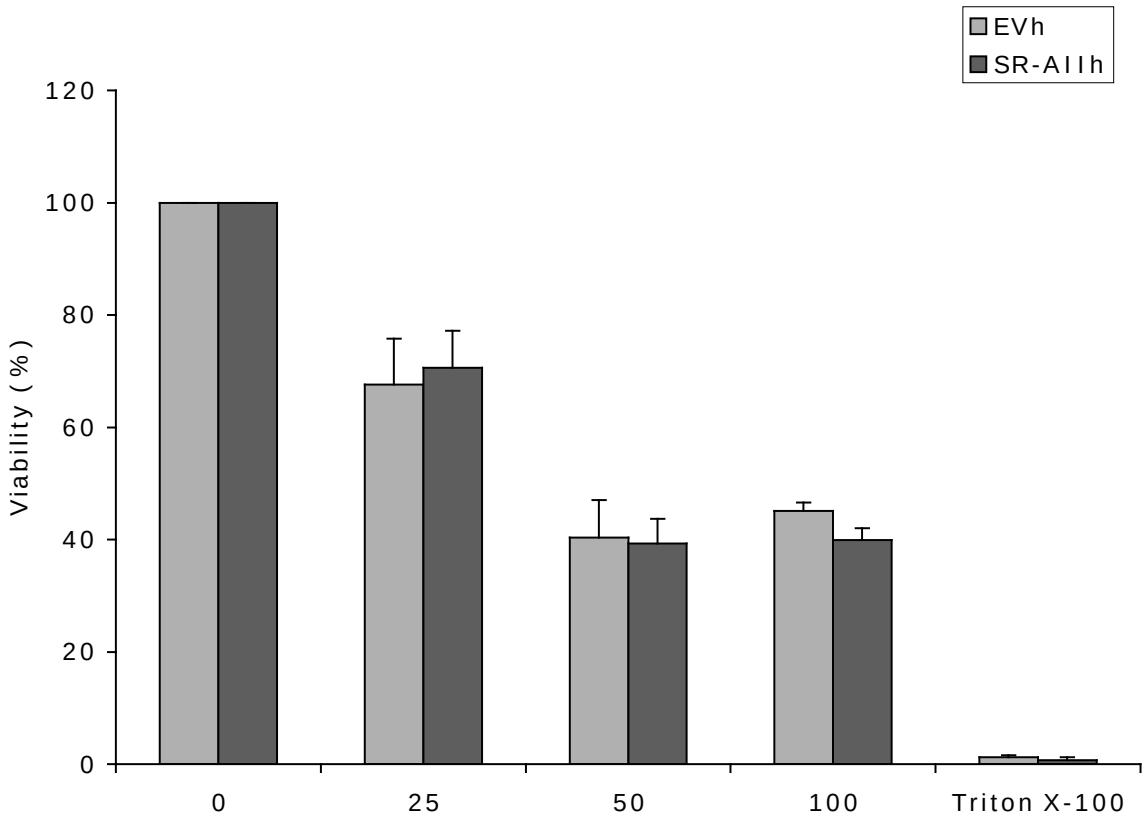

Cells were trypsinized and plated 24 hours prior to exposure at 50,000 cells in a 96-well plate. Silica was added to a final dose of 25, 50 and 100 µg/cm^2 per well. After 24 hours of exposure, viability was measured using CellTiter96 Aqueous One Solution Reagent. Values were normalized considering that cells exposed to media only have 100% of viability.

Figure 3.21

LDH Release by SR-AIIn Transfected Cells Exposed to 50 µg/cm2 of Silica and Treated With SR-As Inhibitors (N=2)

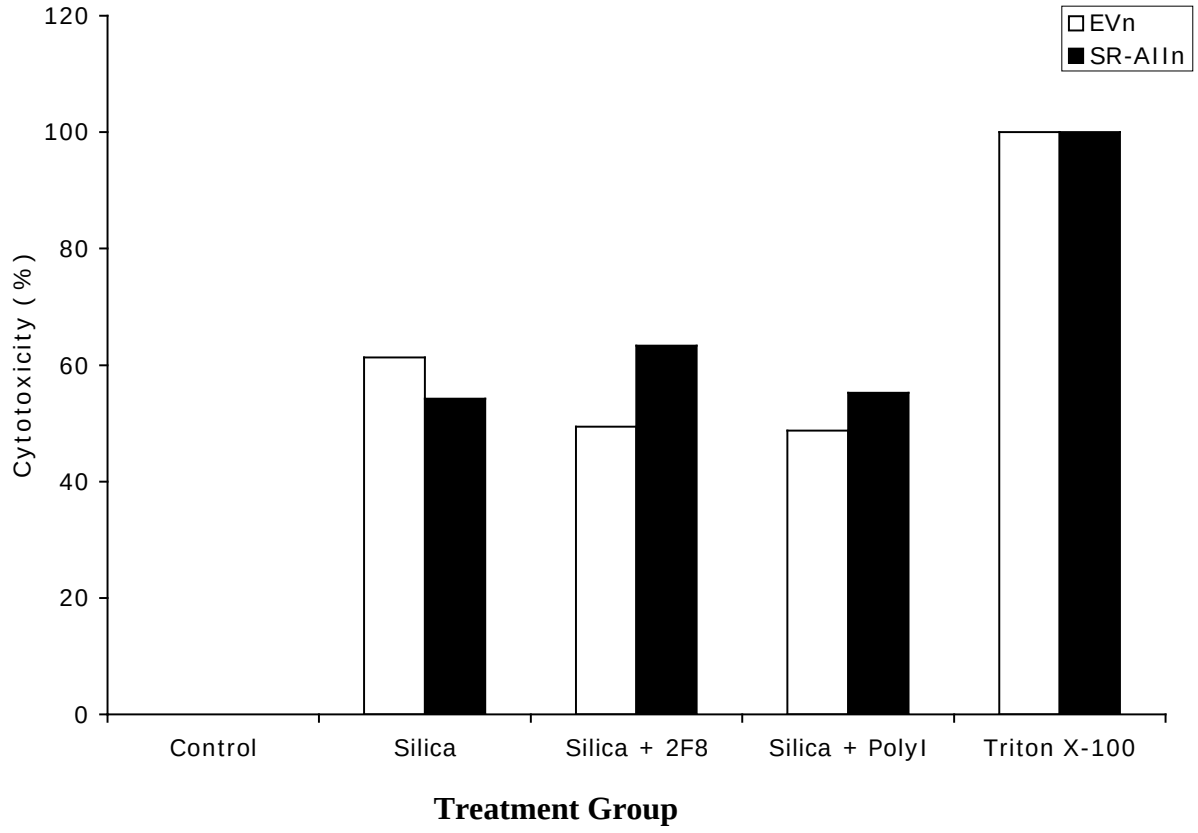

Cells were trypsinized and plated 24 hours prior to exposure at 50,000 cells in a 96-well plate. The SR-A inhibitors 2F8 blocking antibody (specific for SRA-I/II) and poly I (nonspecific for SR-AI/II) were used 30 minutes before silica exposure. Then silica was added to a final dose of 50 µg/cm^2 per well. After 24 hours of exposure, cytotoxicity was approached detecting LDH release using Cytotoxic Detection Assay (LDH). Values were normalized considering that cells exposed to media only have no LDH release and cells exposed to Triton X-100 1% have 100% of LDH release.

Figure 3.22

DNA Sequence of Mutated CD204

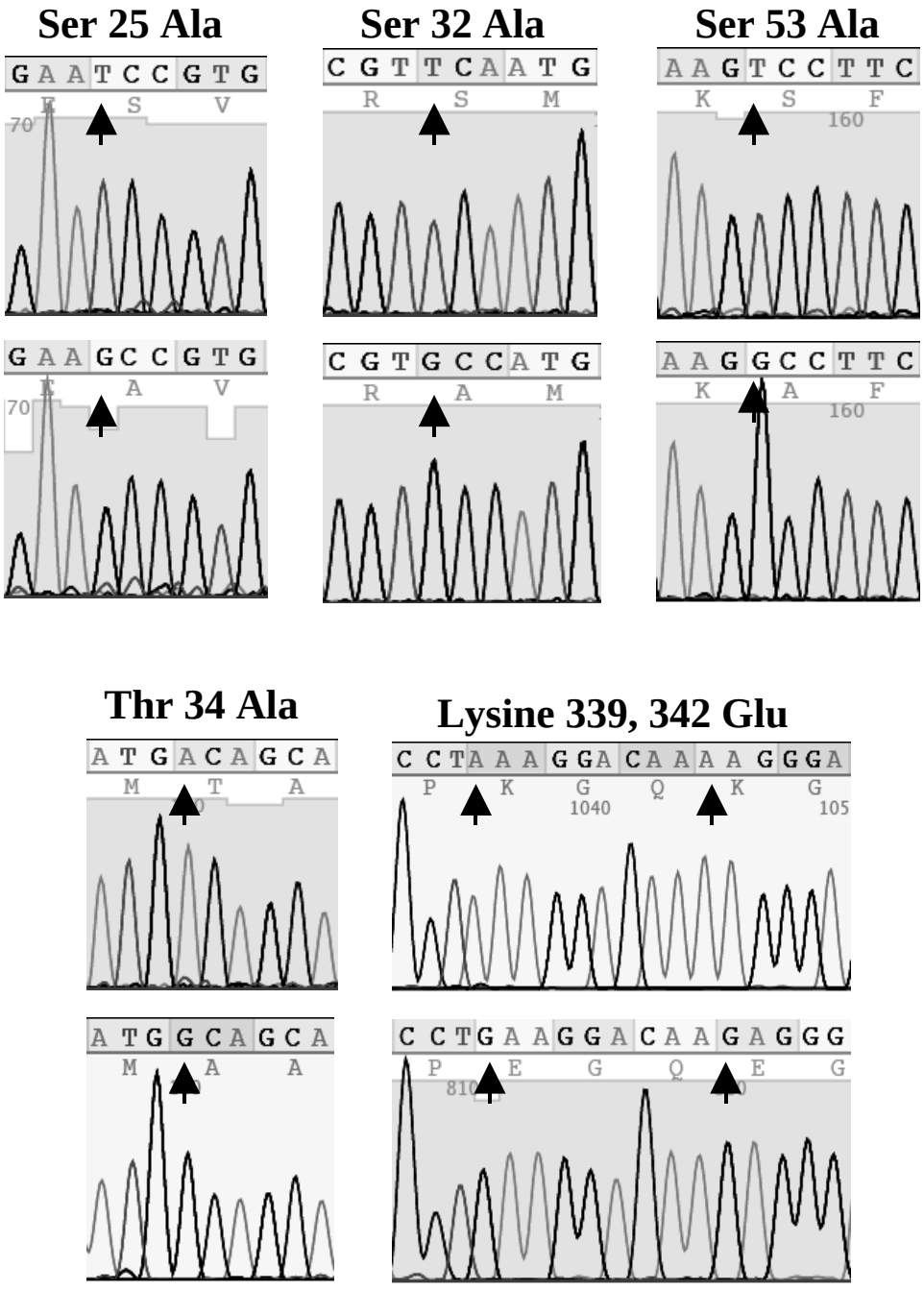

Chromatograms corresponding to the DNA sequences of the mutations inserted in murine SR-AII, as described in the Methods section. Arrowheads point to the mutated bases.

Figure 3.23

IP and WB of Mutated SRAIIn Protein in Transfected CHO Cells

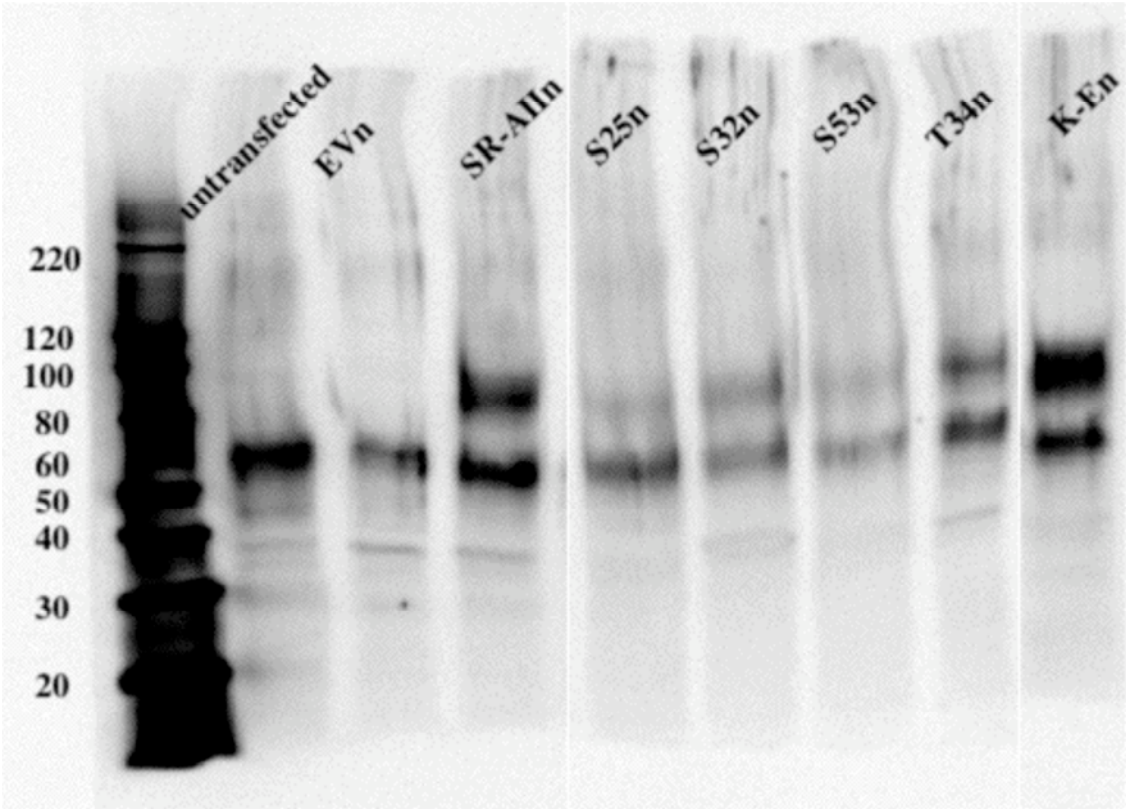

Ten million cells were lysed and IP with 2F8 antibody and protein G agarose. IP cell lysate was electhrophoresed and transferred to a nitrocellulose membrane for WB with monoclonal antibody anti-6X His tag. Bands were detected by enhanced chemiluminescence (ECL).

Figure 3.24

Uptake of AcLDL by Mutated SR-AIIn Transfected Cells (N=3-6)

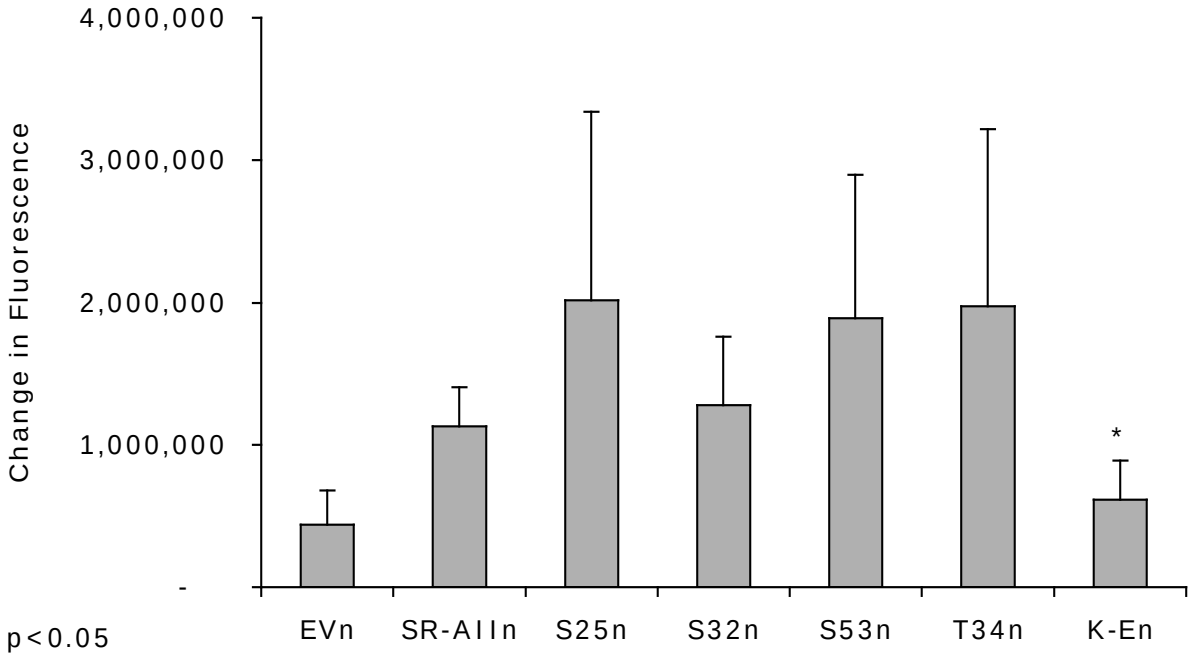

Transfected Construct

Uptake of AcLDL by CHO cells transfected with mutated SRA-II constructs. Cells were exposed to fluorescence labeled AcLDL for 90 minutes. Quantification was performed using a Laser Scan Cytometer. Differences with its respective unexposed control were analyzed.

Figure 3.25

DNA Fragmentation Detected by TiterTACS in Mutated SRA-IIn Transfected Cells After Silica Exposure (N=3-5)

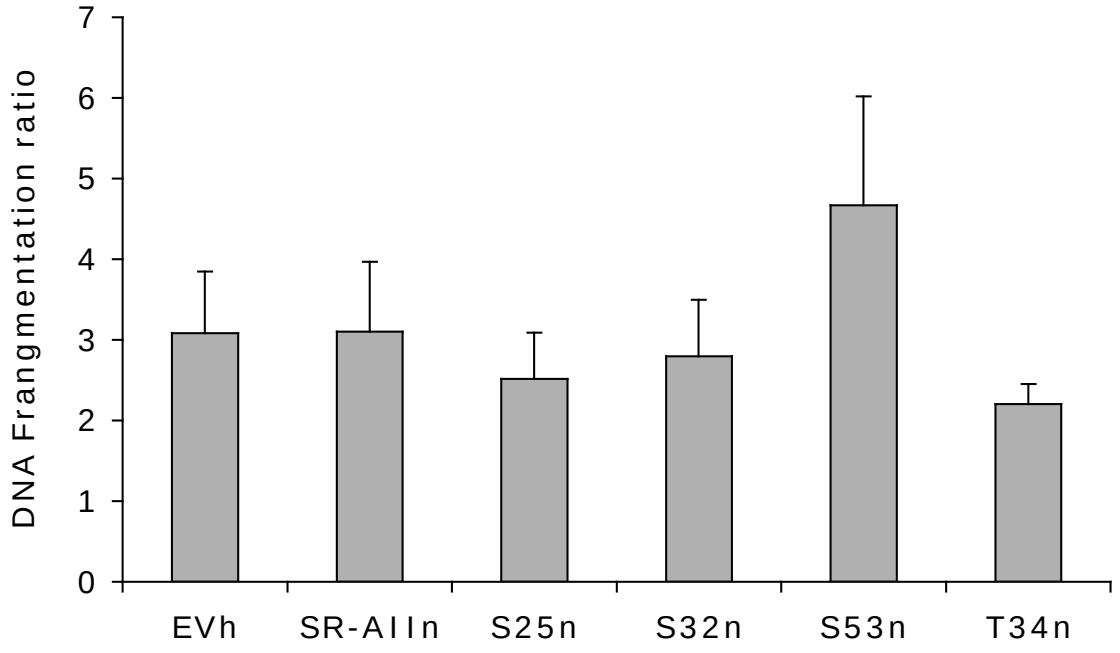

Cells were scraped and plated 24 hours prior to exposure at 2 $x10^5$ cell in a volume of 200 µl per well in a 96 well plate. Then culture media was changed and silica added to a final concentration of 66.7 µg/cm^2. Cells were exposed to silica for 24 hours. TiterTACS was used to detect in situ DNA fragmentation. Absorbance was measured. at 450 nm. Ratios with its respective unexposed control were analyzed.

Figure 3.26

Caspase-3 Activity in Mutated SR-AIIn Transfected Cells After Silica Exposure
(N=6)

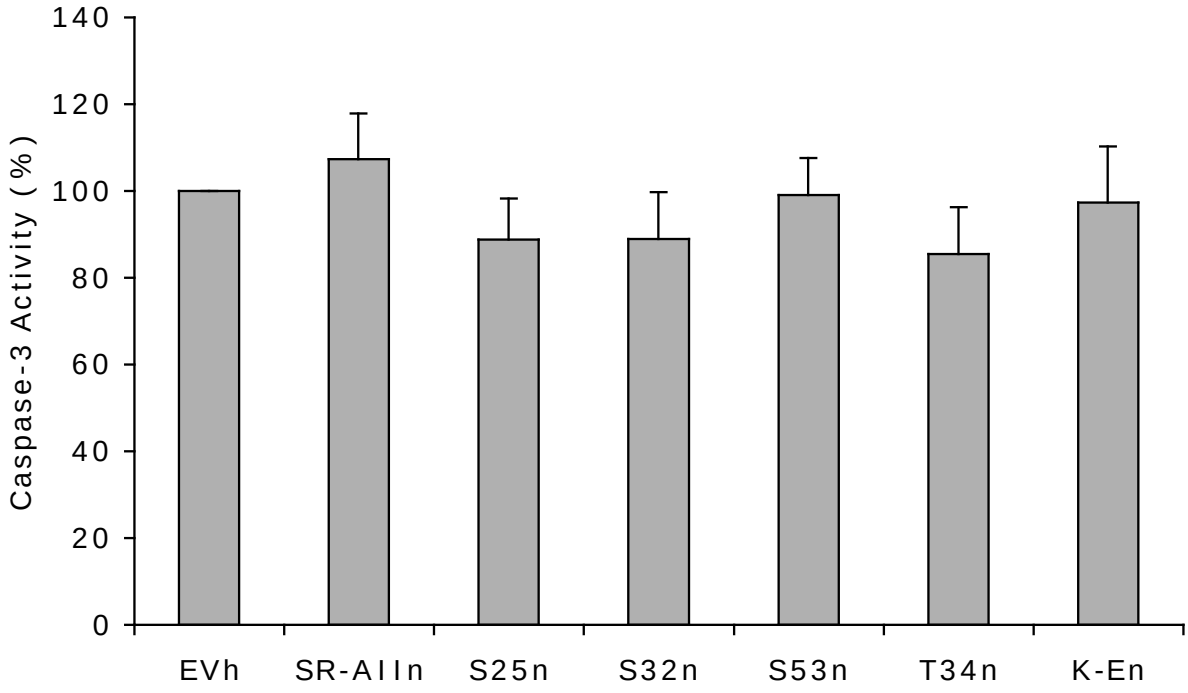

Cells were scraped and plated 24 hours prior to exposure at 2 $x10^5$ cell in a volume of 100 µl per well in a 96 well plate. Cell culture media was changed at exposure time. Silica was added to a final concentration of 50 $\mu g/cm^2$ and cells were exposed to silica for 24 hours before performing any assessment. Caspase-3 activity was detected using the Caspase-3 Activity Assay for High Throughput Screening. Fluorescence was detected at an excitation wavelength of 400 nm and emission wavelength of 505 nm. Ratios with its respective unexposed control were analyzed and normalized to 100% for the transfection control.

Figure 3.27

PCR Product Confirmatory of SR-AIh and SR-AIIh Incorporation into Genomic CHO Cells

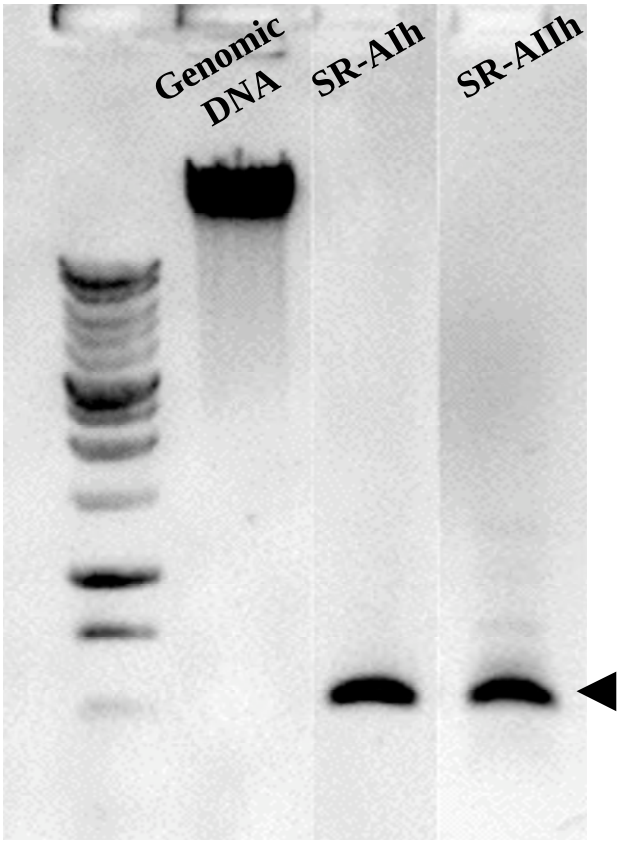

Genomic DNA was isolated from 1-2 million transfected cells. DNA was amplified by PCR using a T7 primer corresponding to vector sequence, and a SR-AII primer. Then PCR product was run in a 0.8% agarose gel. Arrowhead shows PCR product band.

Figure 3.28

Uptake of AcLDL by SR-AIh and SR-AIIh Transfected CHO Cells (N=6)

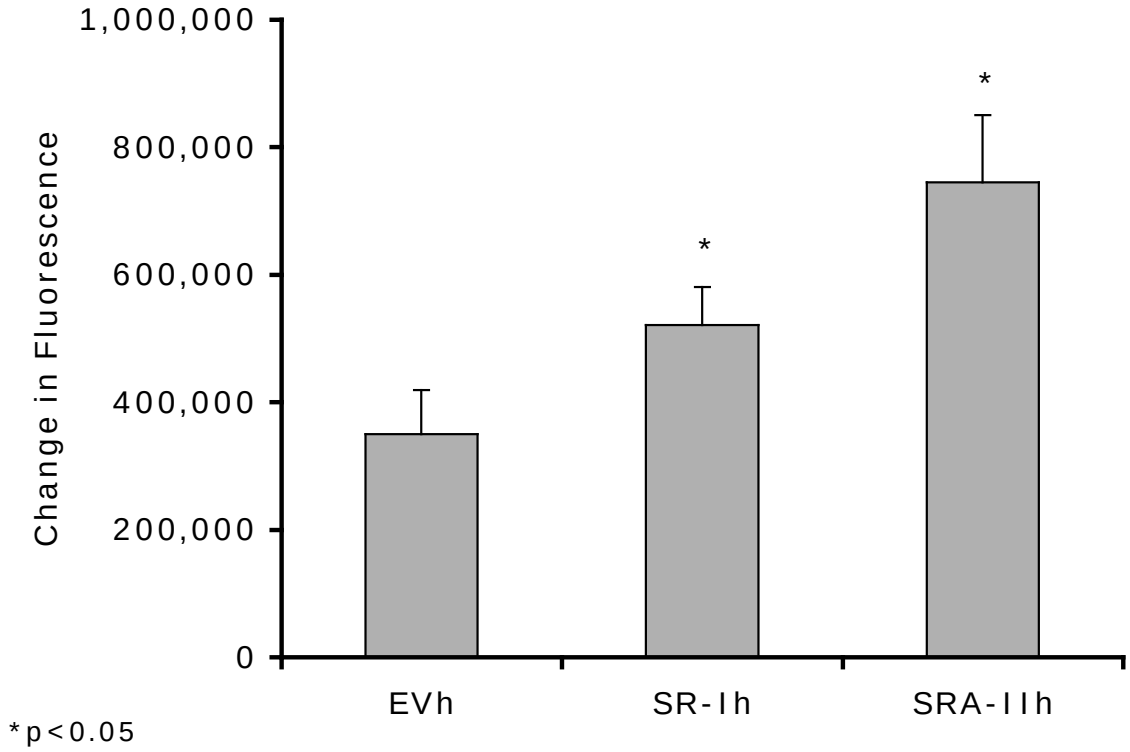

Uptake of AcLDL by CHO cells transfected with SRA-Ih and SR-AIIh. Cells were exposed to fluorescence labeled AcLDL for 90 minutes. Quantification was performed using a Laser Scan Cytometer. Differences with its respective unexposed control were analyzed.

Figure 3.29

Inhibition of AcLDL Uptake in SR-AIh and SR-AIIh Transfected Cells (N=6)

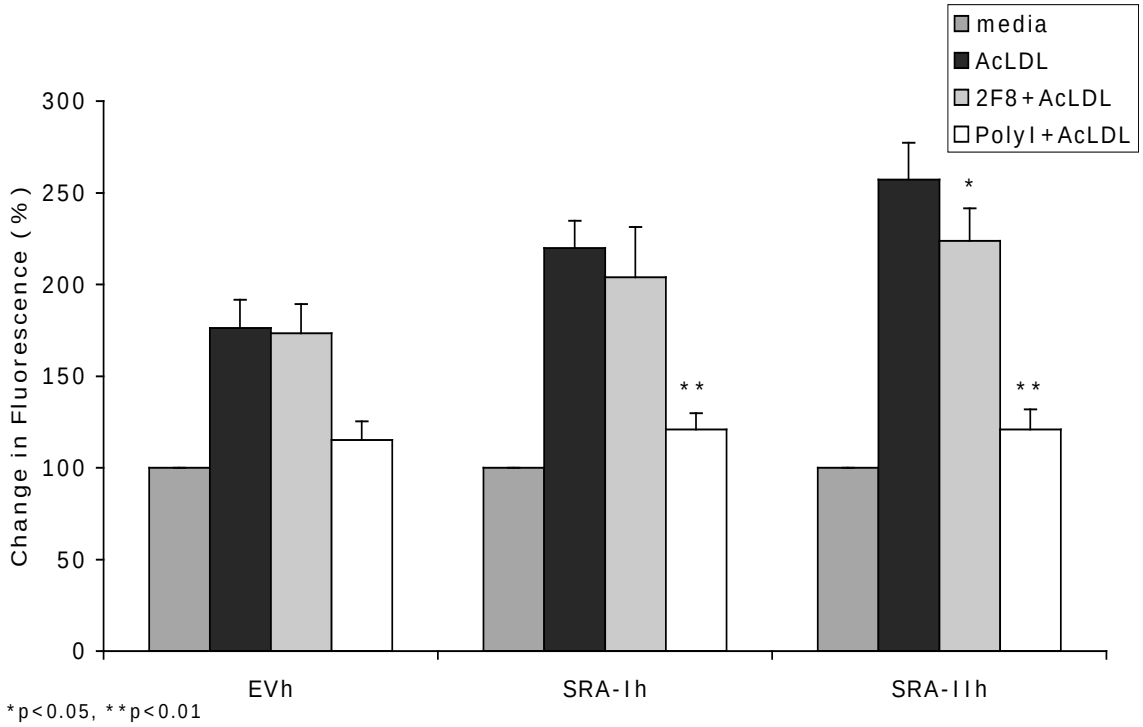

Uptake of AcLDL by transfected CHO cells with SR-AIh and SRA-IIh when exposed to the SR-A inhibitors (ligands in a competition assay). 2F8 a specific SRA-I/II ligand (blocking antibody) and poly I a nonspecific ligand were used. Cells were pre-incubated 30 minutes with SR-A inhibitors before being exposed to fluorescence labeled AcLDL for 90 minutes. Quantification was performed using a Laser Scan Cytometer. Ratios with its respective unexposed control were analyzed and normalized to 100% for the control non-exposed group.

Figure 3.30

Change in Side Scatter in SR-AIh and SR-AIIh in Transfected Cells After Silica Exposure
(N=2)

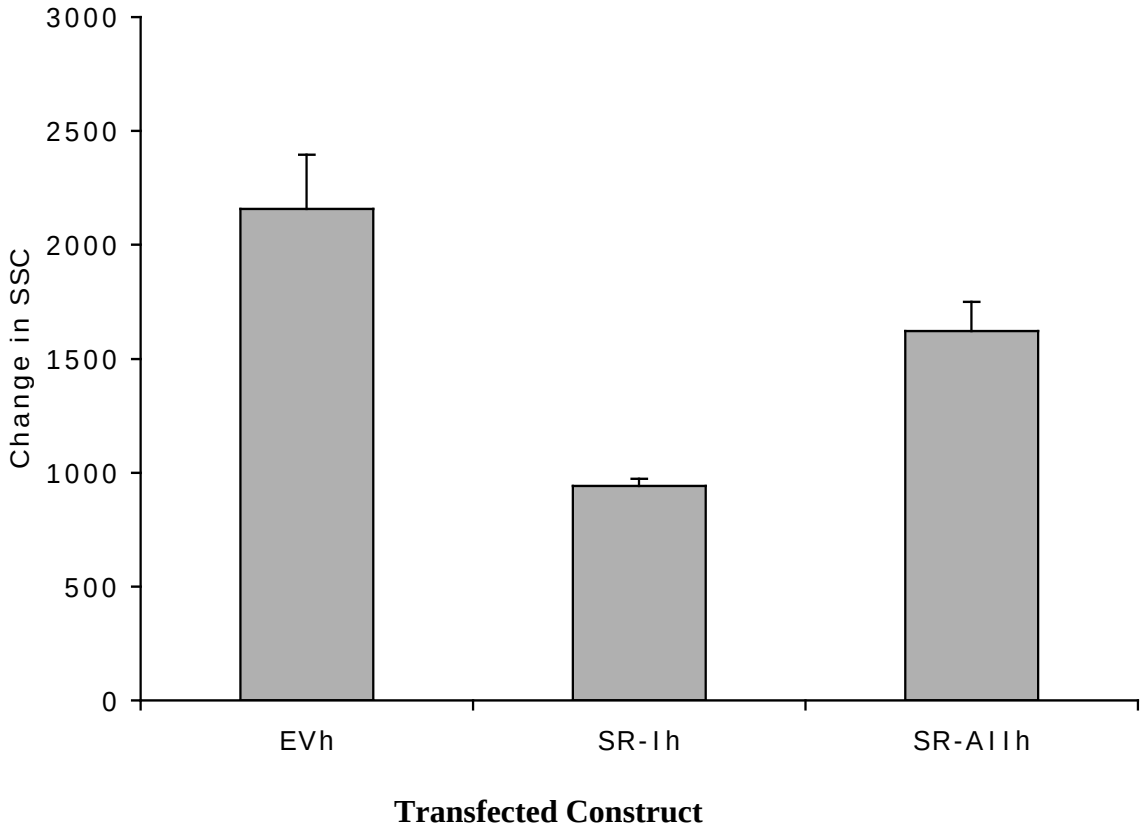

One million cells were exposed to silica at a concentration of 150 µg/ml in an end-over-end rotator for 90 minutes at 37ºC. Silica binding/uptake was quantified evaluating cell granularity by flow cytometric right angle scatter (RAS). Differences with its respective unexposed control were analyzed.

Figure 3.31

TUNEL Assay in SR-AIh and SR-AIIh Transfected Cells After Silica Exposure
(N=4)

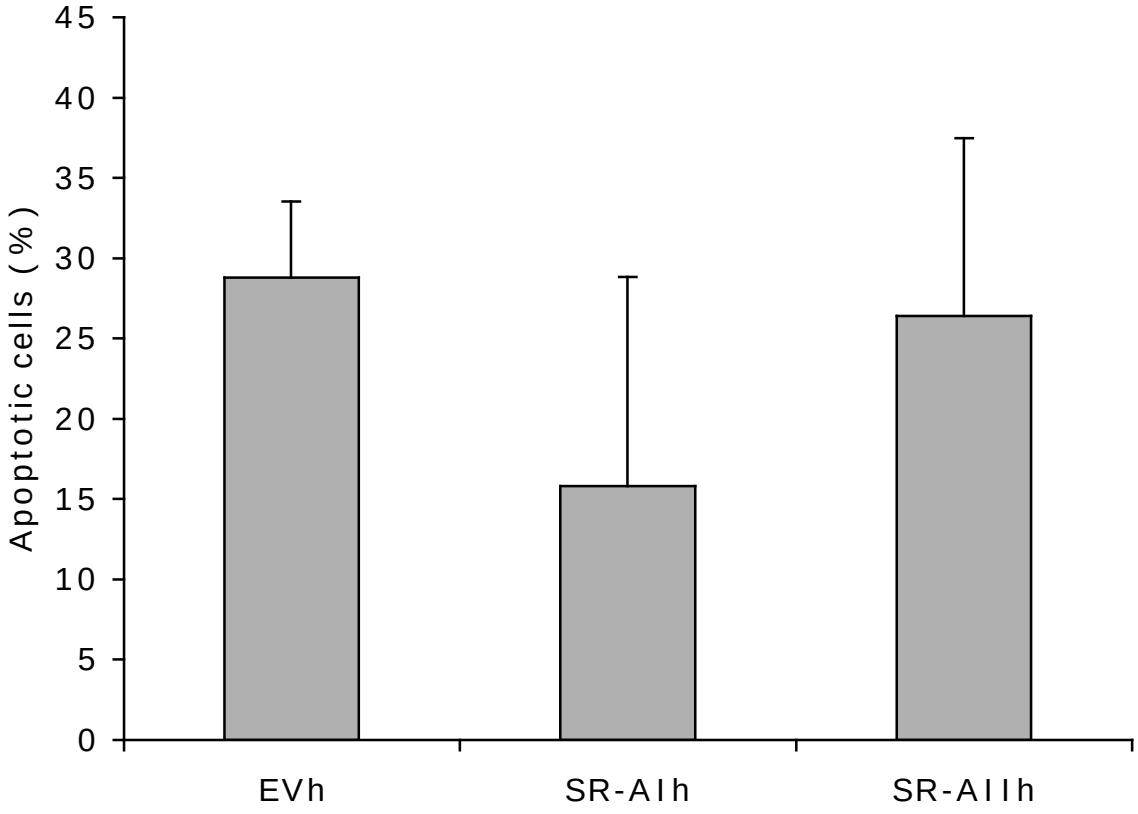

Cells were scraped and 1.5 x 10^6 cells were transfered to 25 cm^2 flasks and preincubated for 48 hours. Silica was added at a final concentration of 50 µg/cm^2. After 24 hour-exposure cells were trypsinized, washed and transferred to fresh tubes for DNA labeling using the APO-BrdU TUNEL Assay Kit. Cells were fixed, stained, and analyzed by flow cytometry. Differences in percentage with its respective unexposed control were analyzed

Figure 3.32

LDH Release by SR-AIh and SR-AIIh Transfected Cells After Silica Exposure
(N=8)

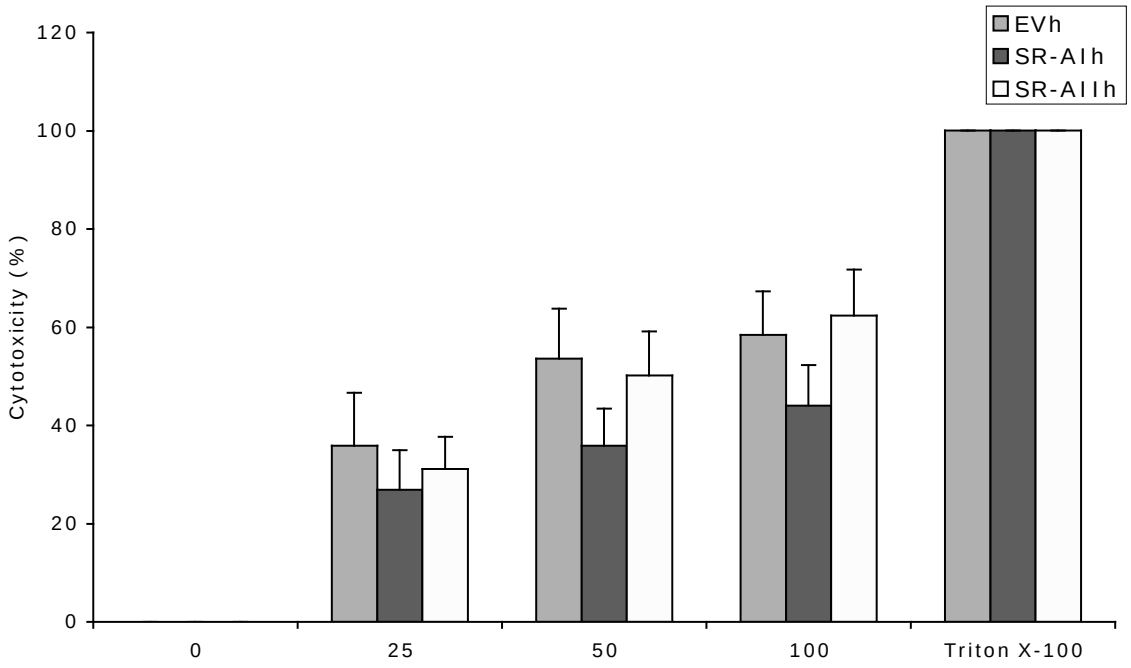

Silica (µg/cm^2)

Cells were trypsinized and plated 24 hours prior to exposure at 50,000 cells in a 96-well plate. Silica was added to a final dose of 25, 50 and 100 µg/cm^2 per well. After 24 hours of exposure, cytotoxicity was approached detecting LDH release using Cytotoxic Detection Assay (LDH). Values were normalized considering that cells exposed to media only have no LDH release and cells exposed to Triton X-100 1% have 100% of LDH release.

Figure 3.33

Silica Induced Cytotoxicity in SR-AIh and SR-AIIh Transfected Cells (N=3)

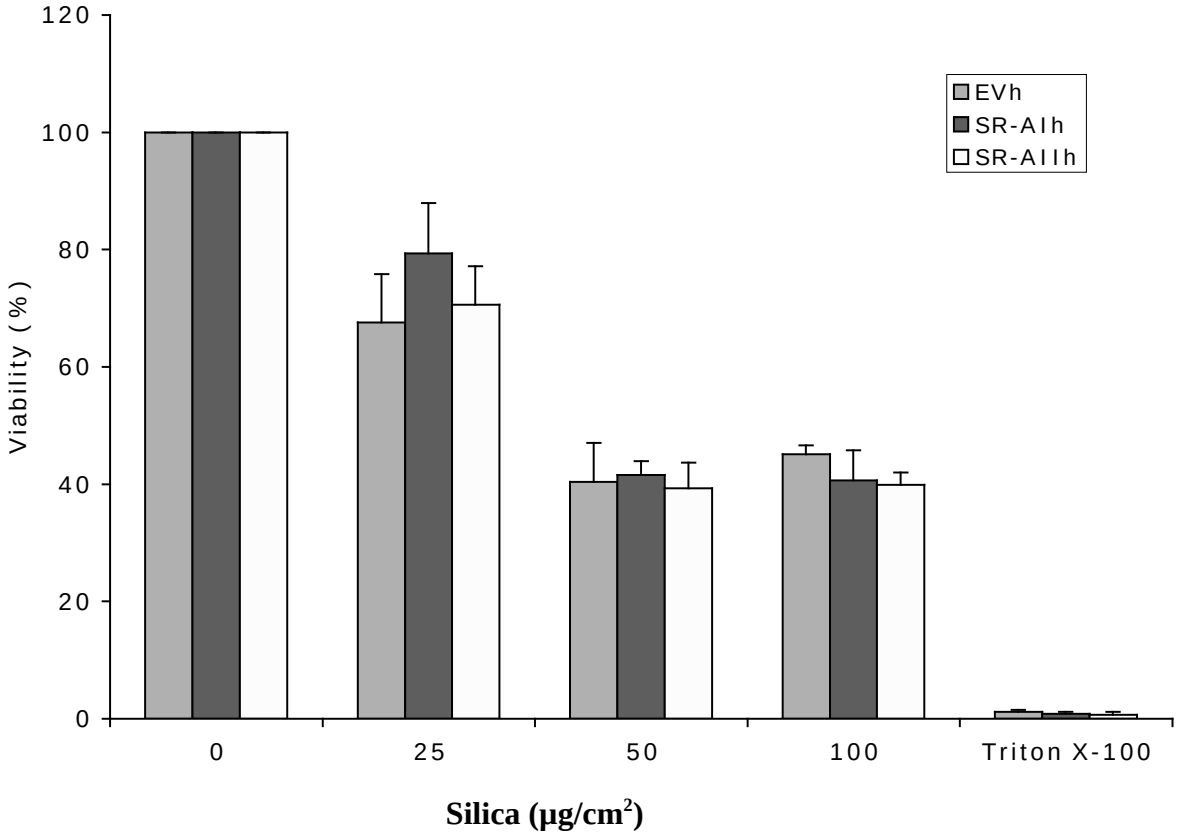

Cells were trypsinized and plated 24 hours prior to exposure at 50,000 cells in a 96-well plate. Silica was added to a final dose of 25, 50 and 100 µg/cm^2 per well. After 24 hours of exposure, viability was measured using CellTiter96 Aqueous One Solution Reagent. Values were normalized considering that cells exposed to media only have 100% of viability.

Chapter 4

Final Discussion

The cause of most ILDs is still unknown. In this study two environmental/occupational agents implicated in causing ILD were studied: crocidolite asbestos and silica. Both agents can activate inflammation and produce direct injury to the resident pulmonary cells (Rimal et al., 2005; Rom, Travis et al., 1991). In the asbestos study, crocidolite alone could not induce either inflammation (prostacyclin production) or cytotoxicity. In the first case, it required the presence of an RGD protein coating the fibers, and for the second case one factor or more factors present in the fetal bovine serum was required. Garcia et al described that human umbilical vein endothelial cells released prostacyclin after amosite asbestos exposure (Garcia, Gray et al., 1988), Donaldson et al postulated the involvement of an RGD protein in the cell detachment induced by the exposure of amosite to A549 cells (human alveolar type II cell line) (Donaldson, Miller et al., 1993), and Boylan et al describe the role of vitronectin in crocidolite internalization by mesothelial cells (Boylan, Sanan et al., 1995). No previous study has described the role of RGD proteins in crocidolite-induced prostacyclin release by murine alveolar type II cells. In addition there is no previous report describing two separate responses, such as inflammation and cytotoxicity, in the same group of cells after crocidolite exposure. These findings show the complexity of the different ways cells could respond to crocidolite exposure.

In the silica study, our system expressing SR-AI or SR-AII was not sufficient to induce apoptosis or cytotoxicity with silica exposure and probably other factors or co-

receptors are necessary. These two studies have in common that the agent by itself (asbestos or silica) is not sufficient to induce activation/damage of cells. Multiple interactions with other factors such as ECM proteins (e.g. vitronectin), different receptors expressed on the surface of cells (e.g. integrins), activation status of the cell environment, etc. All these variables together (at the right time and in the right place) may be required to initiate and maintain the response required to produce ILD.

Future Directions

Role of Asbestos in Lung Epithelial Cells

- Determine the role of prostacyclin in the ILD animal model: Because prostacyclin protects and attenuates lung fibrosis in the bleomycin-induced pulmonary fibrosis model, it will be interesting to determine if decrease in prostacyclin levels correlate with the development of ILD in different animal models, and also if prostacyclin therapy could prevent or attenuate the progression of the disease.

- Determine the role of each VNR and VNR inhibitors in the ILD animal model: VNR interaction induced prostacyclin biosynthesis, but also VNR bind LAP inducing activation of TGFβ a key factor in the fibrotic process. So, it is important to characterize which VNRs are binding coated asbestos and which ones bind LAP activating TGFβ in the ILD animal model. This will provide more alternatives for intervention by blocking the VNRs promoting lung fibrosis.

- Determine the role of Cox 2 inhibitors in the progression of ILD. The use of Cox inhibitors is very popular currently. In this study, prostacyclin production was Cox 2 mediated. So it is important to determine if blocking prostacyclin production using Cox 2 inhibitors will accelerate the development of ILD in the animal model.

- Determine the role of “RGD” proteins in the progression of ILD. Because RGD proteins (e.g. vitronectin) were involved in the prostacyclin production, it would be interesting to characterize what RGD proteins in the BAL are coating the fibers in order to allow cell interaction. This will provide alternative ways for future intervention.

Role of Scavenger Receptors in Silica Binding and Apoptosis

- Identification of proteins that bind the cytoplasmic domain of SR-A I/II after silica binding. More studies characterizing the proteins associated to SR-AI/II activation after silica binding are required in order to understand how the apoptotic signal is initiated.
- Determine the role of SR-A I/II inhibitors in the ILD animal model. It is necessary to determine the effect of SR-AI/II inhibitors in the ILD animal model in order to develop alternatives to future intervention
- Determine the role of human SR-A I/II in binding and apoptosis when expressed in a human cell line. More studies characterizing the human SR-AI/II in silica binding and silica-induced apoptosis are necessary to understand its role in ILD.

References

Abdalah, R., Wei, L., Francis, K., & Yu, S. P. (2006). Valinomycin-induced apoptosis in Chinese hamster ovary cells. *Neurosci Lett, 405*(1-2), 68-73.

Andersson, L., & Freeman, M. W. (1998). Functional changes in scavenger receptor binding conformation are induced by charge mutants spanning the entire collagen domain. *J Biol Chem, 273*(31), 19592-19601.

Aronoff, D. M., Peres, C. M., Serezani, C. H., Ballinger, M. N., Carstens, J. K., Coleman, N., et al. (2007). Synthetic prostacyclin analogs differentially regulate macrophage function via distinct analog-receptor binding specificities. *J Immunol, 178*(3), 1628-1634.

Arredouani, M. S., & Kobzik, L. (2004). The structure and function of marco, a macrophage class a scavenger receptor. *Cell Mol Biol (Noisy-le-grand), 50 Online Pub*, OL657-665.

Ashkenas, J., Penman, M., Vasile, E., Acton, S., Freeman, M., & Krieger, M. (1993). Structures and high and low affinity ligand binding properties of murine type I and type II macrophage scavenger receptors. *J Lipid Res, 34*(6), 983-1000.

Belton, O., Byrne, D., Kearney, D., Leahy, A., & Fitzgerald, D. J. (2000). Cyclooxygenase-1 and -2-dependent prostacyclin formation in patients with atherosclerosis. *Circulation, 102*(8), 840-845.

Bissonnette, E., Carre, B., Dubois, C., & Rola-Pleszczynski, M. (1990). Inhibition of alveolar macrophage cytotoxicity by asbestos: possible role of prostaglandins. *J Leukoc Biol, 47*(2), 129-134.

Boylan, A. M., Sanan, D. A., Sheppard, D., & Broaddus, V. C. (1995). Vitronectin enhances internalization of crocidolite asbestos by rabbit pleural mesothelial cells via the integrin alpha v beta 5. *J Clin Invest, 96*(4), 1987-2001.

Burri, P. H., & Weibel, E. R. (1973). *Rontgendiagnostik der Lunge* (7th ed.). Bern: Huber.

Caughey, G. E., Cleland, L. G., Penglis, P. S., Gamble, J. R., & James, M. J. (2001). Roles of cyclooxygenase (COX)-1 and COX-2 in prostanoid production by human endothelial cells: selective up-regulation of prostacyclin synthesis by COX-2. *J Immunol, 167*(5), 2831-2838.

Chao, S. K., Hamilton, R. F., Pfau, J. C., & Holian, A. (2001). Cell surface regulation of silica-induced apoptosis by the SR-A scavenger receptor in a murine lung macrophage cell line (MH-S). *Toxicol Appl Pharmacol, 174*(1), 10-16.

Chen, Y., Sankala, M., Ojala, J. R., Sun, Y., Tuuttila, A., Isenman, D. E., et al. (2006). A phage display screen and binding studies with acetylated LDL provide evidence for the importance of the scavenger receptor cysteine-rich (SRCR) domain in the ligand-binding function of MARCO. *J Biol Chem*.

Clement, A., Henrion-Caude, A., & Fauroux, B. (2004). The pathogenesis of interstitial lung diseases in children. *Paediatr Respir Rev, 5*(2), 94-97.

Converse, P. J. (2006, 05/12/2006). *Integrin, Alpha-V; ITGAV*. Retrieved 02/07/2007, 2007, from http://www.ncbi.nlm.nih.gov/entrez/dispomim.cgi?id=193210

Covey, S. (2006). *The Silicate Class*. Retrieved 01/06/2007, 2007, from http://mineral.galleries.com/Minerals/SILICATE/Class.htm

Cutler, N. S., Graves-Deal, R., LaFleur, B. J., Gao, Z., Boman, B. M., Whitehead, R. H., et al. (2003). Stromal production of prostacyclin confers an antiapoptotic effect to colonic epithelial cells. *Cancer Res, 63*(8), 1748-1751.

DiDonato, D., & Brasaemle, D. L. (2003). Fixation methods for the study of lipid droplets by immunofluorescence microscopy. *J Histochem Cytochem, 51*(6), 773-780.

Doi, T., Higashino, K., Kurihara, Y., Wada, Y., Miyazaki, T., Nakamura, H., et al. (1993). Charged collagen structure mediates the recognition of negatively charged macromolecules by macrophage scavenger receptors. *J Biol Chem, 268*(3), 2126-2133.

Donaldson, K., Miller, B. G., Sara, E., Slight, J., & Brown, R. C. (1993). Asbestos fibre length-dependent detachment injury to alveolar epithelial cells in vitro: role of a fibronectin-binding receptor. *Int J Exp Pathol, 74*(3), 243-250.

Dufva, M., Svenningsson, A., & Hansson, G. K. (1995). Differential regulation of macrophage scavenger receptor isoforms: mRNA quantification using the polymerase chain reaction. *J Lipid Res, 36*(11), 2282-2290.

Enterline, P. E., & Henderson, V. (1973). Type of asbestos and respiratory cancer in the asbestos industry. *Arch Environ Health, 27*(5), 312-317.

Faust, R. A. (1995). *Toxicity Summary for Asbestos*. Retrieved 04/13/2007, 2007, from riskassessment.ornl.gov/documents/Asbestos.pdf

Finkelstein, J. N., & Barrett, E. G. (2000). Alterations in Gene expression in Pulmonary Cells Following Particle Interactions. In P. Gehr & J. Heyder (Eds.), *Particle-Lung Interactions* (pp. 379-399). New York: Marcel Dekker, Inc.

Fong, L. G., & Le, D. (1999). The processing of ligands by the class A scavenger receptor is dependent on signal information located in the cytoplasmic domain. *J Biol Chem, 274*(51), 36808-36816.

Franks, L. M., Carbonell, A. W., Hemmings, V. J., & Riddle, P. N. (1976). Metastasizing tumors from serum-supplemented and serum-free cell lines from a C57BL mouse lung tumor. *Cancer Res, 36*(3), 1049-1055.

Fraser, I., Hughes, D., & Gordon, S. (1993). Divalent cation-independent macrophage adhesion inhibited by monoclonal antibody to murine scavenger receptor. *Nature, 364*(6435), 343-346.

Fraser, R. S., Colman, N., & Muller, N. (2005). *Synopsis of Diseases of the Chest* (3rd ed.): Elsevier/Saunders.

Garcia, J. G., Dodson, R. F., & Callahan, K. S. (1989). Effect of environmental particulates on cultured human and bovine endothelium. Cellular injury via an oxidant-dependent pathway. *Lab Invest, 61*(1), 53-61.

Garcia, J. G., Gray, L. D., Dodson, R. F., & Callahan, K. S. (1988). Asbestos-induced endothelial cell activation and injury. Demonstration of fiber phagocytosis and oxidant-dependent toxicity. *Am Rev Respir Dis, 138*(4), 958-964.

Geng, Y., Kodama, T., & Hansson, G. K. (1994). Differential expression of scavenger receptor isoforms during monocyte-macrophage differentiation and foam cell formation. *Arterioscler Thromb, 14*(5), 798-806.

Giancotti, F. G. (2000). Complexity and specificity of integrin signalling. *Nat Cell Biol, 2*(1), E13-14.

Giancotti, F. G., & Ruoslahti, E. (1999). Integrin signaling. *Science, 285*(5430), 1028-1032.

Goldstein, J. L., Ho, Y. K., Basu, S. K., & Brown, M. S. (1979). Binding site on macrophages that mediates uptake and degradation of acetylated low density lipoprotein, producing massive cholesterol deposition. *Proc Natl Acad Sci U S A, 76*(1), 333-337.

Gordon, S. (2002). Pattern recognition receptors: doubling up for the innate immune response. *Cell, 111*(7), 927-930.

Gough, P. J., Greaves, D. R., & Gordon, S. (1998). A naturally occurring isoform of the human macrophage scavenger receptor (SR-A) gene generated by alternative splicing blocks modified LDL uptake. *J Lipid Res, 39*(3), 531-543.

Gross, T. J., & Hunninghake, G. W. (2001). Idiopathic pulmonary fibrosis. *N Engl J Med, 345*(7), 517-525.

Hamilton, R. F., de Villiers, W. J., & Holian, A. (2000). Class A type II scavenger receptor mediates silica-induced apoptosis in Chinese hamster ovary cell line. *Toxicol Appl Pharmacol, 162*(2), 100-106.

Hamilton, R. F., Iyer, L. L., & Holian, A. (1996). Asbestos induces apoptosis in human alveolar macrophages. *Am J Physiol, 271*(5 Pt 1), L813-819.

Hamilton, R. F., Jr., Thakur, S. A., Mayfair, J. K., & Holian, A. (2006). MARCO mediates silica uptake and toxicity in alveolar macrophages from C57BL/6 mice. *J Biol Chem, 281*(45), 34218-34226.

Hampton, R. Y., Golenbock, D. T., Penman, M., Krieger, M., & Raetz, C. R. (1991). Recognition and plasma clearance of endotoxin by scavenger receptors. *Nature, 352*(6333), 342-344.

Hayman, E. G., Pierschbacher, M. D., Ohgren, Y., & Ruoslahti, E. (1983). Serum spreading factor (vitronectin) is present at the cell surface and in tissues. *Proc Natl Acad Sci U S A, 80*(13), 4003-4007.

Helliwell, R. J., Adams, L. F., & Mitchell, M. D. (2004). Prostaglandin synthases: recent developments and a novel hypothesis. *Prostaglandins Leukot Essent Fatty Acids, 70*(2), 101-113.

Iyer, R., Hamilton, R. F., Li, L., & Holian, A. (1996). Silica-induced apoptosis mediated via scavenger receptor in human alveolar macrophages. *Toxicol Appl Pharmacol, 141*(1), 84-92.

Jiang, Y., Oliver, P., Davies, K. E., & Platt, N. (2006). Identification and characterization of murine SCARA5, a novel class a scavenger receptor that is expressed by populations of epithelial cells. *J Biol Chem, 281*(17), 11834-11845.

Kalgutkar, A. S., Marnett, A. B., Crews, B. C., Remmel, R. P., & Marnett, L. J. (2000). Ester and amide derivatives of the nonsteroidal antiinflammatory drug, indomethacin, as selective cyclooxygenase-2 inhibitors. *J Med Chem, 43*(15), 2860-2870.

Kamio, K., Liu, X., Sugiura, H., Togo, S., Kobayashi, T., Kawasaki, S., et al. (2007). Prostacyclin Analogues Inhibit Fibroblast Contraction of Collagen Gels Through the cAMP-PKA Pathway. *Am J Respir Cell Mol Biol*.

Kamp, D. W., Dunn, M. M., Sbalchiero, J. S., Knap, A. M., & Weitzman, S. A. (1994). Contrasting effects of alveolar macrophages and neutrophils on asbestos-induced pulmonary epithelial cell injury. *Am J Physiol, 266*(1 Pt 1), L84-91.

Kamp, D. W., Graceffa, P., Pryor, W. A., & Weitzman, S. A. (1992). The role of free radicals in asbestos-induced diseases. *Free Radic Biol Med, 12*(4), 293-315.
Kamp, D. W., Greenberger, M. J., Sbalchierro, J. S., Preusen, S. E., & Weitzman, S. A. (1998). Cigarette smoke augments asbestos-induced alveolar epithelial cell injury: role of free radicals. *Free Radic Biol Med, 25*(6), 728-739.
Kamp, D. W., & Weitzman, S. A. (1997). Asbestosis: clinical spectrum and pathogenic mechanisms. *Proc Soc Exp Biol Med, 214*(1), 12-26.
Kamp, D. W., & Weitzman, S. A. (1999). The molecular basis of asbestos induced lung injury. *Thorax, 54*(7), 638-652.
Kampman, K. A., & McDonald, J. A. (1996). Adhesion Molecules in Lung Morphogenesis. In P. A. Ward & J. C. Fantone (Eds.), *Adhesion Molecules and the Lung* (1st ed., Vol. 90, pp. 99-126). New York: Marcel Dekker, Inc.
Kelley, J. (1998). Occupational Lung Diseases Caused by Asbestos, Silica, and Other Silicates. In G. L. Baum, J. D. Crapo, B. R. Celli & J. B. Karlinsky (Eds.), *Textbook of Pulmonary Diseases* (6th ed., pp. 659-682). Philadelphia: Lippincott-Raven Publishers.
Kerr, J. F., Wyllie, A. H., & Currie, A. R. (1972). Apoptosis: a basic biological phenomenon with wide-ranging implications in tissue kinetics. *Br J Cancer, 26*(4), 239-257.
Khan, A. N., Jones, C., & Macdonald, S. (2004, 01/28/2004). *Asbestos-Related Disease*. Retrieved 11/29/2006, 2006, from http://www.emedicine.com/radio/topic53.htm
Kim, J. G., Keshava, C., Murphy, A. A., Pitas, R. E., & Parthasarathy, S. (1997). Fresh mouse peritoneal macrophages have low scavenger receptor activity. *J Lipid Res, 38*(11), 2207-2215.
Kinnula, V. L., Raivio, K. O., Linnainmaa, K., Ekman, A., & Klockars, M. (1995). Neutrophil and asbestos fiber-induced cytotoxicity in cultured human mesothelial and bronchial epithelial cells. *Free Radic Biol Med, 18*(3), 391-399.
Kodama, T., Freeman, M., Rohrer, L., Zabrecky, J., Matsudaira, P., & Krieger, M. (1990). Type I macrophage scavenger receptor contains alpha-helical and collagen-like coiled coils. *Nature, 343*(6258), 531-535.
Kosswig, N., Rice, S., Daugherty, A., & Post, S. R. (2003). Class A scavenger receptor-mediated adhesion and internalization require distinct cytoplasmic domains. *J Biol Chem, 278*(36), 34219-34225.
Lecoeur, H. (2002). Nuclear apoptosis detection by flow cytometry: influence of endogenous endonucleases. *Exp Cell Res, 277*(1), 1-14.
Liu, W., Ernst, J. D., & Broaddus, V. C. (2000). Phagocytosis of crocidolite asbestos induces oxidative stress, DNA damage, and apoptosis in mesothelial cells. *Am J Respir Cell Mol Biol, 23*(3), 371-378.
Liu, X., Conner, H., Kobayashi, T., Kim, H., Wen, F., Abe, S., et al. (2005). Cigarette smoke extract induces DNA damage but not apoptosis in human bronchial epithelial cells. *Am J Respir Cell Mol Biol, 33*(2), 121-129.
Lobner, D. (2000). Comparison of the LDH and MTT assays for quantifying cell death: validity for neuronal apoptosis? *J Neurosci Methods, 96*(2), 147-152.
Lovborg, H., Gullbo, J., & Larsson, R. (2005). Screening for apoptosis--classical and emerging techniques. *Anticancer Drugs, 16*(6), 593-599.

Lovgren, A. K., Jania, L. A., Hartney, J. M., Parsons, K. K., Audoly, L. P., Fitzgerald, G. A., et al. (2006). COX-2-derived prostacyclin protects against bleomycin-induced pulmonary fibrosis. *Am J Physiol Lung Cell Mol Physiol, 291*(2), L144-156.

MacCorkle, R. A., Slattery, S. D., Nash, D. R., & Brinkley, B. R. (2006). Intracellular protein binding to asbestos induces aneuploidy in human lung fibroblasts. *Cell Motil Cytoskeleton, 63*(10), 646-657.

Marieb, E. N., & Hoehn, K. (2007). *Human Anatomy & Physiology* (7th ed.). San Francisco: Pearson Benjamin Cummings.

Mason, R. J., Schwarz, M. I., Hunninghake, G. W., & Musson, R. A. (1999). NHLBI Workshop Summary. Pharmacological therapy for idiopathic pulmonary fibrosis. Past, present, and future. *Am J Respir Crit Care Med, 160*(5 Pt 1), 1771-1777.

McClellan, R. O. (1999). Ambient Airbone Particulate Matter. Toxicology and Standards. In D. E. Gardner, J. D. Crapo & R. O. McClellan (Eds.), *Toxicology of The Lung* (3rd ed., pp. 289-341). Ann Arbor: Taylor & Francis.

McClellan, R. O., & Miller, F. J. (1997). An overview of EPA's proposed revision of the particulate matter standard. *CIIT Activities, 17*(4), 1-22.

McKusick, V. A. (1989, 07/18/1994). *Vitronectin; VTN*. Retrieved 02/07/2007, 2007, from http://www.ncbi.nlm.nih.gov/entrez/dispomim.cgi?id=193190

McKusick, V. A. (2001, 02/27/2003). *Prostaglandin I2 synthase; PTGIS*. Retrieved 11/28/2006, 2006, from http://www.ncbi.nlm.nih.gov/entrez/dispomim.cgi?id=601699

Miki, S., Tsukada, S., Nakamura, Y., Aimoto, S., Hojo, H., Sato, B., et al. (1996). Functional and possible physical association of scavenger receptor with cytoplasmic tyrosine kinase Lyn in monocytic THP-1-derived macrophages. *FEBS Lett., 399*(3), 241-244.

Morimoto, K., Wada, Y., Hinagata, J., Imanishi, T., Kodama, T., & Doi, T. (1999). VXFD in the cytoplasmic domain of macrophage scavenger receptors mediates their efficient internalization and cell-surface expression. *Biol Pharm Bull, 22*(10), 1022-1026.

Mossman, B. T., Bignon, J., Corn, M., Seaton, A., & Gee, J. B. (1990). Asbestos: scientific developments and implications for public policy. *Science, 247*(4940), 294-301.

Mossman, B. T., & Churg, A. (1998). Mechanisms in the pathogenesis of asbestosis and silicosis. *Am J Respir Crit Care Med, 157*(5 Pt 1), 1666-1680.

Mossman, B. T., & Gee, J. B. (1989). Asbestos-related diseases. *N Engl J Med, 320*(26), 1721-1730.

Mossman, B. T., Kamp, D. W., & Weitzman, S. A. (1996). Mechanisms of carcinogenesis and clinical features of asbestos-associated cancers. *Cancer Invest, 14*(5), 466-480.

Mossman, B. T., Surinrut, P., Brinton, B. T., Marsh, J. P., Heintz, N. H., Lindau-Shepard, B., et al. (1996). Transfection of a manganese-containing superoxide dismutase gene into hamster tracheal epithelial cells ameliorates asbestos-mediated cytotoxicity. *Free Radic Biol Med, 21*(2), 125-131.

Munger, J. S., Huang, X., Kawakatsu, H., Griffiths, M. J., Dalton, S. L., Wu, J., et al. (1999). The integrin alpha v beta 6 binds and activates latent TGF beta 1: a

mechanism for regulating pulmonary inflammation and fibrosis. *Cell, 96*(3), 319-328.

Murakami, S., Nagaya, N., Itoh, T., Kataoka, M., Iwase, T., Horio, T., et al. (2006). Prostacyclin agonist with thromboxane synthase inhibitory activity (ONO-1301) attenuates bleomycin-induced pulmonary fibrosis in mice. *Am J Physiol Lung Cell Mol Physiol, 290*(1), L59-65.

Murphy, J. E., Tedbury, P. R., Homer-Vanniasinkam, S., Walker, J. H., & Ponnambalam, S. (2005). Biochemistry and cell biology of mammalian scavenger receptors. *Atherosclerosis, 182*(1), 1-15.

Murphy, J. F., Steele, C., Belton, O., & Fitzgerald, D. J. (2003). Induction of cyclooxygenase-1 and -2 modulates angiogenic responses to engagement of alphavbeta3. *Br J Haematol, 121*(1), 157-164.

Nakamura, K., Funakoshi, H., Tokunaga, F., & Nakamura, T. (2001). Molecular cloning of a mouse scavenger receptor with C-type lectin (SRCL)(1), a novel member of the scavenger receptor family. *Biochim Biophys Acta, 1522*(1), 53-58.

Nakamura, T., Hinagata, J., Tanaka, T., Imanishi, T., Wada, Y., Kodama, T., et al. (2002). HSP90, HSP70, and GAPDH directly interact with the cytoplasmic domain of macrophage scavenger receptors. *Biochem.Biophys.Res.Commun., 290*(2), 858-864.

Nemery, B., Bast, A., Behr, J., Borm, P. J., Bourke, S. J., Camus, P. H., et al. (2001). Interstitial lung disease induced by exogenous agents: factors governing susceptibility. *Eur Respir J Suppl, 32*, 30s-42s.

Obot, C. J., Morandi, M. T., Beebe, T. P., Hamilton, R. F., & Holian, A. (2002). Surface components of airborne particulate matter induce macrophage apoptosis through scavenger receptors. *Toxicol Appl Pharmacol, 184*(2), 98-106.

Ottaviani, M. F., Venturi, F., Pokhrel, M. R., Schmutz, T., & Bossmann, S. H. (2001). Physicochemical Studies on the Adsorption Properties of Asbestos. *J Colloid Interface Sci, 238*(2), 371-380.

Palecanda, A., & Kobzik, L. (2000). Alveolar macrophage-environmental particle interaction: analysis by flow cytometry. *Methods, 21*(3), 241-247.

Pande, P., Mosleh, T. A., & Aust, A. E. (2006). Role of alphavbeta5 integrin receptor in endocytosis of crocidolite and its effect on intracellular glutathione levels in human lung epithelial (A549) cells. *Toxicol Appl Pharmacol, 210*(1-2), 70-77.

Peiser, L., & Gordon, S. (2001). The function of scavenger receptors expressed by macrophages and their role in the regulation of inflammation. *Microbes Infect, 3*(2), 149-159.

Peterson, M. W., & Schwartz, D. A. (1999). Effects of Fiber Aerosols on the Lung and Chest Wall. In D. L. Swift & W. M. Foster (Eds.), *Air Pollutants and the Respiratory Tract* (1st ed., Vol. 128, pp. 219-250). New York: Marcel Dekker, Inc.

Pittet, J. F., Griffiths, M. J., Geiser, T., Kaminski, N., Dalton, S. L., Huang, X., et al. (2001). TGF-beta is a critical mediator of acute lung injury. *J Clin Invest, 107*(12), 1537-1544.

Plaetzer, K., Kiesslich, T., Oberdanner, C. B., & Krammer, B. (2005). Apoptosis following photodynamic tumor therapy: induction, mechanisms and detection. *Curr Pharm Des, 11*(9), 1151-1165.

Platt, N., & Gordon, S. (2001). Is the class A macrophage scavenger receptor (SR-A) multifunctional? - The mouse's tale. *J.Clin.Invest, 108*(5), 649-654.

Powel, F. L. (1998). Structure and Function of the Respiratory System. In L. R. Johnson (Ed.), *Essential Medical Physiology* (2nd ed., pp. 239-254). Philadelphia: Lippincott-Raven Publishers.

Raabe, O. G. (1999). Respiratory Exposure to Air Pollutants. In D. L. Swift & W. M. Foster (Eds.), *Air Pollutants and the Respiratory Tract* (1st ed., Vol. 128, pp. 39-73). New York: Marcel Dekker, Inc.

Resnick, D., Freedman, N. J., Xu, S., & Krieger, M. (1993). Secreted extracellular domains of macrophage scavenger receptors form elongated trimers which specifically bind crocidolite asbestos. *J Biol Chem, 268*(5), 3538-3545.

Rimal, B., Greenberg, A. K., & Rom, W. N. (2005). Basic pathogenetic mechanisms in silicosis: current understanding. *Curr Opin Pulm Med, 11*(2), 169-173.

Roberts, K., Yokoyama, W. M., Kehn, P. J., & Shevach, E. M. (1991). The vitronectin receptor serves as an accessory molecule for the activation of a subset of gamma/delta T cells. *J Exp Med, 173*(1), 231-240.

Rom, W. N., Travis, W. D., & Brody, A. R. (1991). Cellular and molecular basis of the asbestos-related diseases. *Am Rev Respir Dis, 143*(2), 408-422.

Ruoslahti, E. (2003). The RGD story: a personal account. *Matrix Biol, 22*(6), 459-465.

Samet, J. M. (2000). Occupational Pulmonary Disorders. In L. Goldman & J. C. Bennett (Eds.), *Cecil Textbook of Medicine* (21st ed., pp. 419-424). Philadelphia: W.B. Saunders Company.

Schvartz, I., Seger, D., & Shaltiel, S. (1999). Vitronectin. *Int J Biochem Cell Biol, 31*(5), 539-544.

Seiffert, D. (1997). Constitutive and regulated expression of vitronectin. *Histol Histopathol, 12*(3), 787-797.

Sheppard, D. (2005). Integrin-mediated activation of latent transforming growth factor beta. *Cancer Metastasis Rev, 24*(3), 395-402.

Stoner, G. D., Kikkawa, Y., Kniazeff, A. J., Miyai, K., & Wagner, R. M. (1975). Clonal isolation of epithelial cells from mouse lung adenoma. *Cancer Res, 35*(8), 2177-2185.

Takagi, J. (2004). Structural basis for ligand recognition by RGD (Arg-Gly-Asp)-dependent integrins. *Biochem Soc Trans, 32*(Pt3), 403-406.

Tannock, I. F., & Lee, C. (2001). Evidence against apoptosis as a major mechanism for reproductive cell death following treatment of cell lines with anti-cancer drugs. *Br J Cancer, 84*(1), 100-105.

Tatrai, E., Brozik, M., Kovacikova, Z., & Horvath, M. (2005). The effect of asbestos and stone-wool fibres on some chemokines and redox system of pulmonary alveolar macrophages and pneumocytes type II. *Biomed Pap Med Fac Univ Palacky Olomouc Czech Repub, 149*(2), 357-361.

Thornberry, N. A., & Lazebnik, Y. (1998). Caspases: enemies within. *Science, 281*(5381), 1312-1316.

Toews, G. B. (2000). Interstitial Lung Disease. In L. Goldman & J. C. Bennett (Eds.), *Cecil Textbook of Medicine* (21st ed., pp. 409-419). Philadelphia: W.B. Saunders Company.

Tsuda, A., Stringer, B. K., Mijailovich, S. M., Rogers, R. A., Hamada, K., & Gray, M. L. (1999). Alveolar cell stretching in the presence of fibrous particles induces interleukin-8 responses. *Am J Respir Cell Mol Biol, 21*(4), 455-462.

Wagner, G. R. (1997). Asbestosis and silicosis. *Lancet, 349*(9061), 1311-1315.

Wang, L., Antonini, J. M., Rojanasakul, Y., Castranova, V., Scabilloni, J. F., & Mercer, R. R. (2003). Potential role of apoptotic macrophages in pulmonary inflammation and fibrosis. *J Cell Physiol, 194*(2), 215-224.

Wang, L., Scabilloni, J. F., Antonini, J. M., Rojanasakul, Y., Castranova, V., & Mercer, R. R. (2005). Induction of Secondary Apoptosis, Inflammation and Lung Fibrosis After Intratracheal Instillation of Apoptotic Cells in Rats. *Am J Physiol Lung Cell Mol Physiol*.

Weibel, E. R. (1963). *Morphometry of The Human Lung* (7th ed.). New York: Springer-Verlag.

Whitehead, P. (2001). *Silicate Mineralogy*. Retrieved 01/06/2007, 2007, from http://tesla.jcu.edu.au/Schools/Earth/EA1001/Mineralogy/Silicates.html

Wu, J., Liu, W., Koenig, K., Idell, S., & Broaddus, V. C. (2000). Vitronectin adsorption to chrysotile asbestos increases fiber phagocytosis and toxicity for mesothelial cells. *Am J Physiol Lung Cell Mol Physiol, 279*(5), L916-923.

Yamamoto, K., Nishimura, N., Doi, T., Imanishi, T., Kodama, T., Suzuki, K., et al. (1997). The lysine cluster in the collagen-like domain of the scavenger receptor provides for its ligand binding and ligand specificity. *FEBS Lett, 414*(2), 182-186.

Yun, Z., Takagi, M., & Yoshida, T. (2001). Effect of antioxidants on the apoptosis of CHO cells and production of tissue plasminogen activator in suspension culture. *J Biosci Bioeng, 91*(6), 581-585.